

Alternative Methods for Assessing Air Quality and Energy Strategies for Developing Countries: A Case Study on Cuba

THÈSE N° 9010 (2018)

PRÉSENTÉE LE 6 DÉCEMBRE 2018

À LA FACULTÉ DE L'ENVIRONNEMENT NATUREL, ARCHITECTURAL ET CONSTRUIT
LABORATOIRE DE SYSTÈMES D'INFORMATION GÉOGRAPHIQUE
PROGRAMME DOCTORAL EN GÉNIE CIVIL ET ENVIRONNEMENT

ÉCOLE POLYTECHNIQUE FÉDÉRALE DE LAUSANNE

POUR L'OBTENTION DU GRADE DE DOCTEUR ÈS SCIENCES

PAR

Jessie MADRAZO BACALLAO

acceptée sur proposition du jury:

Prof. S. Takahama, président du jury
Prof. F. Golay, Prof. A. Clappier, directeurs de thèse
Prof. M. Z. Jacobson, rapporteur
Dr Ph. Thunis, rapporteur
Prof. F. Marechal, rapporteur



ÉCOLE POLYTECHNIQUE
FÉDÉRALE DE LAUSANNE

Suisse
2018

Overview

Project

Title:	<i>Alternative Methods for Assessing Air Quality and Energy Strategies for Developing Countries: A Case Study on Cuba</i>
Candidate:	Jessie Madrazo (LASIG, EPFL)
Supervision:	Prof. François Golay (LASIG, EPFL) Prof. Alain Clappier (Univ. Strasbourg)
Doctoral Committee:	Prof. Satoshi Takahama (APRL, EPFL) Prof. François Marechal (IPESE, EPFL) Prof. Mark Z. Jacobson (Stanford University) Dr. Philippe Thunis (JRC, European Commission)
Enrollment date:	Sep. 1, 2014
Host institute:	Ecole Polytechnique Fédérale de Lausanne (EPFL) Doctoral Program in Civil and Environmental Engineering (EDCE) Geographic Information Systems Laboratory (LASIG)

Contact

Postal address:	EPFL ENAC IIE LASIG GC D2 415 (Batiment GC) Station 18 CH-1015 Lausanne
Office:	GCD2415
Phone:	+41 78 926 80 22
Email:	jessie.madrado@epfl.ch

*“The ability to simplify means to eliminate unnecessary so that the necessary may speak”
Hans Hofmann, Keys to Manifesting Your Destiny.*

*a mis padres, Martha Bacallao y Jorge Madrazo
a mi mas grande apoyo spiritual, Maritza Bacallao
a mi compañero de vida, Juan Miguel Valdes
... su amor y apoyo hicieron esto posible*

Abstract

The worldwide increasing energy consumption is mainly based on fossil fuel which leads to a large number of environmental problems. Indeed, the combustion of fossil fuels releases into the atmosphere different greenhouse gases, as well as harmful pollutants. Greenhouse gases are responsible for climate change while harmful pollutants cause air quality degradation. Moreover, fossil fuel resources are limited and their depletion will happen sooner or later. Governments of the whole world are urged to take relevant measures and policies to design and implement strategies for energy transition. To support their choices, different modelling and decision support approaches have been developed, mainly in industrialized countries. However, these approaches usually lack coherent integration and rely on expensive and often unavailable detailed data, especially in developing countries.

This PhD aims at develop alternative method for the assessment of air quality and energy strategies in the framework of developing countries. A key aspect is the simplifications of intrinsic techniques so as to facilitate the assessment of different strategies. Examples of this approach include the reduction of computational time, the development of inexpensive methodologies to obtain data or simply the creation of benchmarks and indicators to support the choices. The developed methods are implemented in Cuba which seems an excellent test case to design and apply energy strategies for developing countries. On the one hand, the climate of country presents good opportunities for renewable energy sources integration (e.g. solar and biomass). On the other hand, the embargo imposed by the United States in 1960 started to have dramatic consequences on the energy supply of the island when the help of Russia stopped in 1990. It is now a political issue for the Cuban authorities to improve their energy independency.

The first part of this work deals with methods intended to assess emission abatements and air quality strategies. For this purpose, an air pollution measurement campaign was carried out in Havana. It provided data to implement and improve a pre-existing methodology capable of estimating Cuban vehicle emission factors. The statistical analysis of the measurement campaign results pointed-out the traffic as responsible of around 50% of the particulate matter concentration in the street and identified vehicles pre-1980s as the most polluting technologies. This work also demonstrates the usability of an emission inventory designed for air quality simulations. Statistical and benchmarking tools helped to pinpoint differences between global and regional inventories, and identify where efforts should concentrate for improving emission data. A regional emission inventory was used as input in CHIMERE air quality model to simulate the evolution of air pollution during the year 2015. Then, a series of emission reduction scenarios have been computed to set up simplified algebraic relationships (i.e. so-called Source-Receptor Relationship) capable of predicting the impacts on concentration levels resulting from regional emission abatement strategies, while being more time-efficient than traditional methods.

The last part is dedicated to explore scenarios for the energy transition of Cuba. To this end, the energy fluxes between resources, technologies and final demand was computed for the year 2015. A set of scenarios were then designed on the basis of different mix of energy resources. The first scenario is considered as a base-line projection and corresponds to the strategy of the Cuban ministry of energy. Three other scenarios evaluate the consequences of Cuba's use of renewable resources to fulfill a growing percentage of electricity demand. These scenarios have been compared according to three criteria that seemed the most relevant for the country geopolitical and economic situation: energy security (degree of dependence from energy imports), sustainability of the energy resources and population exposure to harmful pollutants. Overall, the results indicated that energy security and sustainability increase with wind and solar penetration at different rates. A penetration rate of 20% of the demand significantly decreases fossil fuel requirements and imports. Once raised to 50%, Cuba can achieve complete energy independence. The scenario which fulfils 100% of the electricity demands from solar and wind resources shows the maximum of sustainability. Not surprisingly, the penetration of renewables had positive effects on air quality.

Keywords: air pollution measurements, emission inventory, real-world emission factor, air quality management, source-receptor relationship, energy management, energy planning, Cuba.

Resumé

La consommation mondiale croissante d'énergie est principalement basée sur la consommation de carburants fossiles ce qui entraîne un grand nombre de problèmes environnementaux. En effet, la combustion de ces carburants fossiles dégage dans l'atmosphère différents gaz à effet de serre, ainsi que de nombreux polluants nocifs. Les gaz à effet de serre sont responsables du changement climatique globale, tandis que les polluants nocifs entraînent la dégradation de la qualité de l'air. De plus, les ressources en carburants fossiles sont limitées et cette ressource s'épuisera tôt ou tard. Les gouvernements du monde entier sont de plus en plus sollicités pour concevoir et mettre en œuvre des stratégies de transition énergétique. Dans ce but, différentes approches de modélisation et d'aide à la décision ont été développées, principalement dans les pays industrialisés. Ces approches nécessitent d'intégrer beaucoup de différents facteurs. Elles s'appuient sur des données détaillées coûteuses et souvent indisponibles, en particulier dans les pays en développement.

Cette thèse vise à concevoir des méthodes alternatives adaptées aux pays en voie de développement pour évaluer la qualité de l'air et les stratégies énergétiques dans ces pays. Cuba a été choisie pour ce travail car il s'agit d'un excellent cas test pour concevoir et appliquer des stratégies énergétiques adaptées pays en voie de développement. D'une part, le climat à Cuba est particulièrement propice à l'intégration des sources d'énergie renouvelables (par exemple, l'énergie solaire et la biomasse). D'autre part, l'embargo imposé par les États-Unis en 1960 a commencé à produire des effets dramatiques sur l'approvisionnement énergétique de l'île lorsque l'aide de la Russie s'est arrêtée en 1990. C'est désormais un enjeu politique pour les autorités cubaines d'améliorer leur indépendance énergétique.

La première partie de ce travail porte sur l'étude de la qualité de l'air. Une campagne de mesure de la pollution atmosphérique a été menée à La Havane. Une méthodologie préexistante a été améliorée pour estimer le facteur d'émission des véhicules cubains en utilisant le minimum de moyens possibles. L'analyse statistique des résultats de la campagne de mesures a mis en évidence que le trafic était responsable d'environ 50% de la concentration de particules dans l'une des rues principales de La Havane et a identifié les véhicules d'avant 1980 comme les technologies les plus polluantes. Un inventaire des émissions a été calculé pour la ville de La Havane. Cet inventaire a été utilisé comme une donnée d'entrée du modèle de qualité de l'air CHIMERE afin de simuler l'évolution de la pollution atmosphérique au cours de l'année 2015. Une série de scénarios de réduction des émissions ont été calculés pour établir des relations Source-Récepteur (SRR). Ces SRR sont capables de prédire très rapidement (quelques minutes pour les SRR au lieu de quelques jours pour le modèle CHIMERE) l'impact de n'importe quelle stratégie de réduction sur la qualité de l'air.

La dernière partie de ce travail est consacrée à la conception et à la comparaison de différents scénarios énergétiques pour Cuba. Les flux d'énergie entre la demande en énergie et les ressources énergétiques disponibles ont été calculés pour l'année 2015. La demande en énergie a été estimée pour l'année 2030 et différents scénarios basés sur différents mix de ressources énergétiques ont été conçus. Un premier scénario correspond à la stratégie du ministère cubain de l'énergie. Trois scénarios mettent en œuvre des ressources solaires et éoliennes pour fournir un pourcentage croissant de la demande en énergie électrique. Ces scénarios ont été comparés selon trois critères qui semblaient les plus pertinents pour Cuba compte tenu de sa situation géopolitique et économique: la sécurité énergétique (degré de dépendance vis-à-vis des importations énergétiques), la durabilité des ressources énergétiques et l'exposition des populations aux polluants nocifs. Les différents scénarios ont montré que lorsque l'énergie éolienne et l'énergie solaire fournissent 20% de la demande en électricité, les besoins en combustibles fossiles (que ce soit domestiques ou importés) sont considérablement réduits et cela, sans avoir recours au stockage de l'énergie. Au-delà d'une pénétration d'environ 20% à 25% de l'énergie éolienne et solaire, le stockage de l'énergie devient nécessaire. Mais lorsque cette pénétration atteint 50%, Cuba devient totalement indépendante des importations d'énergie. Le scénario où le solaire et le vent fournissent 100% de la demande électrique est celui qui maximise la durabilité des ressources et améliore le plus la qualité de l'air.

Mots-clés: mesures de la pollution atmosphérique, inventaire des émissions, facteur d'émission réel, gestion de la qualité de l'air, relation source-récepteur, gestion de l'énergie, planification énergétique, Cuba.

Acknowledges

First, I would like to thank my advisors, Prof. François Golay, who gave me the opportunity to do this thesis and Prof. Alain Clappier for his constant guidance and support during my research. Many thanks to both of you for all explanations, patience and constant motivation, good mood and advices that were priceless.

I would also like to thank Prof. François Marechal for his support to the research project and Prof. Mark Z. Jacobson for hosting me in his laboratory at Stanford University. I also thanks Dr Ph. Philippe Thunis for its comments and feedback to this document

An special gratitude goes out to Prof. Luis Carlos Belalcazar and Marco Guevara for the scientific support and pertinent comments.

My gratitude also goes to the research teams of CUBAENERGIA and CECONT in Cuba for providing support with obtaining data, as well as to the Swiss institutions that provided me funding support for this work; these include Swiss Government Excellence Scholarships program, the Cooperation and Development Center (CODEV), the Swiss National Science Foundation (SNF) and the foundation Erna Hamburger.

I am also grateful to the Association UrbamoCUBA.ch and his president M. Remy Fankhauser for the funding and logistical support provided during the measurement campaign we developed in Havana.

Finally, I want to thank all the people from the LASIG, Professors, PhD and McS Students, with special mention to Solange Duruz, Matthew Parkan and Annie Guillaume for all the help, the fun and the motivation during these years.

Contents

1	Introduction	1
1.1	Motivation	1
1.2	Focus of research and objective	1
1.3	Outline	3
2	Evidence of traffic-generated air pollution in Havana	6
2.1	Introduction	7
2.2	Measurement campaign	7
2.3	Result and discussion	9
2.3.1	Traffic flows	9
2.3.2	Concentration levels	9
2.3.3	Meteorological parameters	9
2.3.4	Statistical relationships between traffic flows, pollutant concentration and wind forces	13
2.4	Conclusions	15
3	Low-cost methodology to estimate vehicle emission factors	18
3.1	Introduction	19
3.2	Sampling location and data	19
3.3	Methods	20
3.3.1	Basic assumptions	20
3.3.2	Dilution factor	21
3.3.3	Time averaging	22
3.4	Results and discussion	22
3.4.1	Multiple linear regression	22
3.4.2	Principal component regression	25
3.4.3	Considering uncertainties in EF estimations	27
3.4.4	Comparisons with available studies	27
3.5	EFs for air pollution policy purposes	28
3.6	Conclusions	31
4	Screening differences between a local inventory and the Emissions Database for Global Atmospheric Research (EDGAR)	35
4.1	Introduction	36
4.2	Data and Method	37
4.2.1	Local inventory	37
4.2.2	EDGAR inventory	41
4.2.3	Benchmarking tools	41
4.3	Results and discussion	41
4.4	Conclusions	45
5	Setting a Source-Receptor Relationship (SRR) for the assessment of emission reduction strategies over Cuba	49
5.1	Introduction	50
5.2	Model set up	50
5.2.1	Emission inventory	50

5.2.2	Meteorological fields	51
5.3	Statistical analysis	51
5.3.1	Relationships between the main species	51
5.3.2	Relationship between abatement scenarios	55
5.4	Source-Receptor relationship	56
5.4.1	Methodology	56
5.4.2	Application for NO _x , PM ₂₅ and SOMO35	57
5.4.3	Improvements for PM ₂₅ and SOMO35	58
5.4.4	Absolute values, PM ₂₅ , SOMO35 and NO ₂ estimates	59
5.5	Conclusions	60
6	Cuban's energy strategy into 2030: General design features toward a sustainable transition	64
6.1	Introduction	65
6.2	Overview of the Cuban energy system	65
6.2.1	The situation in 2015	65
6.2.2	The projection into 2030	68
6.2.3	Environmental concerns	70
6.2.4	Comparison between 2015 and 2030	70
6.3	Alternative scenarios for the Cuban energy mix	71
6.3.1	Insights in energy demand	71
6.3.2	Insights in potential resources	71
6.3.3	Matching electric power supply with demand	74
6.3.4	Scenarios development	77
6.4	Results	78
6.5	Summary and conclusions	79
7	Summary of main contributions and outlook	83
7.1	Alternatives techniques for reliable assessments of emission abatement strategies, the case of Cuba	84
7.2	General design features toward a sustainable energy transition. The case of Cuba	85
7.3	Recommendations	86
7.4	Outlook	87

List of Figures

1.1	Overview of energy system and air quality links	2
2.1	Measurement site and location of the street Simon Bolivar in Havana city (Red point). Adapted from Google earth map: (a) Street top view with the meteorological station – 1, the traffic video recording – 2 and pollutant measurement devices – 3. (b) Street elevation view	8
2.2	Traffic data	10
2.3	Average diurnal variations of PM10, NO2 and SO2	11
2.4	Wind roses: average diurnal variation of wind forces	12
2.5	Bivariate polar plots	14
3.1	Data collection site (Simon Bolivar Street). 1: Thermo-Scientific ADR 1500 profiler and traffic video recording. 2: AIRDAM anemometer. Adapted from Google Earth.	20
3.2	Results of the multiple regression for different averaging times. (a) Correlation coefficient. (b-e) EF refers the coefficients of the regression or PM10 emission factors, and $\pm\sigma$ is the standard deviation of the coefficients. (f) The intercept and $\pm\sigma$ is the standard deviation of the intercept. (g) Significance levels of the regression coefficients.	23
3.3	Results of the principal component regression for different averaging time periods. (a) Correlation coefficient. (b-e) EF is the PM10 emission factor, i.e., the coefficients of the regression; $\pm\sigma$ is the standard deviation of the coefficients. (f) Background concentrations: the intercept $\pm\sigma$ is the standard deviation of the intercept.	26
3.4	Probability density functions. The curves express the range of variation of PM10 EFs (mg km-1 veh-1) by vehicle category.	27
3.5	Comparison of PM10 concentration levels ($\mu\text{g m}^{-3}$) from on-road vehicles under four scenarios. Red and black arrows indicate the minimum and maximum percent of reduction expected on the street.	30
3.6	Projection lines of PM10 concentration levels based on reductions from 55 to 10 ($\mu\text{g m}^{-3}$), as expected from decreasing the number of light-duty vehicles from 1000 to 0 along with an increase in passengers that travel on buses from 65 to 100% and/or changing light-duty vehicle capacities. (See 3.8). The percentages on the right (red and black) indicate the minimum and maximum reductions expected on the street.	31
4.1	Spatial comparison of CO, NMVOC, PM10, NOx, SO2 and CH4 emissions in ton/year; differences as EDGAR - Local EI: (a) SNAP-7 (b) SNAP-1,3,4. Pollutants are mentioned in the legend of each panel.	42
4.2	Bar plot on horizontal axes: comparison of CO, NMVOC, NOx, PM10, SO2 and CH4 emissions of local inventory with EDGAR data.	43
4.3	Diamond diagram: Activity-emission factor diagram for the macro-sectors SNAP-1,3,4 and SNAP-7, and pollutants CO, NMVOC, NOx, PPM10, SO2, CH4	44
4.4	Diamond diagram for SNAP-7 with cell by cell ratios. The circles represent coarse comparison by pollutant. The point cloud presents a cell by cell comparison	44
4.5	Diamond diagram for SNAP-7 with cell by cell ratios. The circles represent coarse comparison by pollutant. The point cloud presents a cell by cell comparison	45
5.1	Bipolar plot showing relationships between hourly mean of PPM, PM25, NOx, NO2, O3 day and night, as well as the indicator SOMO35.	52

5.2	Scatter plots of NO _x mean vs PPM mean (top-left), NO _x mean vs O ₃ night mean (top-right), O ₃ day vs SOMO35 (bottom-left) and NO _x mean vs NO ₂ mean (bottom-right). Fit line in red colour.	53
5.3	Cuba's pollution maps from CTM simulation	54
5.4	Comparison between simulations resulting from simultaneous precursor reductions and the estimates made from individual precursor reductions.	56
5.5	Regions selected for validating the SRR.	57
5.6	Comparison between CTM and SRR bell-shape approach for yearly PM ₂₅ , NO _x , SOMO35, with emission reductions applied over Havana, Cienfuegos and Santiago de Cuba at 20 and 80%. Blue dotted lines represent the ± 10 error range	58
5.7	Comparison between CTM and SRR improvement strategies for yearly PM ₂₅ and O ₃ day, with emission reductions applied over Havana, Cienfuegos and Santiago de Cuba at 20%. . .	59
5.8	Comparison between CTM and SRR for absolute NO ₂ , PM ₂₅ and SOMO35, with emission reductions applied over Havana, Cienfuegos and Santiago de Cuba at 80%.	60
6.1	Energy flow Sankey diagram of Cuba for the year 2015	67
6.2	Trend of energy demand from 2002 to 2015	68
6.3	Energy flow Sankey diagram of Cuba for the year 2030	69
6.4	Trend of sugarcane production from 2005 to 2015	72
6.5	Land surface (km ²) required to meet Cuban electricity demand from solar, wind and biomass resources	73
6.6	Energy fluxes between the intermittent sources, the storage, the demand and the backup: a) the intermittent sources provide enough energy to entirely fulfil the demand, b) the storage completes the intermittent sources to supply the demand, c) intermittent sources and storage are not sufficient to entirely power the demand, so it is necessary to use a backup energy source. . .	75
6.7	Backup energy, storage capacity and backup capacity calculated for different solar installed capacity expressed according to the different percentages of the electricity demand supplied by the solar energy.	77
6.8	Comparison between scenarios for 2030	78
7.1	Interdependencies of the research in air quality domain and main contributions (*)	84
7.2	Main contribution in energy system domain	85

List of Tables

2.1	Significant correlations (i.e. p-value < 0.05) among pollutants and vehicular flow: A significance level of 0.05 indicates that the risk of concluding that a correlation exists -i.e. changes in vehicle categories are related to changes in pollutant concentration levels- is 5% levels. . . .	13
3.1	Parameter settings used in dispersion model (OSPM)	22
3.2	Summary of multiple linear regressions – MLR; results (in mg km ⁻¹ veh ⁻¹) for averaging times 5'-90'. Avg. EF: an average of coefficients for an emission factors; Std. Dev of the Avg. EF: the standard deviation of coefficients with respect to the mean; Avg. of the EFs Std. Dev: the average of the standard deviations of the coefficients. Total Std. Dev: summation of the square root of the sum of squared standard deviations; Std. Dev of the Avg. EF and Avg. of the EF's Std. Dev.	24
3.3	Summary of the multiple linear regression–MLR; results (in mg km ⁻¹ veh ⁻¹) for averaging times 40'-60'. Avg. EF: an average of the coefficients for an emission factor; Std. Dev of the Avg. EF: the standard deviation of the coefficients with respect to the mean; Avg. of the EF's Std. Dev: the average of the standard deviations of the coefficients; Total Std. Dev: summation of the square root of the sum of squared standard deviations; Std. Dev of the Avg. EF and Avg. of the EF's Std. Dev.	24
3.4	Correlations matrix of predictor variables for a time period of 50'.	25
3.5	Summary of the principal component regression (PCR) results (in mg km ⁻¹ veh ⁻¹) for averaging times 40'-60'. Avg. EF: the average of the coefficients for an emission factor; Std. Dev of the Avg. EF: the standard deviation of the coefficients with respect to the mean; Avg. of the EF's Std. Dev: the average of the standard deviations of the coefficients; Total Std. Dev: summation of the square root of the sum of squared standard deviations; Std. Dev of the Avg. EF and Avg. of the EF's Std. Dev.	25
3.6	Estimated traffic emission factors (mg km ⁻¹ veh ⁻¹) for 33.3% vehicle fractions from the PDFs	28
3.7	Estimated PM10 hourly diurnal concentration levels (ug m ⁻³)	29
3.8	Passenger transport capacity used for projections.	30
4.1	SNAP sectors classification. Source: CORINAIR / SNAP 97 version 1.0 dated 20/03/1998. .	37
4.2	Vehicle categories. The total number of vehicles was set according the vehicle registration system office of Havana. Average mileage in a working day is collected from literature. . . .	38
4.3	Street categories: Havana road network categorized according to the Cuban technical standards NC 53-80 y NC 53-81. These norms provide a functional classification of urban and rural streets. Road network lengths were measured by category from the world editable Open Street Map QGIS plugin.	39
4.4	EMISENS input data. Activity levels disaggregated by vehicle and road categories (veh.km/h)	39
4.5	Emission factors (g/km-veh) by vehicle category (Passenger vehicles and light gasoline vehicles, including small vans (AG), Passenger vehicles and light diesel vehicles, including small vans (AD), Heavy vehicles and Trucks(HT), Buses (B), Motorcycles (MT))and compound including Carbon monoxide (CO), nitrogen oxides (NOx), volatile organic compounds (NMVOC), particulate matter (PM10), methane (CH4) and sulfur dioxide (SO2).	40

4.6	Stationary sources, data available. Example entities: (HOSJT) Hospital “Julio Trigo”, (GEAPO) Electrogen Group “Apolo”, (GEMAN) Electrogen, Group “Managua”, (ANTAC) Iron-steel company “Antillana de acero”, (REFÑL) Crude-oil refinery “Nico Lopez” Column head description: (a) latitude (degree); (b) longitud (degree); (c) SNAP sector; (d) regimen (hrs/day); (e) regimen (days/week); (f) EF-Nox (g/s) national; (g) EF-SO2 (g/s) national; (h) EF-PM10 (g/s) national; (i) EF-PM2.5 (g/s) national; (j) EF-CO (g/s) international reference; (k) EF-NMVOC (g/s) international reference	40
5.1	Overview of PCA results, correlations (Corr) and loadings (Contrib) of variables with respect to the main principal components (PC)	53
5.2	Set of emission reduction scenarios needed to implement the SRR over Cuba. Scenario 1 represents the base-case set-up in Sec.5.3.2, while the other scenarios are computed applying the % emission reductions as shown in table.	57
6.1	Energy demands (GWh) by key sectors in 2015. Adapted from (ONE, 2016)	66
6.2	Electricity production (GWh) 2015: Technologies and resources	66
6.3	Electricity production 2030: Technologies and resources	69
6.4	Potential of energy resources in Cuba	73
6.5	List of alternative scenarios for 2030	77
6.6	Indicators 2030	78

Chapter 1

Introduction

1.1 Motivation

The world energy consumption has been increasing since the beginning of the 20th century. The major part of this consumption is based on fossil fuels (EIA, 2016); coal, oil and natural gas have ignited homes and machinery for centuries, driving civilization forward. However, as human development augmented, the unsustainability of such energy became apparent. The combustion of fossil fuels releases different greenhouse gases into the atmosphere (Prather et al. 1994; WER 2016), such as carbon dioxide (CO₂), as well as harmful pollutants (WHO Regional Office for Europe 2016), like particulate matters (PM), and nitrogen oxides (NO_x). Greenhouse gases are responsible for climate change while harmful pollutants cause air quality degradation. Moreover, fossil fuel resources deteriorate; their depletion will happen sooner or later (Höök et al. 2013). The global supplies deterioration, as well as the growing impact on the environment will influence more and more our future economic activities (Yeager et al. 2012). Energy transition is inevitable and is indeed one of the most crucial challenges for our modern societies.

Current solutions are mainly based on the implementation of new technologies able to reduce fossil fuel consumption (increasing energy efficiency and/or using renewable energy re-sources) and its environmental impacts. Their diversification creates many opportunities, but enlarged complexity leads to increased challenges (WER 2016). Indeed, the implementation of new technologies affects the lifestyle of the population (Sutton 2013), and depends on the geographical, economic, social and cultural context of the region involved. Consequently, a single and global solution is not an option. Air quality and energy policies as well as choices regarding fuel mixes and renewable energy source targets can largely differ between regions. Each country must have the possibility to choose the most adapted strategies to its specificities while remaining consistent with the global context.

The need to adapt decision to the local context is especially relevant when comparing developed and developing countries (Vandaele et al. 2015). Efficient air quality or energy strategies in developed countries are often not adapted for developing countries (Vanderschuren et al. 2010); similarly studies performed for developed countries to find best sets of solutions cannot simply be extrapolated for developing countries. Moreover, such studies are difficult to perform in developing countries (Urban 2009), as they usually require data and computer performances which are not available. Presently, developing countries have to take decisions for supporting their future development (Girardin et al. 2010; Hanif 2017). However, without adapted decision aid tools, capable of covering the range of interests of low-income economies, the planning are likely to be (highly) misfit.

1.2 Focus of research and objective

In this regard, the main goal of the work presented here is to develop alternative methods for the assessment of air quality and energy strategies in the framework of developing countries. A key aspect is the simplification of intrinsic methods so that it facilitates the assessment by, for example, reducing

computational time, developing inexpensive methodologies to obtain data or simply providing analysis, benchmarking or indicators to support the choices.

Broadly, the study of an energy system (see Fig.1.1) starts by identifying the resources available in the region, with particular attention to ‘alternative’ resources whose potentials have not yet been fully valorised (e.g. biomass, sunlight or wind), and the services which should be satisfied. Conversion technologies can either use a resource to directly satisfy a service (e.g. the generation of electricity from biomass) or they can produce an intermediate product that needs to be further converted through another technology to satisfy a service (e.g. the production of a liquid fuel from biomass that can be converted into mobility by means of a defined type of vehicle). As technologies reliant on fossil fuels, greenhouse and harmful pollutants are emitted. In this perspective, most of the researches focus on exploring trade-offs between energy efficiency and emissions (Moret et al., 2015) but are more limited regarding the consequences on air pollution. Although actions to reduce fossil energy consumption may imply drops in emissions, the concentration levels of particular pollutants can rise; this is due to the complex nature of physical-chemical processes (Carnevale et al. 2014) leading to the formation of secondary pollutants (e.g. NO_x and O₃ which are part of the same chemical reactive process). Thus, energy strategies resulting optimal from an energy efficiency and economic point of view could be counter-productive to air quality.

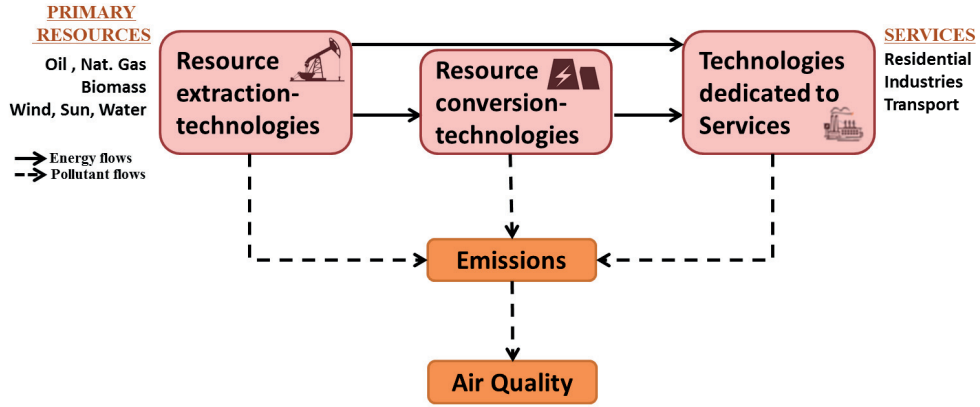


Figure 1.1: Overview of energy system and air quality links

Along this work, a first part of modelling support will be devoted to develop methods for the assessment of emissions and air quality impacts in the framework of developing countries. A second part contributes to a better understanding of the effects that energy planning decisions (i.e. choices among technologies and primary resources) have on the country development –energy security and sustainability. It provides general design features to progressively mutate a country energy mix into a more independent system.

The developed methods are implemented in Cuba. Cuba is an excellent test case to develop and apply such methods. On the one hand, the climate of the country presents good opportunities for renewable energy sources integration (e.g. solar and biomass) (Alonso et al. 2010; IAEA 2008; Panfil et al. 2017). On the other hand, the embargo imposed by the United States in 1960 has had dramatic consequences on the energy supply of the island since the help of Russia stopped in 1990 (Käkönen et al. 2014). It is now a political issue for the Cuban authorities to improve their energy independency. The government is therefore urged to take decisions to adapt the energy supply system. Unfortunately, past experience has shown that governmental decisions generally lack long term vision (cf. Suarez et al. 2012) and often consist in choosing technologies that require minimal investment costs, while neglecting use costs and indirect costs related to environmental impacts. Therefore, the development of innovative methods joined with the use of adapted modelling support in order to design air quality and energy strategies has a particular importance for the country. Existing studies (Belt 2010; Eras et al. 2017), even energy policies (see in Davis et al. 2017; Käkönen et al. 2014 Cuban Energy Revolution), have been focussing on residential, power and industrial sectors, so that preliminary information can be compiled from them. However, the share of transportation technologies and services, their level of emissions, pollution contributions and influences in the complete system is currently much less addressed. For this reason, this work also stresses on the transportation sector -data gathering, methods and analysis.

For each chapter, updated scientific approaches are selected and assessed. Their usability in the context of Cuba is examined, and methodologies adapted to the scarcity of data and computational resources are designed and validated.

1.3 Outline

A brief overview of the individual chapters is given below, along with the research contributions in this thesis.

Chapter 2 presents the results of an air pollution measurement campaign carried out in Havana, Cuba for evidencing transport-generated pollution. Previous works on measuring pollution (Martínez Varona et al. 2018; Molina Esquivel et al. 2011, 2017) have shown limitations, basically in sampling periods, to represent conditions where pollutant concentrations fluctuate, such as those generated by transport. We measured traffic volumes, meteorological parameters and pollutant concentration levels (i.e. PM10, SO2 and NO2) over shorter-time periods (1h); and showed how vehicular traffic influences concentration levels under specific meteorological conditions.

Chapter 3 deals with the task of determining vehicle emission factors, which is an important parameter for the development of reliable transport emission inventories and for evaluating the impact of technological changes in the sector. This estimation typically requires data from advanced (and expensive) monitoring systems. In the absence, simpler (lower-cost) measuring systems, as presented in Chapter 2, were used and a novel approach (Madrado et al. 2018a fundamented in Belalcazar et al. 2009) designed to accurately estimate vehicle emission factors. Additionally, we explore the potential of technological scenarios for the abatement of air pollution in Havana.

Chapter 4 deals with the gaps between global and regional emission inventories (Madrado et al. 2018b). Facing the scarcity of national inventories, the global ones must be used for air quality simulations. The implementation of benchmarking tools (Thunis et al. 2016a) and statistical analysis help the identification of differences between both inventories as well as the acquisition of insights in possible explanations. This enables to make decisions regarding the usability/reliability of emission inventories, as well as to indicate where efforts should be concentrated for improving less accurate data.

Chapter 5 presents an example study which sets up a Source-Receptor relationship over Cuba. This is a simplified approach (Clappier et al. 2015; Pisoni et al. 2017) which mimics the results of complex deterministic chemical transport models (CTM). It can provide substantial help on designing strategies in the context of developing countries since it is low-demanding in computational time. Its setting requires a previous statistical analysis of CTM responses for gaining insights into the behaviour and key relationships among pollutants, their emission precursors and the possible set of scenarios. Additionally, two different techniques are presented and implemented in order to improve the performance of the Cuban SRR.

Chapter 6 explores scenarios for the Cuban energy transition and proposes an outlook for policy framework. An overview of the Cuba's energy system and its short-term projection is presented. Thereafter, the challenges involved are discussed, which basically arise from the current reliance on fossil fuels and imports. General design features were identified to progressively mutate the Cuban energy mix into a more independent system. A set of indicators regarding criteria as energy security, sustainability and air quality are presented in order to facilitate the analysis of the mix.

Chapter 7 concludes this thesis discussing the prospects and remaining challenges on air quality and energy decision problems in low-income countries and gives potential future directions for research in these domains.

References

- Alonso, M. F., K. M. Longo, S. R. Freitas, R. Mello da Fonseca, V. Marécal, M. Pirre, and L. G. Klenner (2010). “An urban emissions inventory for South America and its application in numerical modeling of atmospheric chemical composition at local and regional scales”. In: *Atmospheric Environment* 44.39, pp. 5072–5083.
- Belalcazar, L. C., O. Fuhrer, M. D. Ho, E. Zarate, and A. Clappier (2009). “Estimation of road traffic emission factors from a long term tracer study”. In: *Atmospheric Environment* 43.36, pp. 5830–5837.
- Belt, J. A. B. (2010). *The Electric Power Sector in Cuba : Potential Ways to Increase Efficiency and Sustainability*. Tech. rep.
- Carnevale, C., G. Finzi, A. Pederzoli, E. Turrini, M. Volta, G. Guariso, R. Gianfreda, G. Maffei, E. Pisoni, P. Thunis, L. Markl-Hummel, N. Blond, A. Clappier, V. Dujardin, C. Weber, and G. Perron (2014). “Exploring trade-offs between air pollutants through an Integrated Assessment Model.” In: *The Science of the total environment* 481, pp. 7–16.
- Clappier, A., E. Pisoni, and P. Thunis (2015). “A new approach to design source–receptor relationships for air quality modelling”. In: *Environmental Modelling & Software* 74, pp. 66–74.
- Davis, C. and T. Piconne (2017). *Executive Summary of the expert seminar: "Sustainable development; the path to economic growth in Cuba*. Tech. rep. June 2017, pp. 1–8.
- Eras, J. C. and L. Hens (2017). “The Biomass Based Electricity Generation Potential of the Province of Cienfuegos, Cuba”. In: *Waste and Biomass Valorization* 8.6, pp. 2075–2085.
- Girardin, L., F. Marechal, M. Dubuis, N. Calame-Darbellay, and D. Favrat (2010). “EnerGis: A geographical information based system for the evaluation of integrated energy conversion systems in urban areas”. In: *Energy* 35.2, pp. 830–840.
- Hanif, I. (2017). “Economics-energy-environment nexus in Latin America and the Caribbean”. In: *Energy* 141, pp. 170–178.
- Höök, M. and X. Tang (2013). “Depletion of fossil fuels and anthropogenic climate change — A review”. In: *Energy Policy* 52, pp. 797–809.
- IAEA (2008). *Cuba: A country profile on sustainable energy development*. Tech. rep.
- Käkönen, M., H. Kaisti, and J. Luukkanen (2014). *Energy Revolution in Cuba : Pioneering for the Future* ? January.
- Madrazo, J. and A. Clappier (2018a). “Low-cost methodology to estimate vehicle emission factors”. In: *Atmospheric Pollution Research* 9.2, pp. 322–332.
- Madrazo, J., A. Clappier, L. Carlos, O. Cuesta, H. Contreras, and F. Golay (2018b). “Screening differences between a local inventory and the Emissions Database for Global Atmospheric Research (EDGAR)”. In: *Science of the Total Environment* 631-632, pp. 934–941.
- Martínez Varona, M., M. Vila Guzmán, A. Pérez Cabrera, and A. Fernández Arocha (2018). “Presencia de metales pesados en material particulado en aire . Estación de monitoreo INHEM , Centro Habana”. In: *Biblioteca Ecosolar Cd*, pp. 1–10.
- Molina Esquivel, E., G. P. Zayas, M. Martínez Varona, I. P. Hernández, R. G. Gala, F. A. Ugalde, and J. F. Maldonado (2011). “Comportamiento de las fracciones fina y gruesa de PM10 en la estación de monitoreo de calidad del aire en Centro Habana . Campaña 2006-2007”. In: *Higiene y sanidad ambiental* 820-826.11, pp. 820–826.
- Molina Esquivel, E., E. Meneses Ruiz, L. M. Turtós Carbonell, M. Guzmán Vila, D. Alonso García, M. Martínez Varona, C. González, and G. Pérez (2017). “Comportamiento de las fracciones PM10 y PM25 en tres zonas de La Habana (2012)”. In: *Higiene y sanidad ambiental* 17.4, pp. 1553–1564.
- Panfil, M., D. Whittle, and K. Sinverman-Roati (2017). *The Cuban Electric Grid. Lesson and recommendations for Cuba’s electric sector*. Tech. rep. Environmental Defense Fund (EDF).
- Pisoni, E., A. Clappier, B. Degraeuwe, and P. Thunis (2017). “Adding spatial flexibility to source-receptor relationships for air quality modeling”. In: *Environmental Modelling and Software* 90, pp. 68–77.
- Prather, M. J. and J. A. Logan (1994). “COMBUSTION’S IMPACT ON THE GLOBAL ATMOSPHERE”. In: pp. 1513–1527.
- Suarez, J., P. Anibal, R. Faxas, and O. Pérez (2012). “Energy , environment and development in Cuba”. In: *Renewable and Sustainable Energy Reviews* 16.5, pp. 2724–2731.
- Sutton, B. (2013). “The Effects of Technology in Society and Education”. Education and Human Development Master’s Theses. 192. The college at Brockport: State University of New York.

- Thunis, P., B. Degraeuwe, K. Cuvelier, M. Guevara, L. Tarrason, and A. Clappier (2016a). “A novel approach to screen and compare emission inventories”. In: *Air Quality, Atmosphere and Health* 9.4, pp. 325–333.
- Urban, F. (2009). *Sustainable energy for developing countries*.
- Vandaele, N. and W. Porter (2015). “Renewable Energy in Developing and Developed Nations : Outlooks to 2040”. In: 15.3, pp. 1–7.
- Vanderschuren, M., T. Lane, and W. Korver (2010). “Managing energy demand through transport policy: What can South Africa learn from Europe?” In: *Energy Policy* 38.2, pp. 826–831.
- WER (2016). *World Energy Resources*. Tech. rep. Energy Council World.
- WHO Regional Office for Europe (2016). *Health risk assessment of air pollution - general principles*. Tech. rep.
- Yeager, K., F. Dayo, B. Fisher, R. Fouquet, A. Gilau, and H.-H. Rogner (2012). “Chapter 6 - Energy and Economy”. In: *Global Energy Assessment - Toward a Sustainable Future*. Cambridge University Press, Cambridge, UK, New York, NY, USA, and the International Institute for Applied Systems Analysis, Laxenburg, Austria, pp. 385–422.

Chapter 2

Evidence of traffic-generated air pollution in Havana

In Havana, transport is blamed as a likely source of pollution issues. It is usually supported on arguments referring to a vehicle fleet mainly made of old cars (i.e. most models are 1950s U.S or 1980s Russian) with poor technical conditions. Most of the existing studies are based on measurements from passive samplers collected for 24 hours, which may not be representative of conditions where pollutant concentrations (particles or gases) fluctuate or are not homogeneous, such as transport-related pollution. Our goal in this article is to explore the transport-generated pollution by seeing short-time correlations between traffic flows, pollutant concentrations and meteorological parameters. To do that, statistical relationships among all variables were analysed. It reveals that PM₁₀, NO₂ and SO₂ concentration levels are influenced by vehicular traffic, mainly at low speed winds blowing perpendicular to the street axis. Furthermore, southeast and northeast wind forces drag pollution from sources other than traffic. These conclusions depend on the specific meteorological conditions of the Cuban summer season at the measurement area. A more complete analysis must be expected when more data are available.

Note: This chapter is the *preprint* version of an article accepted for publication in the journal Atmosphere. August 2018 (copyright owner as specified in the journal)

List of authors:
Jessie Madrazo, Alain Clappier, Osvaldo Cuesta, Luis Carlos Belalcazar, Yosvany Gonzalez, Javier Bolufé, Carlos Sosa, Ernesto Carrillo, Ricardo Manso, Yaniel Canciano, François Golay

2.1 Introduction

Nowadays most of the population is affected by the proximity of urban areas. According to a United Nations report (UN, 2014), 54% of the current world's population live in cities and an increase to 66% is expected by 2050. Unfortunately, the high concentration of human activities (i.e. heating, transport, nutrition, hygiene, health and other needs) in urban areas involves emissions from the consumption of fossil fuel energy sources, and therefore, large amounts of pollutants are released daily into the urban atmosphere. The impacts of this phenomenon on human health are well known; air pollution triggers stroke, cardiovascular and respiratory diseases, which are featured among the top 10 killers in the world (WHO 2017).

Latin American cities also increase deterioration of air quality (Bell et al. 2011; Hanif 2017; Román-collado et al. 2018). According to Gouveia et al. 2018, Mexico City, Santiago de Chile, Sao Paulo and Rio de Janeiro host nearly 43 million people and have a large children population exposed to levels of air pollution well above those recommended by the World Health Organization (WHO) guidelines. Statistical evaluations showed significant impacts of air pollution on respiratory mortality of children (Gouveia et al. 2018), and health risks markedly higher near sources of pollution. The pollution stemming from transport has been significant and growing (Faiz et al. 1995).

In Havana, epidemiologic studies pointed out associations of health hazards in proportion to ambient PM_{2.5}, PM₁₀, NO₂ and SO₂: Molina Esquivel et al. 1996 found out increased risk of lung cancer by predominant residence (during 40 years) in SO₂ and PM₁₀ high polluted areas; Molina Esquivel et al. 2011 reported high PM₁₀ concentration associated with morbidity and mortality rates; daily mean black smoke concentration increments of 20 μ g/m³ and SO₂ were associated with increments of 2.4% on children acute respiratory infections on October 1996 - March 1998 (Romero Placeres et al. 2004); and correlations between daily mean concentration measurements, meteorological parameters (i.e. temperature, wind speed and direction) and respiratory morbidity indicators showed respiratory diseases highly influenced by PM₁₀ values reaching WHO risk limits on October 1996 - September 1997 (Molina Esquivel et al. 2001a,c). Most of these studies recurrently point PM out as the pollutant with major impact on Havana citizen health, and blame the poor technical condition of vehicles for high levels of PM_{2.5} and PM₁₀ pollution (Molina Esquivel et al. 2015, 2017).

The blaming of transport as a likely source of Havana pollution issues is usually supported by arguments referring to a vehicle fleet mainly composed of old vehicles (most models are 1950s U.S or 1980s Russian) with low fuel efficiency and high emission systems (cf. Ding et al. 2004; Martinez Varona et al. 2011; Molina Esquivel et al. 2001b,c, 2011, 2017; Romero Placeres et al. 2004). Merely a few studies managed tools reporting evidences (cf. Martínez Varona et al. 2018; Molina Esquivel et al. 2015). Their measurements have been obtained from passive samplers collecting for 24 hours, then followed by laboratory chemical analysis: For PM, it used low volume gravimetric analytical methods, while SO₂ and NO₂ gases used to be measured by diffusive devices (spectrophotometric, absorption method) with a minimum sampling exposition of 24 hours. These setting techniques may not represent conditions where pollutant concentrations (particles or gases) fluctuate or are not homogeneous, such as transport-related pollution. Up to now, evidencing traffic-related air pollution is challenging since passive monitoring can only detect the concentration of ambient air pollution caused by various factors as a whole (Cuesta-Santos et al. 2012; Pan et al. 2016).

In this article, we explore the traffic-generated pollution in Havana by analysing shorter-time correlations between traffic flows, pollutant concentrations and meteorological parameters. We consider that it avoid the difficulty of evidencing out the traffic-related air pollution from the ambient air pollution. A measurement campaign was carried out in an important street of Havana where traffic volumes, some traffic-related pollutants (i.e. PM₁₀, SO₂ and NO₂) and meteorological parameters were rated with proper temporal resolution. Then, statistical relationships among all variables were analysed, it aims to show how strong pollutant measurements are influenced by traffic flows during specific meteorological episodes.

2.2 Measurement campaign

The measurement campaign took place in Simon Bolivar Street (cf. Fig.2.1), close to the centre of Havana over 10 days of summer 2015. Simon Bolivar is an urban corridor built before the beginning of 20th century in which important daily commuting movements take place. It is about 12 meters wide and east-west direction. The surrounding buildings of about 15 meters of average height classify the street as an urban canyon (ratio height/width = 1.25).



Figure 2.1: Measurement site and location of the street Simon Bolivar in Havana city (Red point). Adapted from Google earth map: (a) Street top view with the meteorological station – 1, the traffic video recording – 2 and pollutant measurement devices – 3. (b) Street elevation view

Diurnal traffic flow along the street was continuously recorded with a GoPro video camera placed on the north side of the street, about 200 meters away from the nearest traffic light intersection at a proper elevation to capture all traffic lanes (see Fig.2.1 for more details). Traffic volumes were manually counted after-campaign from the video recordings and aggregated into clearly identifiable categories: i.e. motorcycles, modern cars, median-age cars which are vehicles of Russian origin, old-age cars which are vehicles of American origin, high-capacity buses, low-capacity buses and trucks.

PM₁₀, NO₂ and SO₂ air pollution measurement devices were installed at 1.5 meters height. A Thermo-Scientific ADR 1500 was used for PM; it incorporates light scattering photometry, optical sensing and electronic processing techniques to measure precisely a selected size of suspended particles down to $1\mu\text{g}/\text{m}^3$. We set it to provide real-time PM₁₀ concentrations every minute from 7:00 to 19:00. The concentrations of pollutant gases were captured from chemical adsorption (i.e. a chemical reaction between the given gas and an adsorbing substance). CT-112 and CT-212 bearers (Volberg, 1982) of Tetrachloromercurate -TCM and Potassium iodide -KI substances were used as sorbent tubes sampling for one-hour step at accurately known flow rates of 1.0 and 0,25 L/min. They were measured by visible spectrophotometric techniques at 540nm and 575nm wavelength respectively. The mass of gases in each tube were determined from calibration curves, and then, concentration levels of SO₂ and NO₂ calculated by applying the correspondent conversion factors, i.e. 2.830 for SO₂ and 17.294 for NO₂. For both pollutant gases, the limits of detection (LOD) and quantitation (LOQ) were 0.1 and $500\mu\text{g}/\text{m}^3$ respectively. All pollutant measurements were stopped during rainfall episodes discarding events of substantial pollutant concentration decline for washing out particles and absorbing pollutants.

A meteorological station and radio wave transmission housing were placed on the roof of the nearest building. This edifice is the highest point (20 m high) within a 1km radius. The registered meteorological parameters were temperature, solar radiation, atmospheric pressure, humidity, wind speed and direction. All data were automatically stored in a computer at one-minute step resolution.

2.3 Result and discussion

2.3.1 Traffic flows

More than 15'000 vehicles were counted daily over the campaign period (see Fig.2.2). The fleet mainly comprises light-duty cars; i.e. modern age cars (27.6%); medium age cars (16.2%); old age cars (33.0%). Merely 8.9% is made of motorcycles and 14.3% of heavy-duty vehicles including buses and trucks. This composition is rather typical in Havana. In Fig. 2.2a, light duty categories, especially old vehicles, display the highest flow variability. In Fig. 2.2b, hourly fluctuations of traffic flow reflects wider but visibly distinguishable peaks; during the morning, traffic increases until 11:00 and then, subtly decreases prior to 17:00 when a new peak appears.

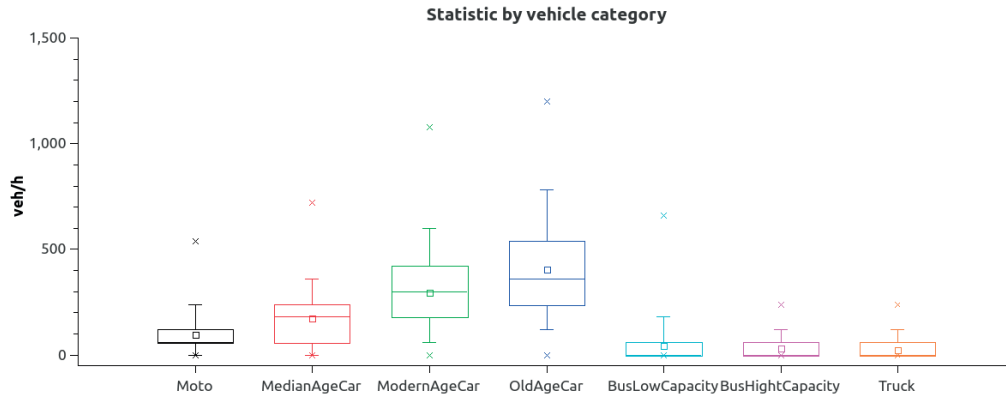
2.3.2 Concentration levels

Hourly diurnal PM10, NO2 and SO2 measurements are shown in Fig.2.3. The PM10 plot was obtained by averaging the one-minute step measurements over one-hour from all data gathered during the campaign. PM10 diurnal concentrations fluctuates close to the mean value ranging from 88 to 115 $\mu\text{g}/\text{m}^3$. NO2 and SO2 ranged from 72-138 $\mu\text{g}/\text{m}^3$ and 14-40 $\mu\text{g}/\text{m}^3$ respectively. These values are higher than mean reported on previous studies for PM10 (30-61 $\mu\text{g}/\text{m}^3$) and exceeded PM10 WHO-threshold (50 $\mu\text{g}/\text{m}^3$), NO2 (8-20 $\mu\text{g}/\text{m}^3$) and SO2 (1.5-24 $\mu\text{g}/\text{m}^3$) (Cruz Rodríguez et al. 2017; Martínez Varona et al. 2013; Molina Esquivel et al. 2001c). These differences could be due to the measurement settings (e.g. sampling height and duration) that differed from the referenced studies. In Fig.2.3, the PM10 fluctuations do not seem to follow completely the increase of the middle-morning traffic (cf. Fig.2.2b) but after 11:00, a better correspondence with traffic profile is observed. NO2 exhibits highest values on morning hours, before 9:00 the pollutant profile seems to be inversely correlated with traffic flows. However, after noontime, NO2 levels fall further and then rise around 15:00 in a modest accordance with the traffic trends. For SO2, the almost constant temporal profile (with exception of some observations going beyond limits) suggests that contributions from stable sources are more important than the vehicle ones. As things stand here, no inferences can be reached as to whether SO2 variations are interrelated with local traffic flows. Indeed, these pollution profiles are indicative; they alone do not provide conclusive insights about the traffic-generated pollution behaviour.

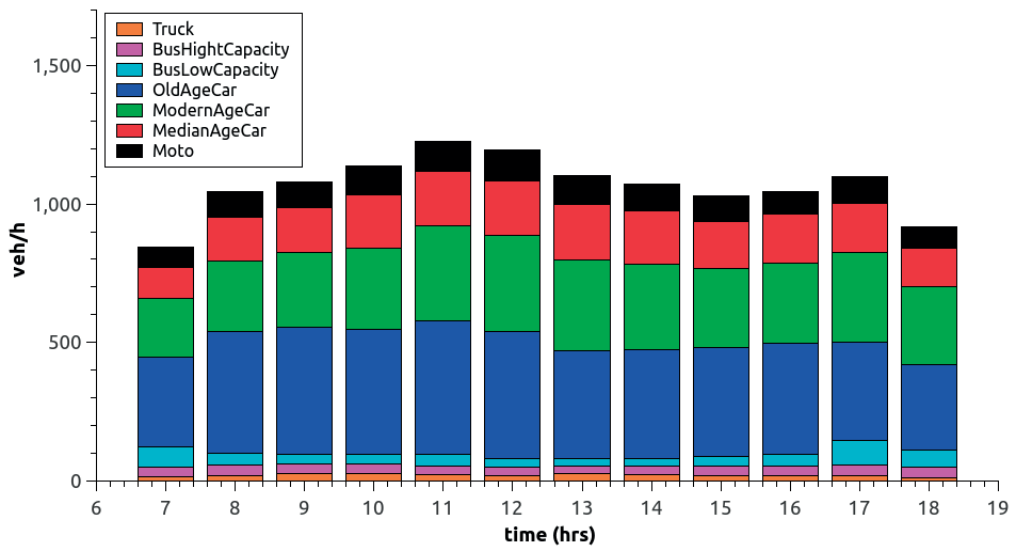
2.3.3 Meteorological parameters

Meteorological data analysis focused on wind speed and direction as high-influencing parameters of pollutant dispersion. Fig.2.4 shows wind roses drawing data at three-hour intervals (i.e. 7:00 -10:00; 10:00 – 13:00; 13:00 – 16:00 and 16:00 to 19:00). Two different regimes can be observed. During the first interval winds come from the south-southeast at a relatively low speed while on the other periods, wind mainly comes from north-northeast at highest speeds. These observations agree with the theory of “Sea-Land Breezes” (Simpson et al. 1977). A delayed offshore breeze can be observed on the first wind rose: At previous night, the land loses heat quickly after the sun sets down and the air above cools too. Water has much higher thermal inertia (i.e. very little day/night temperature change) so the relatively warm air over the sea causes low pressure. Over the land, high surface pressures will form because of the colder air. To compensate, the wind blows from the higher pressure over the land to lower pressure over the sea causing a “land breeze” (Ding et al. 2004). During the middle morning, wind starts the reverse phenomenon on so-called “sea breeze”: The sun heats up both the sea surface and the land. However, water heats up much more slowly than land and so the air above the land will be warmer compared to the air over the sea. This causes a wind blowing from the sea inland.

It is believed that land-sea breezes generate specific pollutant motion regimes inside the street canyon and therefore, influence traffic contributions: According to Berkowicz 1998; Berkowicz et al. 1997 and Kastner-Klein et al. 2003, wind flows at street level and the pollutant recirculation features depend on roof level wind flows. The street level wind inside the recirculation zone forms an angle with the street axis, which is equal to that of wind direction at roof level with respect to the street axis but with transverse component mirror reflected. Outside the recirculation zone, the wind direction is the same as at roof level. As well, the variability of wind directions across the measurement site may explain the existence of different air pollution behaviours.



(a) box plots of vehicle categories



(b) hourly flows

Figure 2.2: Traffic data

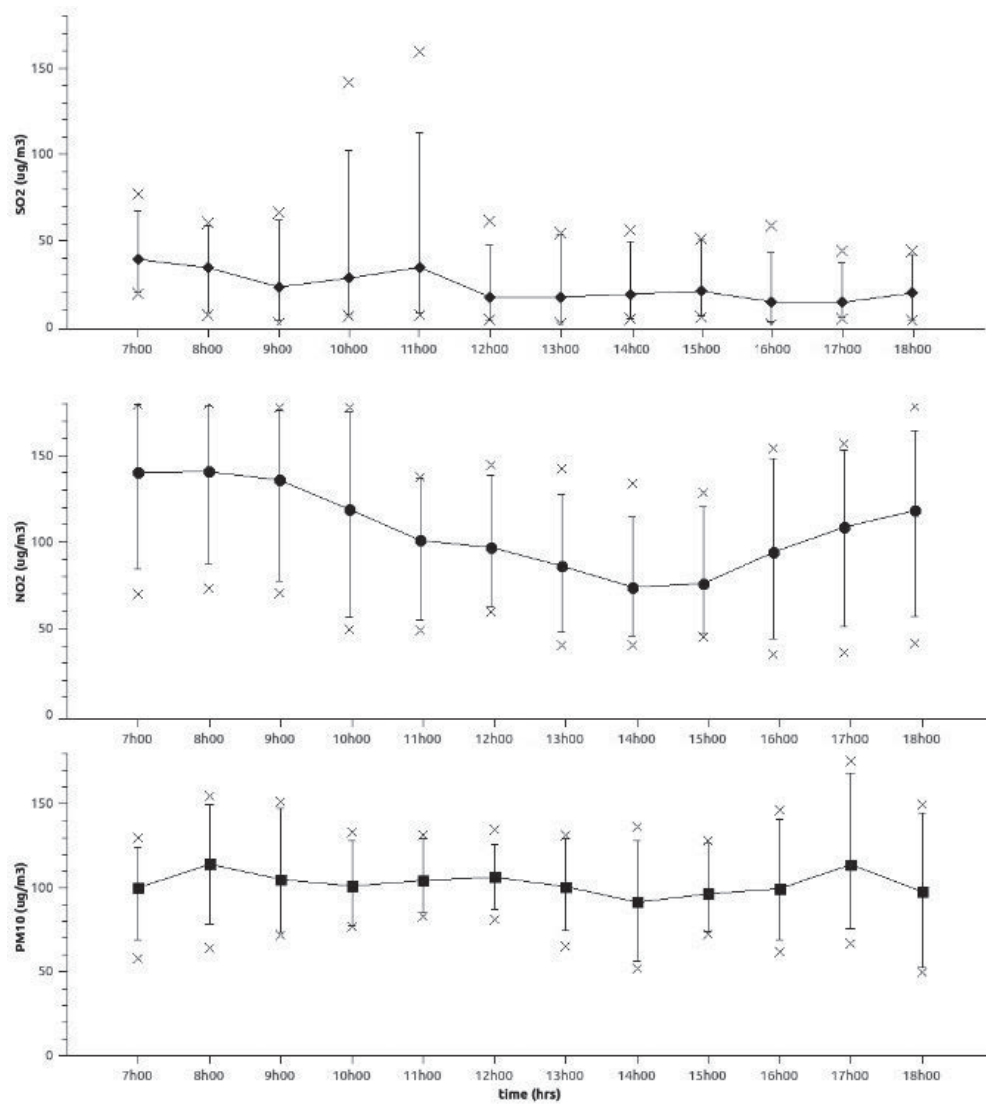
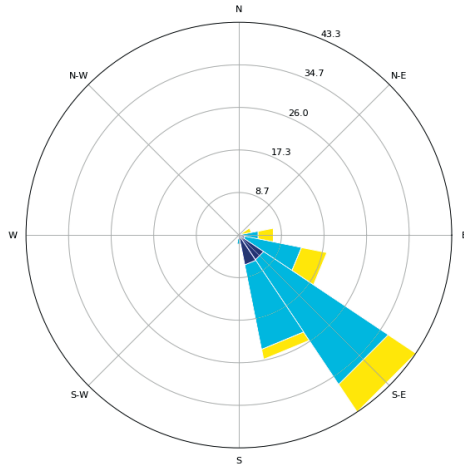
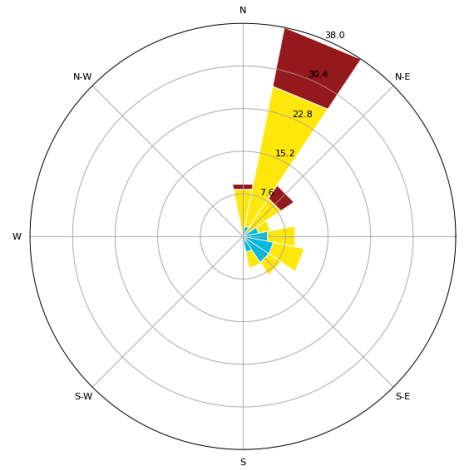


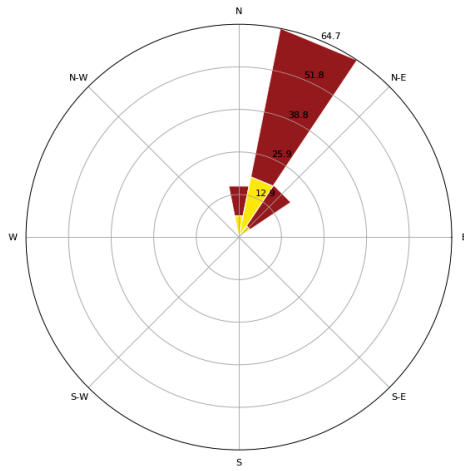
Figure 2.3: Average diurnal variations of PM₁₀, NO₂ and SO₂



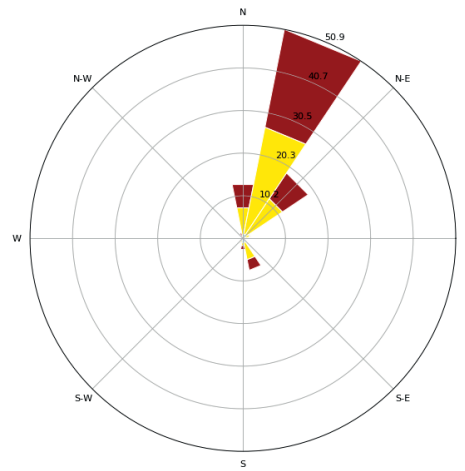
(a) 7h00-10h00



(b) 10h00-13h00



(c) 13h00-16h00



(d) 16h00-19h00

Figure 2.4: Wind roses: average diurnal variation of wind forces

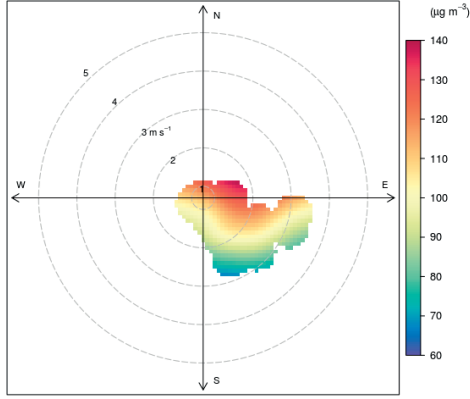
2.3.4 Statistical relationships between traffic flows, pollutant concentration and wind forces

As it was aforementioned, the wind flow regimes are expected to influence pollutant concentration levels since they change the features of pollutant motion and limit the scope of surrounding pollution sources. In Fig.2.5, bivariate polar plots allow for gaining an idea of sources-generated pollution according to prevalent wind flow profiles -i.e. land (7:00-10:00) and sea (13:00-19:00) breezes. During the morning, PM10 tends to be highest ($140\mu\text{g}/\text{m}^3$) under low and perpendicular (with respect to the street axis) wind conditions, pointing to ground level source contributions, such as traffic. NO2 does not vary with the variation of wind speeds, suggesting also traffic contributions. However, it tends to increase (from 100 to $200\mu\text{g}/\text{m}^3$) as wind direction changes from south to east, becoming more significant the contributions from non-traffic sources at high-speed wind. SO2 decreases (from 45 to $20\mu\text{g}/\text{m}^3$) as wind directions change from south to east and remains almost constant under wind speed fluctuations. It points out the influence of ground-level sources for wind blowing in perpendicular to the street axis. During the afternoon, pollutants variations were less pronounced compared to the morning. PM10 subtly increases (from 80 to $100\mu\text{g}/\text{m}^3$) as wind direction goes from southeast to northeast. SO2 tends to peak under high wind speed conditions at northeast; pointing to the existence of important sources other than traffic. NO2 is less influenced by wind conditions.

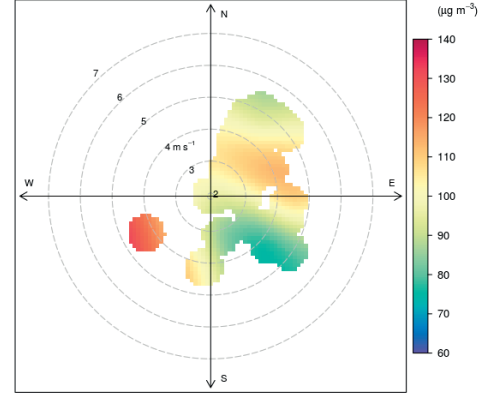
To stand out better the strength of traffic contributions, statically significant correlations among pollutants and flows of specific vehicle categories, including several alternative aggregation schemes, were set. Best results were found by grouping vehicles of similar emission profiles (i.e. buses and trucks were aggregated on “heavy category”, medium and old age light-duty vehicles were aggregated on “MedOld category”, motorcycles and modern light-duty vehicles remain alone categories), see table 2.1. During the morning rises in PM10 are coupled with rises in traffic indicating that PM10 concentration levels were likely induced by vehicle emissions. Moderate are the correlation among SO2 and vehicle emissions, they are mostly influenced by heavy vehicles. During the afternoon, all pollutants correlate acceptably. PM10 and NO2 are highly influenced by heavy vehicles, while SO2 is coupled with changes of old-medium age vehicles. The statistically significant relationships for variables in table 2.1 indicate that the three pollutants do account for traffic contributions which accentuate under specific meteorological conditions.

Table 2.1: Significant correlations (i.e. p-value < 0.05) among pollutants and vehicular flow: A significance level of 0.05 indicates that the risk of concluding that a correlation exists -i.e. changes in vehicle categories are related to changes in pollutant concentration levels- is 5% levels.

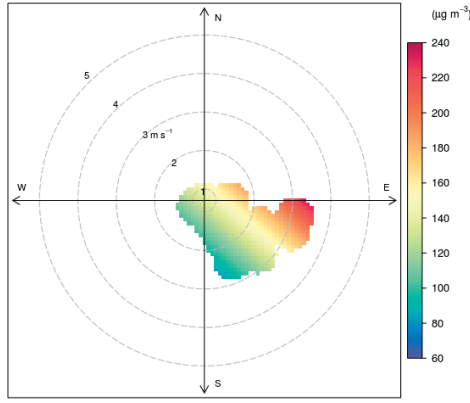
Vehicle categories	Morning 7h00-10h00			Afternoon 13h00-19h00		
	PM_{10}	NO_2	SO_2	PM_{10}	NO_2	SO_2
Motorcycles	0.68	-	-	0.42	0.49	0.36
<i>p-value</i>	7e-04	-	-	6e-03	1e-02	2e-02
Modern-Veh	0.74	-	0.45	0.41	0.47	0.39
<i>p-value</i>	3e-05	-	4e-02	8e-03	2e-02	1e-02
MedOld-Veh	0.78	-	-	-	-	0.54
<i>p-value</i>	1e-04	-	-	-	-	4e-02
Heavy	0.63	-	0.53	0.65	0.63	-
<i>p-value</i>	2e-03	-	1e-02	9e-04	7e-04	-
Total-Veh	0.83	-	-	0.50	0.53	0.39
<i>p-value</i>	7e-06	-	-	1e-02	3e-02	1e-02



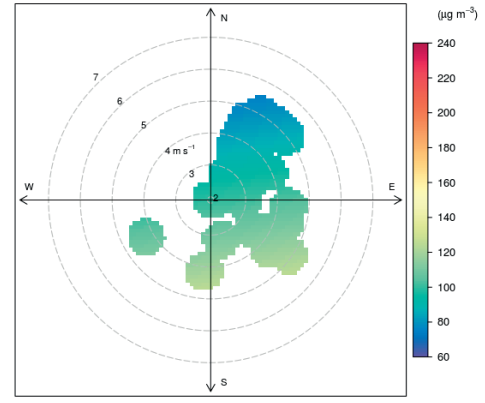
(a) PPM 7h00-10h00



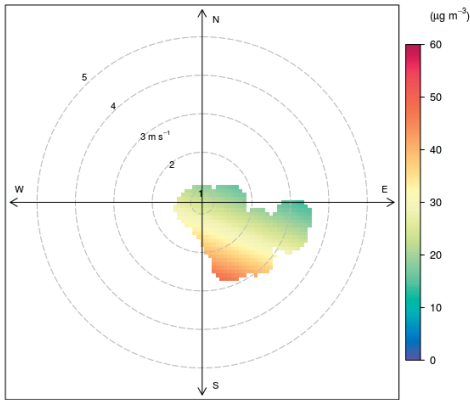
(b) PPM 13h00-19h00



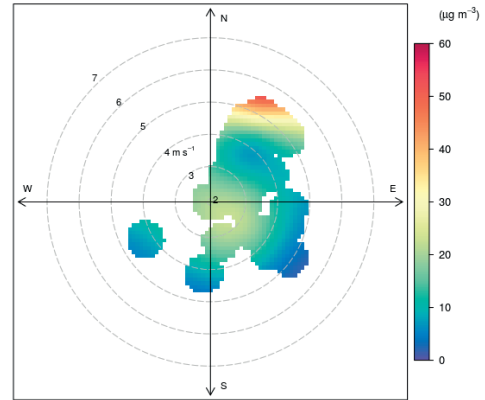
(c) NO2 7h00-10h00



(d) NO2 13h00-19h00



(e) SO2 7h00-10h00



(f) SO2 13h00-19h00

Figure 2.5: Bivariate polar plots

2.4 Conclusions

Aiming at evidencing traffic-generated air pollution in Havana, statistical tools were applied on a set of pollutant, traffic and meteorological measurements (one-hour samples). The statistic significant relationships for hourly traffic and pollutant measurements indicate that PM10, NO2 and SO2 pollution account for traffic contributions. The morning PM10 pollution is mostly influenced by traffic. PM10, NO2 and SO2 traffic-generated pollution increase at low wind speeds blowing perpendicular to the street axis. In addition to traffic, the emissions from other sources seem to be dragged by winds from southeast (morning) and northeast (afternoon) inducing variations, mainly in NO2 and SO2 pollution levels. These conclusions dependent on the specific wind conditions of the Cuban summer season at the measurement area. A more complete analysis is be expected when more data are available for other seasons.

References

- Bell, M. L., L. A. Cifuentes, D. L. Davis, E. Cushing, A. Gusman, and N. Gouveia (2011). "Environmental health indicators and a case study of air pollution in Latin American cities". In: *Environmental Research* 111.1, pp. 57–66.
- Berkowicz, R. (1998). "Street Scale Models." In: *Environmental Pollution*. Ed. by J Fenger, O. Hertel, and F. Palmgren. Springer, Dordrecht. Chap. Urban Air.
- Berkowicz, R. and M. Denmark (1997). *Modelling traffic pollution in streets*. Ministry of Environment and Energy, National Environmental Research Institute.
- Cruz Rodríguez, L. and J. A. Valdivia Pérez (2017). "Cuantificación de la concentración de Zn, Cu, Pb y Cd en partículas menores de 10 m procedentes del aerosol atmosférico. Clasificación de las fuentes contaminantes en la zona de estudio". In: *Revista Killkana Técnica* 1.3, pp. 17–24.
- Cuesta-Santos, O., M. Fonseca, R. Manrique, and E. Carrillo (2012). "Evaluación de la calidad del aire en ciudades de cuba". In: *Memorias de la Convención Internacional Trópico 2012, La Habana, 14 – 18 de Mayo*. ISBN 978-959-282-079-1.
- Ding, A., T. Wang, M. Zhao, T. Wang, and Z. Li (2004). "Simulation of sea-land breezes and a discussion of their implications on the transport of air pollution during a multi-day ozone episode in the Pearl River Delta of China". In: *Atmospheric Research* 38, pp. 6737–6750.
- Faiz, A., S. Gautama, and E. Burkib (1995). "Air pollution from motor vehicles : issues and options for Latin American countries". In: *The Science of the total environment* 169, pp. 303–310.
- Gouveia, N. and W. Leite (2018). "Effects of air pollution on infant and children respiratory mortality in four large Latin-American cities *". In: *Environmental Pollution* 232.
- Hanif, I. (2017). "Economics-energy-environment nexus in Latin America and the Caribbean". In: *Energy* 141, pp. 170–178.
- Kastner-Klein, P., E. Fedorovich, M. Ketzel, R. Berkowicz, and R. Britter (2003). "The modelling of turbulence from traffic in urban dispersion models - Part II: Evaluation against laboratory and full-scale concentration measurements in street canyons". In: *Environmental Fluid Mechanics* 3.2, pp. 145–172.
- Martínez Varona, M., G. Maldonado, E. Molina Esquivel, and A. Fernández (2011). "Concentraciones diarias de contaminantes del aire en La Habana (Cuba)". In: *Higiene y sanidad ambiental* 792, pp. 786–792.
- Martínez Varona, M., E. Molina Esquivel, G. Maldonado Cantillo, M. Guzmán Vila, and D. Alonso García (2013). "Comportamiento de partículas menores de 10 micras mediante dos equipos de monitoreo". In: *Higiene y sanidad ambiental* 13.4, pp. 1060–1065.
- Martínez Varona, M., M. Vila Guzmán, A. Pérez Cabrera, and A. Fernández Arocha (2018). "Presencia de metales pesados en material particulado en aire . Estación de monitoreo INHEM , Centro Habana". In: *Biblioteca Ecosolar Cd*, pp. 1–10.
- Molina Esquivel, E., C. Barceló Pérez, L. A. Bonito Lara, and C. del Puerto Quintana (1996). "Factores de riesgo de cáncer pulmonar en Ciudad de La Habana". In: *Revista Cubana de Higiene y Epidemiología*, pp. 1–8.
- Molina Esquivel, E., L. A. B. Colás, V. P. Díaz, L. Cuellar, and D. Rodríguez (2001a). "Contaminacion Atmosferica y Asma Bronquial". In: *Revista Cubana de Higiene y Epidemiologia* 39(1), pp. 5–15.
- Molina Esquivel, E., L. A. B. Colás, V. P. Díaz, L. Cuellar, and D. Rodríguez (2001b). "Contaminación atmosférica y prevalencia de asma en Centro Habana". In: *Revista Cubana de Higiene y Epidemiologia* 39.1, pp. 5–15.
- Molina Esquivel, E., L. A. Browns Colás, V. Prieto Díaz, M. Bonet Gordea, and L. Cuéllar Luna (2001c). "Crisis de asma y enfermedades respiratorias agudas. Contaminantes atmosféricos y variables meteorológicas en Centro Habana". In: *Revista Cubana Med Gen Integr* 17.1, pp. 10–20.
- Molina Esquivel, E., G. P. Zayas, M. Martínez Varona, I. P. Hernández, R. G. Gala, F. A. Ugalde, and J. F. Maldonado (2011). "Comportamiento de las fracciones fina y gruesa de PM10 en la estación de monitoreo de calidad del aire en Centro Habana . Campaña 2006-2007". In: *Higiene y sanidad ambiental* 820-826.11, pp. 820–826.
- Molina Esquivel, E., M. Martínez Varona, L. M. Turtós Carbonell, E. Meneses Ruiz, S. García Dos, L. F. Cuesta Zedeño, and S. Pire Rivas (2015). "Carbono elemental y orgánico en PM25 y PM10 de zonas urbanas de La Habana (Cuba)". In: *Higiene y sanidad ambiental* 15(3), pp. 1343–1349.
- Molina Esquivel, E., E. Meneses Ruiz, L. M. Turtós Carbonell, M. Guzmán Vila, D. Alonso García, M. Martínez Varona, C. González, and G. Pérez (2017). "Comportamiento de las fracciones PM10 y PM25 en tres zonas de La Habana (2012)". In: *Higiene y sanidad ambiental* 17.4, pp. 1553–1564.

- Pan, L., E. Yao, and Y. Yang (2016). “Impact analysis of traffic-related air pollution based on real-time traffic and basic meteorological information”. In: *Journal of Environmental Management* 183, pp. 510–520.
- Román-collado, R. and A. V. Morales-carrión (2018). “Towards a sustainable growth in Latin America : A multiregional spatial decomposition analysis of the driving forces behind CO₂ emissions changes”. In: *Energy Policy* 115.November 2017, pp. 273–280.
- Romero Placeres, M., M. Lacasaña Navarro, M. Téllez Rojo Solís, A. V. M., and I Romieu (2004). “Contaminación atmosférica, asma bronquial e infecciones respiratorias agudas en menores de edad de La Habana”. In: *Revista Cubana de Higiene y Epidemiología*, pp. 222–223.
- Simpson, J. E., D. A. Mansfield, and J. R. Milford (1977). “Inland penetration of seabreeze fronts”. In: *Quarterly Journ Royal Meteorological Sociaty*.
- WHO (2017). *Air pollution*.

Chapter 3

Low-cost methodology to estimate vehicle emission factors

Road traffic emission factors (EFs) are important parameters in managing air quality. Estimation typically requires data from advanced (and expensive) monitoring systems which remain unavailable in some regions (e.g. in developing countries). In this context, the use of simpler (lower-cost) systems may be more appropriate, but it is essential to guarantee the robustness of EF estimations. This article describes a methodology designed to estimate vehicle EFs from street canyon measurements of traffic fluxes, wind speed and direction, and pollutant concentration levels by using low-cost devices, all samples at a one-minute interval. We use different moving window filters (time periods) to average the raw measurements. Applying standard multiple linear regressions (MLR) and principal component regressions (PCR), we show that there is an optimal smoothing level that best relates traffic episodes and pollutant concentration measurements. An application for PM₁₀'s EFs on four vehicle categories of Havana's fleet shows a preference for PCR over MLR techniques since it reduced the collinearity effects that appear when traffic fluxes are naturally correlated between vehicle categories. The best regression fits ($R > 0.5$ and standard deviation of estimates $< 15\%$) were obtained by averaging data between 40' and 60'; within the boundaries of 95% confidence interval motorcycles have an $EF = 111.1 \pm 2.7$ mg km⁻¹ veh⁻¹; modern, light vehicles have an $EF = 90.6 \pm 11.2$ mg km⁻¹ veh⁻¹; old, light vehicles have an $EF = 125.4 \pm 18.5$ mg km⁻¹ veh⁻¹ and heavy vehicles have an $EF = 415.1 \pm 31.2$ mg km⁻¹ veh⁻¹. We showed that upgrading old light vehicles (i.e. reducing their emission level at least 30%) is a promising scenario for reducing PM₁₀ air pollution in Havana by between 10% and 17%.

Note: This chapter is the accepted manuscript (*preprint*) version of an article published in the journal Atmospheric Pollution Research on March 2018.

Scientific paper: Madrazo, J., Clappier, A., 2018. Low-cost methodology to estimate vehicle emission factors. Atmos. Pollut. Res. 9, 322–332.

Please see the final published version: <https://doi.org/10.1016/j.apr.2017.10.006>. Cited as Madrazo & Clappier 2018

3.1 Introduction

Vehicle traffic is an important contributor to air pollution in many urban areas (Huang et al. 2016; Wang et al. 2017). Sound policy decisions on the control and management of traffic-related pollution depend on a reliable emission inventory and the emission characteristics of the vehicle fleet (Smit et al. 2017). Among others, one important parameter to be evaluated is the emission factor (EF) (Zarate et al. 2007); it characterizes the amount of pollutant emitted per mass of fuel consumed (fuel-based), per distance driven (task-based) or per energy used (task-based) (Brimblecombe et al. 2015). The EF can differ from one country to another depending on vehicle maintenance, driving patterns and fuel brands. More specifically, in developing countries, traffic flow is heterogeneous in nature (Jaikumar et al. 2017), and in most cases, exhaust emission standards fail to represent the real-world emissions from vehicles in these regions.

Different methods have been developed to estimate vehicle EFs. They typically require data from advanced monitoring systems (cf. Amato et al. 2016; Borrego et al. 2016; Ferm et al. 2015; Keuken et al. 2016; Pang et al. 2014); chassis dynamometer tests (Jung et al. 2017; Li et al. 2013; Nakashima et al. 2017; Pang et al. 2014) and on-road methods (Ait-Helal et al. 2015; Kam et al. 2012) are useful for providing accurate information about individual vehicle contributions. Both are often costly and time-consuming, and the number of testable vehicles (i.e., sample size) is limited. Approaches using measurements from road tunnels (Brimblecombe et al. 2015; Riccio et al. 2016; Zhang et al. 2015) and street canyons (Belalcazar et al. 2010; Klose et al. 2009; Vardoulakis et al. 2003) consider the contribution of the fleet in “real-world” driving conditions. Their basic principles are based on a statistical analysis of traffic and concentration episodes under specific pollutant dispersion rates.

In road tunnel studies, airflow conditions are well defined (i.e., by active mechanical ventilation systems or piston effects). Instead, problems might arise from the long pollutant residence time since receptor devices capture both the concentrations generated by passing vehicles and those retained, which could result in an overestimation of emission rates (Gertler et al. 1991). Additionally, if the instruments become saturated, they may not effectively capture the concentration peaks, and consequently, the EF results are underestimated (Brimblecombe et al. 2015). In street canyon studies, even if natural ventilation is reduced by the presence of buildings, the rate at which the street exchanges air with the atmosphere is greater, and the pollutant residence time is shorter compared to road tunnel studies, especially for the larger-sized particles that are greatly affected by gravity. In addition, wind flows are primarily controlled by micro-meteorological effects of urban geometry and dispersion phenomena, such as the mechanical turbulence induced by moving vehicles, and the atmospheric stability conditions are widely studied (e.g., Berkowicz et al. 1997; Huang et al. 2016; Kakosimos et al. 2010; Kastner-Klein et al. 2003; Ketzel et al. 2000; Moradpour et al. 2017; Sokhi et al. 2008).

In this work, we use basic assumptions previously documented in other street canyon studies to estimate EFs. Testing different moving window filters (time periods) to average the raw measurements, we show the optimal smoothing levels that best relate traffic episodes and pollutant concentration measurements. To do that, we collected traffic counts and average concentration measurements by one-minute time steps. The pollutant dispersion is also quantified at one-minute steps by modelling the changes (low-cost estimation) on meteorological and traffic constraints.

In section 3.2, we start with a brief description of the measurement campaign: data collection and processing. In section 3.3, we explain the methodology, detailing the most important assumptions for estimating EFs. The results of a case study are presented in section 3.4 (EFs of particulate matter -PM10- for Havana’s vehicle fleet); then, we assess the performances of the methodology used for different averaging times. Finally, in section 3.5, we discuss the effect of changing PM10 EF values under several abatement scenarios.

3.2 Sampling location and data

For this study, we examine data obtained over a 10-days measurement campaign in Havana in summer 2015. Data collection occurred in an urban canyon (see Fig.3.1 Simon Bolivar Street with west-east direction). Data include traffic volume, wind speed and direction, and PM10 concentration levels.

Traffic was recorded on videotapes and then manually counted at a temporal resolution of 1’. The fleet of vehicles was classified into four clearly identifiable categories, i.e., motorcycles; modern light-duty cars (post-1980s); old light-duty cars (pre-1980s and of Russian or American origin); and heavy vehicles,



Figure 3.1: Data collection site (Simon Bolivar Street). 1: Thermo-Scientific ADR 1500 profiler and traffic video recording. 2: AIRDAM anemometer. Adapted from Google Earth.

including buses and trucks. No visual differentiation could be made in terms of technology or fuel system injection since many cars have been modernized with new parts (e.g., engines and disk brakes).

Wind speed and direction data were automatically registered from an IRDAM – WST7000C anemometer placed on the roof of the highest building (at a height of 13.6 m) within a 1-km radius; any other accurate meteorological station could be used. PM10 concentrations were recorded using a Thermo-Scientific ADR 1500 profiler (a device based on a highly sensitive light-scattering photometer technique) installed at a height of 1.5 metres on the southern side of the street canyon.

3.3 Methods

3.3.1 Basic assumptions

Due to the short distances between sources and receptors inside street canyons, only very fast chemical reactions significantly influence the measured concentrations (Berkowicz et al. 1997). This enables us to ignore the chemical transformations of slowly reacting gases. Therefore, a linear relationship between released emissions and measured concentrations is valid (Palmgren et al. 1999), leading to the following equation:

$$C^t = D^t E^t + C_0^t \quad (3.1)$$

where C^t (g m⁻³) and E^t (g m⁻¹ s⁻¹) are the concentration and the traffic-related emissions at a time “t”, respectively. The linearity between C^t and E^t is defined by two parameters: C_0^t (g m⁻³), which corresponds to the concentration level at the receptor location when emissions are from sources other than street traffic, and D^t (s m⁻²), which is a dilution factor that quantifies the dispersion resulting from turbulence induced either by atmosphere flows or vehicle movements. The traffic-related emission is a summation of all contributions of individual vehicle activities. Considering vehicles in a specific category “i” (e.g., light vehicles, motorcycles, heavy vehicles), traffic-related emission results in the following:

$$E^t = \sum_i E_i^t = \sum_i N_i^t e_i \quad (3.2)$$

Where E_i^t are the emissions released by all the vehicles of category “i” at time “t”; N_i^t is the flux of vehicles belonging to category “i” in (veh-km h-1); and e_i is the emission factor of the vehicles of category “i” (in g km-1 veh-1), which quantifies the amount of pollutant released by one vehicle travelling for 1-km.

Combining equations 3.1 and 3.2, we obtain the following:

$$C^t = \sum_i D^t N_i^t e_i + C_0^t \quad (3.3)$$

Assuming that e_i is constant with the vehicle category, C_0^t and $D^t N_i^t$ data are expected to be multi-linearly related at each time “t”. Note that N_i^t and C^t are measured data (i.e., vehicles fluxes and concentrations), while D^t depends on elements that induce turbulence in the street canyon, such as meteorology or vehicle movements, and these elements can be measured (see Sec.3.3.2). Only e_i and C_0^t remain as unknown values.

3.3.2 Dilution factor

Previous studies have used predictions in wind tunnel simulations (Bruce et al. 2005; Huang et al. 2016) or have relied on gaseous tracers (Belalcazar et al. 2009; Zhang et al. 2015) as a measure of pollutant dilution. Our approach calculates exhaust emission dilution rates through modelling. Indeed, a plethora of dispersion models specially developed for, or simply used in, street canyon applications are available. There are no clear-cut distinctions between different categories, and models might be classified into groups according to their physical or mathematical principles (e.g., reduced-scale, box, Gaussian, CFD) and their level of complexity (e.g., screening, semi-empirical, numerical) (Vardoulakis et al. 2003). Accurate predictions are, in most cases, a function of meteorology, street geometry, receptor location and traffic volume.

In this work, we used the semi-empirical Operational Street Pollution Model—OSPM (Berkowicz et al. 1997). The model choice was selected based on several aspects: it is robust and fast, contains all the essential parameters and dependencies observed in field data, and has been extensively validated for various street canyon types (Kakosimos et al. 2010). In addition, it has been previously used for similar purposes (e.g., Ketzel et al. 2003; Klose et al. 2009). Concentrations of exhaust gases are calculated using a combination of a plume model for the direct impact of vehicle-emitted pollutants and a box model that enables computation of the additional impacts due to pollutants recirculated within the street by the vortex flow (i.e. traffic-induced turbulence). For more details on the physical principles behind the modelling concept, the reader is referred to the original papers, e.g., Berkowicz 2000; Berkowicz et al. 1997; Kakosimos et al. 2010.

According to Klose et al. 2009, pollutant dilution can be effectively simulated as a function of the turbulence induced by large-scale wind and vehicle motion. Parameters, such as fleet composition, street geometry, temperature and roof-level wind speed and direction, need to be defined implicitly for computing traffic-related emissions and concentrations. We performed simulations that use the experimental street canyon geometry and the in situ receptor location. Data provided by traffic counting (i.e., the composition and flux of vehicles) and by roof-level wind measurements were summarized, and their ranges were split into intervals (see table 3.1). Then, for every possible combination of the predefined step-values (i.e. for the percent of light-duty vehicles, wind speed and direction), the slope of the linear regression plot of emissions vs. concentrations (i.e. resulting from the varying total number of vehicles) were presented as the corresponding dilution factor (rf. eq.3.1).

Note that fleet composition settings differentiate only light- and heavy-duty categories; an increase in the percent of light-duty vehicles “ α ” (i.e. sum of motorcycles, modern and old cars) forces the fraction of heavy-duty vehicles to decrease proportionally. A three-dimensional array of wind speed, wind direction and proportion of light-duty vehicles is provided, and then we estimate dilution factors as a dependency of these parameters:

$$D = f(\alpha, wd, ws) \quad (3.4)$$

Hence, a dilution factor could be easily interpolated if turbulence is induced by parameters within the ranges shown in table 3.1.

Table 3.1: Parameter settings used in dispersion model (OSPM)

Parameters		Range	Interv.Step
Vehicle flux	total number of vehicles	0-2000 veh h^{-1}	200 veh h^{-1}
	% light-duty vehicles (α)	0-100%	10%
Wind flows	wind speed (ws)	0-6.3 m s^{-1}	0.8 m s^{-1}
	wind direction (wd)	0°-359°	15°

3.3.3 Time averaging

The literature suggests a wide spectrum of averaging times, e.g., 5, 15, 30 or 60 minutes (Belalcazar et al. 2009; Klose et al. 2009; Rey deCastro et al. 2008; Shunxi et al. 2009), to assess the relationship between the raw data of pollutant emissions and concentrations. Most time frames reflect the temporal resolution of the data, but in reality, phenomena of chemical and mainly physical origins within the canyon could influence them. In this study, we utilized data sampled at one-minute intervals. Based on eq. 3.3, we aim to identify an averaging time that best relates “ C^t ” and “ $D^t N_i^t$ ” data to maximize the robustness of the emission factor “ e_i ” estimations. Over a given time frame, emissions and concentrations are averaged as follows:

$$\langle C^t \rangle = \frac{1}{n_t} \sum_{t=1}^{n_t} C^t \quad (3.5)$$

$$\langle E^t \rangle = \sum_i \left\{ \frac{1}{n_t} \sum_{t=1}^{n_t} (D^t N_i^t) e_i \right\} = \sum_i \langle D^t N_i^t \rangle e_i \quad (3.6)$$

where n_t is the number of one-minute steps involved in computing the average.

Combining eq. 3.5 and 3.6, we generalize the multilinear relationship between emissions and concentrations (rf. eq.3.3):

$$\langle C^t \rangle = \sum_i \langle D^t N_i^t \rangle e_i + C_0 \quad (3.7)$$

Then, e_i can be approximated using the coefficients of the multiple linear regression (MLR) between $\langle C^t \rangle$ and $\langle D^t N_i^t \rangle$ data.

C_0 is interpreted as the intercept of the linear fit, so it is expected to be constant over the averaging time. Considering that it is a statistical value that characterizes the concentration measured at the receptor location when there is no street traffic, i.e., a background on the bottom, it likely varies with the temporal variation of external contributions. Nevertheless, their temporal variability is expected -and therefore assumed- not to be statistically significant in comparison with the contributions of vehicles on the street.

3.4 Results and discussion

The methodology described in the previous section was implemented to estimate PM10 EFs of the vehicle fleet in Havana. Different averaging times, “ n_t ”, ranging from 5’ to 90’, were tested.

The quality of the regression fit is assessed by two criteria: (i) the global correlation coefficient, “R”, which is a measure of how well the EFs can be predicted using the MLR model from eq.3.7. The closer this value is to 1, the better the multilinear fit is. (ii) The standard deviation, “ σ ”, of each estimate, which measures how precisely the model estimates the unknown coefficient value. The smaller these values, the more precise the regression estimates (e_i -coefficients and $-C_0$ intercept).

3.4.1 Multiple linear regression

Fig.3.2a shows the correlation coefficient “R” at different averaging times, which range from 5’ to 90’. In Fig 3.2b-f, the black points denote the coefficients (e_i as PM10 EFs in mg m⁻¹ veh⁻¹ by vehicle category) and the intercept (C_0 as PM10 in mg m⁻³) from the MLR model. The red and green lines follow the standard deviations “ σ ” of these estimates.

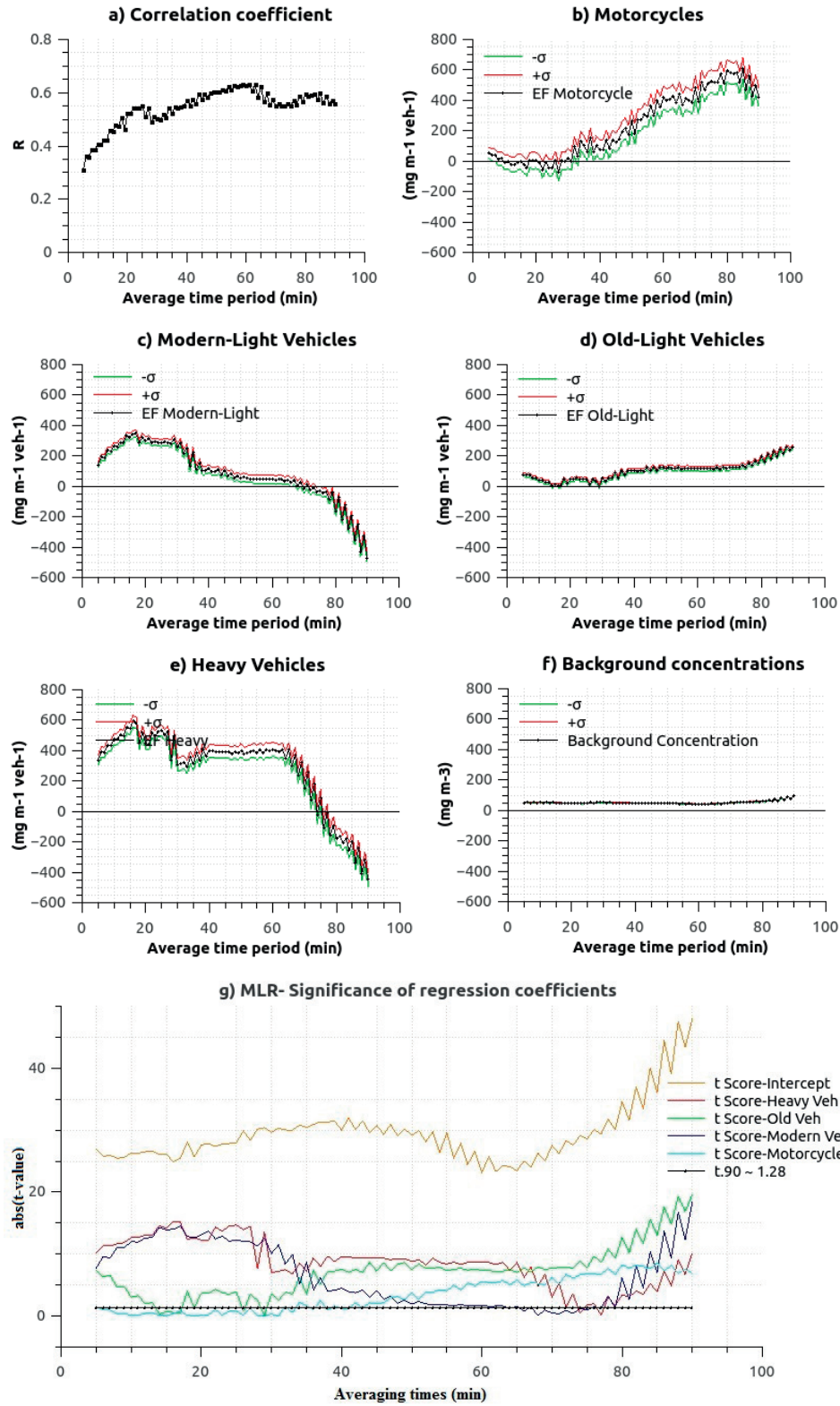


Figure 3.2: Results of the multiple regression for different averaging times. (a) Correlation coefficient. (b-e) EF refers the coefficients of the regression or PM10 emission factors, and $\pm\sigma$ is the standard deviation of the coefficients. (f) The intercept and $\pm\sigma$ is the standard deviation of the intercept. (g) Significance levels of the regression coefficients.

The correlation coefficients were statistically significant for all averaging times (p-values < 6e-06). The best linear fits, i.e., the highest “R” values, were reached at approximately 60’. Overall, the MLR effectively estimates EFs for modern and old light-duty categories with greater precision, i.e., smaller “ σ ” values, than that for motorcycles and heavy vehicles. However, EFs are estimated with similar precision (“ σ ”) by vehicle category, regardless of the averaging time length. To date, we are not able to indicate the specific averaging time that provides the best fit. An overview of the extent of variability for all estimates over the tested averaging times can be seen in table 3.2 : the first row shows the average of the estimates. The standard deviation with respect to this mean (second row) concerns the variability regarding different averaging time lengths. The average of the standard deviations of the estimates (third row) refers to how spread out the set of estimates is across all averaging times. In summation, the square root of the sum of squared standard deviations “ δ ” (i.e., both the standard deviation of the estimates with respect to the mean and the average of the standard deviations of the estimates) describe how much the estimations vary. The variability caused by changes in averaging times is very high, even greater than the average of the individual standard deviations. Consequently, the total standard deviation (fourth row) associated with each EF is greater than the average EF itself.

Table 3.2: Summary of multiple linear regressions – MLR; results (in mg km-1 veh-1) for averaging times 5’-90’. Avg. EF: an average of coefficients for an emission factors; Std. Dev of the Avg. EF: the standard deviation of coefficients with respect to the mean; Avg. of the EFs Std. Dev: the average of the standard deviations of the coefficients. Total Std. Dev: summation of the square root of the sum of squared standard deviations; Std. Dev of the Avg. EF and Avg. of the EF’s Std. Dev.

MLR (5’-90’)					
	Motorcycle	Modern-light veh	Old-light veh	Heavy veh	Backg.conc.
Avg. EF	231.2	85.6	103.5	282.5	51.4
Std. Dev of the Avg. EF	272.4	190.5	107.6	350.3	50.6
Avg. of the EF’s Std. Dev	64.3	25.6	14.3	43.7	1.7
Total Std. Dev (δ)	279.9	192.2	108.5	353.0	50.6

Obviously, not all averaging times offer proper fits, and therefore, it is wrong to consider the entire set. Indeed, we realized that for averaging times <40’ and >60’, the t-value magnitudes of some coefficients are too small (<t_{0.90} 1.28 in Fig.3.2g) to declare them statistically significant. In between 40’ and 60’ (see table 3.3), we found a combination of good fits with estimates less impacted by the averaging time period used; the average standard deviation of the estimates (second row) in this time window decreases. Yet, it is lower than the average of the individual standard deviations (third row) for most of the vehicle categories (i.e., “modern light”, “old light”, and “heavy”).

Table 3.3: Summary of the multiple linear regression–MLR; results (in mg km-1 veh-1) for averaging times 40’-60’. Avg. EF: an average of the coefficients for an emission factor; Std. Dev of the Avg. EF: the standard deviation of the coefficients with respect to the mean; Avg. of the EF’s Std. Dev: the average of the standard deviations of the coefficients; Total Std. Dev: summation of the square root of the sum of squared standard deviations; Std. Dev of the Avg. EF and Avg. of the EF’s Std. Dev.

MLR (40’-60’)					
	Motorcycle	Modern-light veh	Old-light veh	Heavy veh	Backg.conc.
Avg. EF	236.0	65.8	115.6	393.7	45.3
Std. Dev of the Avg. EF	100.6	21.4	8.6	8.6	2.2
Avg. of the EF’s Std. Dev	69.1	26.6	15.0	44.0	1.6
Total Std. Dev (δ)	122.0	34.1	17.3	44.8	2.7

The high extent of variability in the motorcycle estimations is probably due to collinearity effects which arise when predictor variables are naturally correlated with each other -this refers to the presence of linear relationships between the vehicles fluxes of different categories. Indeed, this occurrence affords high global correlation coefficient “R” misrepresenting the MLR model predictions.

The correlations between predictor variables helps on diagnosing the existence of collinearity (Chen-namaneni et al. 2016). As example, table 3.4 shows the correlation matrix of predictors (i.e., parameters $< D^t N_i^t >$ in eq.3.7) for an averaging time of 50’: Data for the “motorcycle”, “modern light” and “old light” categories are highly positively correlated among themselves (Pearson correlation >0.8). This indicates that as the fluxes of vehicles belonging to one of these categories increase, the others also increase, the fluxes of “heavy” appear to be less related (it makes sense since this specific category mainly comprises buses that dominate the city’s form of public transportation). Very similar correlation matrixes are found for other averaging times in the range of 40’-60’.

Table 3.4: Correlations matrix of predictor variables for a time period of 50’.

Correlation matrix	Motorcycle	Modern-light veh	Old-light veh	Heavy veh
Motorcycle	1.00	0.85	0.86	0.58
Modern-Light veh	0.85	1.00	0.84	0.49
Old-Light veh	0.86	0.84	1.00	0.60
Heavy veh	0.58	0.49	0.60	1.00

3.4.2 Principal component regression

Principal component regression (PCR) succeeds in overcoming the collinearity problem that arises when two or more predictor variables are correlated. Based on a principal component analysis (PCA), this procedure converts the set of correlated predictors into a set of linearly uncorrelated variables called principal components (the number of principal components is equal to the number of original predictors). By excluding some of the low-variance principal components in the regression step, the PCR can aptly estimate the regression coefficients that characterize the original model.

When we retain the three principal components with the highest variances, i.e., sufficient to explain 90% of the variance of the original predictor variables, all correlation coefficients remain significant (p-values $< 6e-06$). Although Fig.3.3a shows that “R” is slightly lower based on the PCR than based on the MLR (indicating lower quality in the fits), there is an observed improvement in the estimates of motorcycle EFs (black line in Fig.3.3b), which is almost unaffected by the averaging time lengths. The t-values of all coefficients remain statistically significant between 40’-60’ with a 90% probability (see Fig.3.3g). In table 3.5, we summarize the new estimates and their extent of variability.

Table 3.5: Summary of the principal component regression (PCR) results (in mg km-1 veh-1) for averaging times 40’-60’. Avg. EF: the average of the coefficients for an emission factor; Std. Dev of the Avg. EF: the standard deviation of the coefficients with respect to the mean; Avg. of the EF’s Std. Dev: the average of the standard deviations of the coefficients; Total Std. Dev: summation of the square root of the sum of squared standard deviations; Std. Dev of the Avg. EF and Avg. of the EF’s Std. Dev.

PCR (40’-60’)					
	Motorcycle	Modern-light veh	Old-light veh	Heavy veh	Backg.conc.
Avg. EF	111.1	90.6	125.4	415.1	44.3
Std. Dev of the Avg. EF	9.5	10.6	14.6	22.3	3.0
Avg. of the EF’s Std. Dev	6.2	25.5	42.8	71.5	1.1
Total Std. Dev (δ)	11.3	27.6	45.2	74.9	3.2

We use and recommend the PCR method since it represents a good compromise between fitting quality and estimate accuracy.

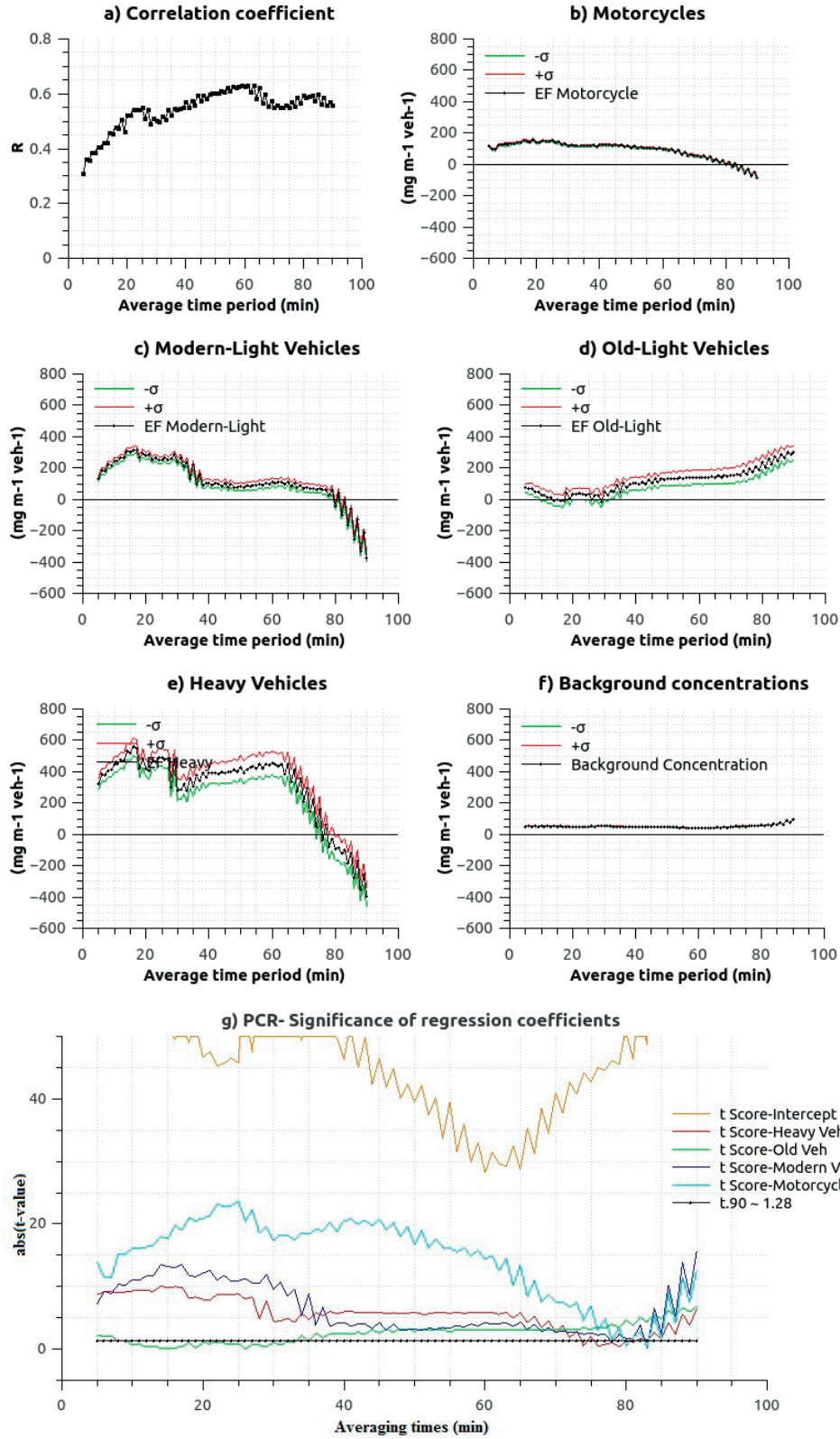


Figure 3.3: Results of the principal component regression for different averaging time periods. (a) Correlation coefficient. (b-e) EF is the PM₁₀ emission factor, i.e., the coefficients of the regression; $\pm\sigma$ is the standard deviation of the coefficients. (f) Background concentrations: the intercept $\pm\sigma$ is the standard deviation of the intercept.

3.4.3 Considering uncertainties in EF estimations

In table 3.5, the total standard deviation may be primarily due to three assumptions: (i) the EFs are constant in each vehicle category; (ii) the background concentration at the receptor location is constant over the averaging time; and (iii) the variability of the dilution factor depends exclusively on the variation of the proportion of light-duty vehicles, wind speed and wind direction.

To capture the uncertainties inherent in such assumptions, we consider the average EFs and total standard deviations, “ δ ”, from the PCR for 40’-60’ using a normal distribution function. The function used to describe the normal distribution is symmetric and valid for pre-defined boundaries of contiguous values (Alamilla-López 2015). We generate a sequence of values from $(EF - 3\delta)$ to $(EF + 3\delta)$ and calculate a probability density function (PDF) for each vehicle category (see Fig.3.4), thereby producing justified estimates of the uncertainties for EFs. Within the boundaries of the 95% confidence interval of the PDF, the EFs are probably within the range bounded by $EF \pm Z \frac{\delta^2}{\sqrt{n}}$ where $Z = 1.96$ for $\alpha = 0.05$. Thus, motorcycles have an $EF = 111.1 \pm 2.7$ mg km⁻¹ veh⁻¹; modern, light vehicles have an $EF = 90.6 \pm 11.2$ mg km⁻¹ veh⁻¹; old, light vehicles have an $EF = 125.4 \pm 18.5$ mg km⁻¹ veh⁻¹; and heavy vehicles have an $EF = 415.1 \pm 31.2$ mg km⁻¹ veh⁻¹. The bounded values are given in absolute terms, and they characterize the range of values within which the EFs of the different categories are assumed to be in, based on the specified level of confidence. They illustrate the scatter in data due to the statistical assumptions made in the linear fitting, but they also consider that the EFs of vehicles in a single category could provide different results due to unavoidable variation in the amount of pollutants that vehicles are emitting. The bounded values account for all contributing uncertainties, including those generated by the assumptions mentioned in the previous paragraph, while the PDFs allow for inferring the probability of finding a vehicle that pollutes more or less within a single category.

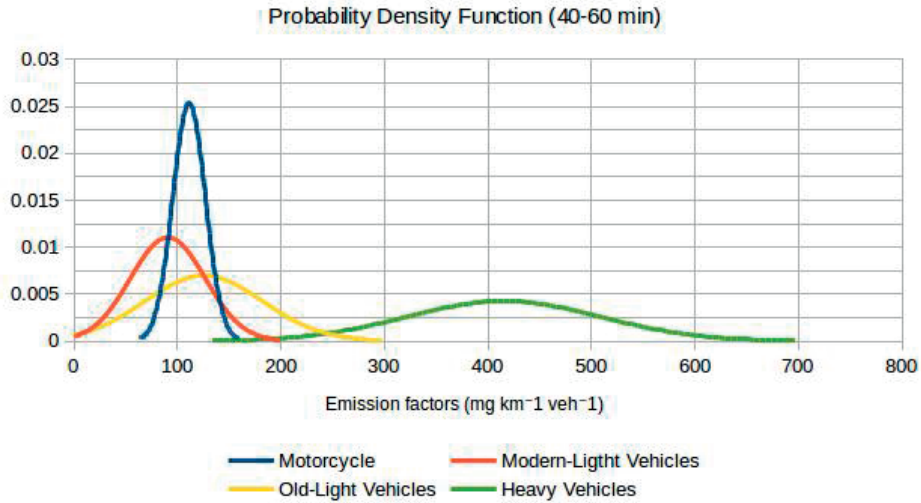


Figure 3.4: Probability density functions. The curves express the range of variation of PM10 EFs (mg km⁻¹ veh⁻¹) by vehicle category.

3.4.4 Comparisons with available studies

Regional differences are commonly expected in vehicle EFs for several reasons, including local applications of emission regulations, local driver behaviours or the quality of the fuel in use. From a literature review conducted by Bond et al. 2004, the average emission rate for light-duty gasoline and diesel is 21.0 ± 14.0 mg km⁻¹ veh⁻¹ (for unit conversions, we assumed average fuel consumption of 0.2 litre km⁻¹) in regions where emission standards have been progressively tightened; pre-1985 cars had average emission rates of approximately 33.6 mg km⁻¹ veh⁻¹. For other regions, an average of 70.0 ± 56.0 mg km⁻¹ veh⁻¹ was used, which is still lower than the values obtained in our study. Yan et al. 2011 relied on measurements from previous studies (Ntziachristos 2001; Ubanwa et al. 2003; Yanowitz et al. 2000) for vehicles built without

standards; they applied values of 7 and 250 mg km⁻¹ veh⁻¹ for light-duty gasoline and diesel vehicles, respectively. Such a large range encompasses our calculated EFs for light-duty vehicles (i.e., modern and old categories). Ntziachristos et al. 2012 reported motorcycle PM₁₀ EFs that comply with European emission standards (i.e., Euro I, Euro II, etc.); the average result was 34 mg km⁻¹ veh⁻¹. For uncontrolled motorcycle technologies, the value of 77 mg km⁻¹ veh⁻¹ was used. These emission rates are lower than the estimates in the present study. From a review of in-use heavy-duty diesel EFs, made by Yanowitz et al. 2000, the average from more than 250 different vehicles reported in 20 worldwide studies was 845.0 ± 56.0 mg km⁻¹ veh⁻¹. For 2008, the value reported by the U.S. EPA (2008) for in-use heavy-duty gasoline vehicles was 316.9 mg km⁻¹ veh⁻¹. In Yan et al. 2011, the proposed average values for heavy-duty vehicles built with and without standards were 280 and 700 mg km⁻¹ veh⁻¹, respectively. Considering that we included diesel and gasoline heavy-duty vehicles in a single category, our estimation aligns with the reference literature.

The fraction of vehicles using the poorest technologies or having the worst maintenance are commonly classified as high-polluting or “super-emitters” (Bond et al. 2004; McCormick et al. 2003; Subramanian et al. 2009; Yan et al. 2011) and contribute significantly to total emissions (Hansen et al. 1990; Lawson 1993; Zhang et al. 1995). The division between super-emitters and normal emitters affects the assumed emission factor for each technology category (Yan et al. 2014). For gasoline vehicles, Bond et al. 2004 reported a super-emitter EF of approximately 280 mg km⁻¹ veh⁻¹; the average value reported by Durbin et al. 1999 and Cadle et al. 1999 was approximately 250 mg km⁻¹ veh⁻¹. For diesel vehicles, in Bond et al. 2004, the average of super-emitters was more than 2 g km⁻¹ veh⁻¹, which is in agreement with studies by McCormick et al. 2003 and Subramanian et al. 2009. The PDFs in Sec.3.4.3 allow us to identify high-polluting vehicles within a single category. We computed the most likely EFs bred from a desired area under the PDFs. In table 3.6, we distinguish three sub-categories by breaking each category into one-third increments (i.e., fractions of 33.3% of vehicles in each sub-category) of the PDF surfaces. According to this fragmentation, we estimate that high-polluting motorcycles and modern-light vehicles have EF values of approximately 118.5 mg km⁻¹ veh⁻¹. For the old-light and heavy categories, the EF values are 170.5 and 491.0 mg km⁻¹ veh⁻¹.

Table 3.6: Estimated traffic emission factors (mg km⁻¹ veh⁻¹) for 33.3% vehicle fractions from the PDFs

Vehicle categories		EFs
Motorcycle	low-polluting	105.1
	medium-polluting	111.8
	high-polluting	118.5
Modern-light veh	low-polluting	63.7
	medium-polluting	91.3
	high-polluting	118.9
Old-light veh	low-polluting	78.4
	medium-polluting	124.2
	high-polluting	170.5
Heavy veh	low-polluting	336.6
	medium-polluting	413.8
	high-polluting	491.0

3.5 EFs for air pollution policy purposes

In this section, we explore the potential of different traffic-related scenarios for the abatement of PM₁₀ air pollution. The scenarios highlight changes in emission factors, e_i , and help assess the expected PM₁₀ reductions that could be reached by upgrading, renewing or restricting the vehicle fleet in Havana. First, we define a reference situation that states the diurnal hourly PM₁₀ concentration levels by considering the following:

1. The background concentration at the receptor location obtained from PCR (Sec.3.4.2, table 3.5).
2. The emission factors, e_i , classified into sub-categories; these are based on the PCR results in Sec.3.4.2 and the PDFs described in Sec.3.4.3, table 3.6.

3. A constant vehicle flux by category, $\langle N_i^t \rangle = N_i$, which is equal to the average of the measurements provided by traffic counting. The induced turbulence through four diurnal periods “P”. Dilution factors $\langle D^t \rangle^p$ are estimated considering minimal variation by period (period 1=7h00-9h00; period 2=9h00-12h00, period 3=12h00-13h00 & 16h00-19h00 period 4=13h00-16h00).

Referring to all these, eq.3.7 can be written as follows:

$$\langle C^t \rangle^p = \sum_i \langle D^t \rangle^p N_i e_i + C_0 \quad (3.8)$$

It considers the contributions of all sources in the street (see table3.7). Traffic sources are responsible for approximately 56% of PM10 air pollution. The largest contributors are old-light and heavy vehicles, in that order. Other sources may include the Havana Refinery and the Thermoelectric power plant, which both have constant operating regime within a 5-km radius from the measurement site, as well as traffic in surrounding streets.

Table 3.7: Estimated PM10 hourly diurnal concentration levels (ug m-3)

Vehicle categories		Hourly diurnal concentration (ug m-3)
Motorcycles	low-polluting	1.4
	medium-polluting	1.5
	high-polluting	1.7
Modern-Light veh	low-polluting	2.2
	medium-polluting	3.2
	high-polluting	4.2
Old-Light veh	low-polluting	5.6
	medium-polluting	8.9
	high-polluting	12.2
Heavy veh	low-polluting	4.0
	medium-polluting	5.0
	high-polluting	5.9
Traffic		55.5(56%)
Background		44.3(44%)
Total		99.8

Thereafter, we forecast the effects of progressive technological improvements (see Fig.3.5). Starting from the largest contributor categories, the first scenario imagines the upgrading of old-light vehicles by reducing their EFs to 78.4 mg km-1 veh-1 (i.e., the EF of low-polluting, old-light vehicles). The second scenario considers a total renewal of this category by reducing their EFs to 63.7 mg km-1 veh-1 (i.e., the EF of low-polluting, modern-light vehicles). In the third scenario, we assume that all light vehicles belong to the modern, low-polluting category. The last scenario adds the upgrading of heavy vehicles by setting the EFs of medium and high polluting vehicles to 336.6 mg km-1 veh-1 (i.e., the EF of low-polluting, heavy vehicles). Fig.3.5 shows the abatements on two percentages: one with respect to the traffic contributions on the street (red arrows), and the other considers the background concentrations (black arrows). The upgrading of vehicles in the old-light category (scenario 1) seems to be the most effective scenario. Alone, this scenario attains half of the PM10 abatement that could be achieved with all cumulative improvements (scenario 4).

If these improvements are implemented across Havana, the background concentrations in any given street would decrease as a result of the reduction of external traffic sources. Then, the percent of reduction with respect to traffic on each street (red arrows) could be greater than the values calculated. Hence, the values indicate the minimum expected abatement for each scenario. Conversely, by adding all possible reductions from sources other than traffic, the corresponding percentage with respect to the contributions on the street (black arrows) indicates the maximum expected abatement for each scenario. These percentages give an idea of the global scope expected (in percent) based on our different technological scenarios.

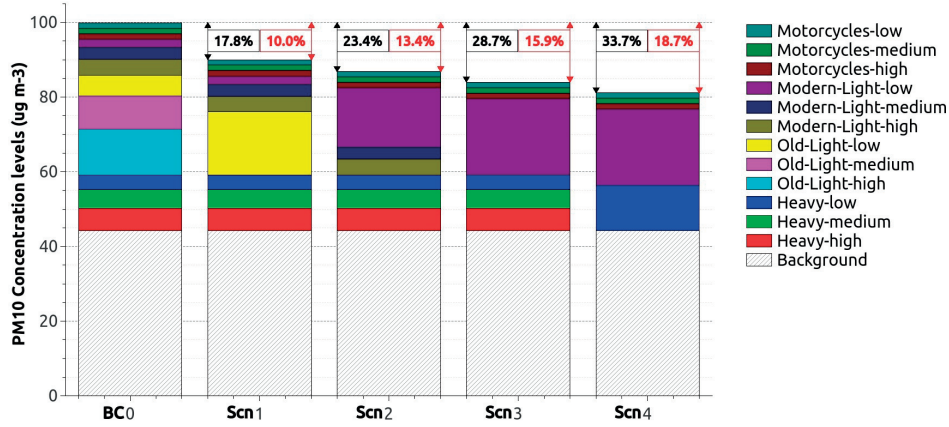


Figure 3.5: Comparison of PM10 concentration levels ($\mu\text{g m}^{-3}$) from on-road vehicles under four scenarios. Red and black arrows indicate the minimum and maximum percent of reduction expected on the street.

Table 3.8: Passenger transport capacity used for projections.

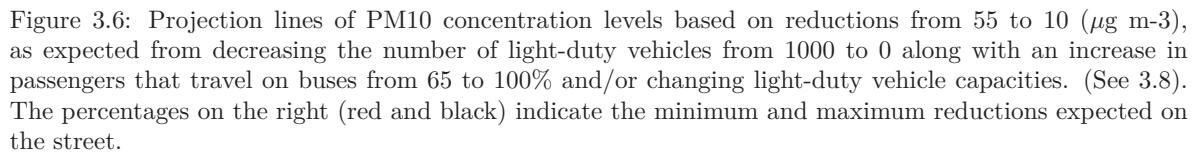
Vehicle categories	Average passenger (η)
Motorcycles	2
Modern-light veh	4
Old-light veh	5
Buses	120
Trucks	1

Greater abatement could be obtained by adding traffic restrictions. This can be seen in Fig. 3.6, which shows the effects of replacing the light-duty traffic, motorcycles and trucks (in that order) with low-polluting buses with 120-passenger capacities. This implies an increase in the number of buses for passengers to travel on.

The black-dotted line represents the evolution of the baseline case. A maximum reduction of $35.5 \mu\text{g m}^{-3}$ (from 55.5 to $20.0 \mu\text{g m}^{-3}$) is expected by restricting the circulation of all light vehicles. Approximately 4 and $5 \mu\text{g m}^{-3}$ of PM10 would be reduced by restricting motorcycles and trucks, respectively. Such situations easily decrease the street PM10 air pollution. For the blue and red dashed lines, we combine the same traffic restrictions with some technological improvements; these consider that all light vehicles exclusively belong to the modern- or old-light categories, respectively. Therefore, these lines (black-dotted, red and blue dashed) could be useful for developing strategies to reduce pollutants. For example, when examining the reduction to $40 \mu\text{g m}^{-3}$ from the “baseline case” (i.e., the start of the black-dotted line), the reduction can be attained either by upgrading light vehicles to modern categories (passing to the blue-dashed line) or by restricting their circulation (moving onto the black-dotted line) to 560 veh h⁻¹, which would require approximately 80% of passengers to travel by bus.

The grey lines add the effects of upgrading light vehicles to modern ones while decreasing the average number of vehicle passengers. In terms of travel comfort, this is a likely future situation that can be considered in Havana; it implies an overall increase in the use of modern vehicles for moving passengers. For example, if the number of passengers is reduced to two and they travel in a modern-light vehicle ($\eta=2$), an increase of $10 \mu\text{g m}^{-3}$ (from 55.5 to $65.4 \mu\text{g m}^{-3}$) would be expected compared to the “baseline case”.

Fig.3.6 also shows the minimum and maximum percentages (axes at right) of reduction that could be expected in the entire city by implementing any of the strategies displayed in the graphs.



In this study, we established a methodology to estimate traffic emission factors from street canyon measurements (low-cost devices) of traffic fluxes, wind forces and concentration levels; all data were collected in one-minute time steps. The methodology was based on the assumption that inside the street canyon and over a given time period, the average traffic emissions are linearly related to the average concentrations of slowly reactive pollutants. Thus, under well-defined wind forces and traffic conditions, a dilution factor was calculated, and multi-linear regression techniques were used for estimating an average emission factor for each vehicle category. The implementation of principal component regressions is preferred over standard multiple regression techniques since it reduces the collinearity effects that appear when traffic fluxes are naturally correlated between vehicle categories. The application for PM₁₀ EFs, four vehicle categories in Havana showed the best regression fits ($R > 0.5$ and standard deviation of estimates $< 15\%$) when averaging the data between 40' and 60'. It was found that traffic sources are responsible for over 50% of PM₁₀ air pollution on the street; among all vehicles, the largest contributors are old, light-duty vehicles. A coarse forecasting indicated that upgrading this category (i.e., a decrease of EF to 78 mg km⁻¹) would be an effective scenario for reducing PM₁₀ air pollution in Havana by between 10 and 17%. The next steps include improvements on dilution factor estimations by generalizing; for example, the effects of street geometry and receptor location. The method is expected to be extended and validated for other pollutants in order to develop sound policies for the control and management of traffic-related pollution in the city of Havana.

References

- Ait-Helal, W., A. Beeldens, E. Boonen, A. Borbon, A. Boréave, M. Cazaunau, H. Chen, V. Daële, Y. Dupart, C. Gaimoz, M. Gallus, C. George, N. Grand, B. Grosselin, H. Herrmann, S. Ifang, R. Kurtenbach, M. Maille, I. Marjanovic, A. Mellouki, K. Miet, F. Mothes, L. Poulain, R. Rabe, P. Zapf, J. Kleffmann, and J.-F. Doussin (2015). “On-road measurements of NMVOCs and NO_x : Determination of light-duty vehicles emission factors from tunnel studies in Brussels city center”. In: *Atmospheric Environment* 122, pp. 799–807.
- Alamilla-López, J. L. (2015). “An Approximation to the Probability Normal Distribution and its Inverse”. In: *Ingeniería, Investigación y Tecnología* 16.4, pp. 605–611.
- Amato, F., O. Favez, M. Pandolfi, A. Alastuey, X. Querol, S. Moukhtar, B. Bruge, S. Verlhac, J. Orza, N. Bonnaire, T. Le Priol, J.-F. Petit, and J. Sciare (2016). “Traffic induced particle resuspension in Paris: Emission factors and source contributions”. In: *Atmospheric Environment* 129, pp. 114–124.
- Belalcázar, L. C., O. Fuhrer, M. D. Ho, E. Zarate, and A. Clappier (2009). “Estimation of road traffic emission factors from a long term tracer study”. In: *Atmospheric Environment* 43.36, pp. 5830–5837.
- Belalcázar, L. C., A. Clappier, N. Blond, T. Flassak, and J. Eichhorn (2010). “An evaluation of the estimation of road traffic emission factors from tracer studies”. In: *Atmospheric Environment* 44.31, pp. 3814–3822.
- Berkowicz, R. (2000). “OSPM - a parameterised street pollution model”. In: *Environmental Monitoring and Assessment* 65, pp. 323–331.
- Berkowicz, R. and M. Denmark (1997). *Modelling traffic pollution in streets*. Ministry of Environment and Energy, National Environmental Research Institute.
- Bond, T. C., D. G. Streets, K. F. Yarber, S. M. Nelson, J. H. Woo, and Z. Klimont (2004). “A technology-based global inventory of black and organic carbon emissions from combustion”. In: *Journal of Geophysical Research D: Atmospheres* 109.14, pp. 1–43.
- Borrego, C., J. H. Amorim, O. Tchepel, D. Dias, S. Rafael, E. Sá, C. Pimentel, T. Fontes, P. Fernandes, S. R. Pereira, J. M. Bandeira, and M. C. Coelho (2016). “Urban scale air quality modelling using detailed traffic emissions estimates”. In: *Atmospheric Environment* 131, pp. 341–351.
- Brimblecombe, P., T. Townsend, C. F. Lau, A. Rakowska, T. L. Chan, G. Močnik, and Z. Ning (2015). “Through-tunnel estimates of vehicle fleet emission factors”. In: *Atmospheric Environment* 123, pp. 180–189.
- Bruce, R. R., R. Coquilla, B. Kuspa, and A. Padilla (2005). *A wind-tunnel study of air re-entrainment from an accidental laboratory exhaust stack release on the UC Davis Watershed Science Research Center*. Tech. rep. November.
- Cadle, S. H., P. A. Mulawa, E. C. Hunsanger, K. Nelson, R. A. Ragazzi, R. Barrett, G. L. Gallagher, D. R. Lawson, K. T. Knapp, and R. Snow (1999). “Composition of light-duty motor vehicle exhaust particulate matter in the Denver, Colorado area”. In: *Environmental Science and Technology* 33.14, pp. 2328–2339.
- Chennamaneni, P. R., R. Echambadi, J. D. Hess, and N. Syam (2016). “Diagnosing harmful collinearity in moderated regressions: A roadmap”. In: *International Journal of Research in Marketing* 33.1, pp. 172–182.
- Durbin, T. D., M. R. Smith, J. M. Norbeck, and T. J. Truex (1999). “Population density, particulate emission characterization, and impact on the particulate inventory of smoking vehicles in the South Coast Air Quality Management District”. In: *Journal of the Air and Waste Management Association* 49.1, pp. 28–38.
- Ferm, M. and K. Sjöberg (2015). “Concentrations and emission factors for PM_{2.5} and PM₁₀ from road traffic in Sweden”. In: *Atmospheric Environment* 119, pp. 211–219.
- Gertler, A. W., W. R. Pierson, J. G. Watson, and R. L. Bradow (1991). *Review and reconciliation of on-road emission factors in the south coast air basin*. Tech. rep.
- Hansen, A. D. A. and H. Rosen (1990). “Individual Measurements of the Emission Factor of Aerosol Black Carbon in Automobile Plumes”. In: *Journal of the Air & Waste Management Association* 40.12, pp. 1654–1657.
- Huang, Y.-d., N.-b. Zengf, Z.-y. Liu, Y. Song, and X. Xu (2016). “Wind tunnel simulation of pollutant dispersion inside street canyons with galleries and multi-level flat roofs”. In: *Journal of Hydrodynamics, Ser. B* 28.5, pp. 801–810.
- Jaikumar, R., S. Shiva Nagendra, and R. Sivanandan (2017). “Modeling of real time exhaust emissions of passenger cars under heterogeneous traffic conditions”. In: *Atmospheric Pollution Research* 8.1, pp. 80–88.

- Jung, S., J. Lim, S. Kwon, S. Jeon, J. Kim, J. Lee, and S. Kim (2017). "Characterization of particulate matter from diesel passenger cars tested on chassis dynamometers". In: *Journal of Environmental Sciences* 54, pp. 21–32.
- Kakosimos, K. E., O. Hertel, M. Ketzel, and R. Berkowicz (2010). "Operational Street Pollution Model (OSPM) - A review of performed application and validation studies, and future prospects". In: *Environmental Chemistry* 7.6, pp. 485–503.
- Kam, W., J. W. Liacos, J. J. Schauer, R. J. Delfino, and C. Sioutas (2012). "On-road emission factors of PM pollutants for light-duty vehicles (LDVs) based on urban street driving conditions". In: *Atmospheric Environment* 61, pp. 378–386.
- Kastner-Klein, P., E. Fedorovich, M. Ketzel, R. Berkowicz, and R. Britter (2003). "The modelling of turbulence from traffic in urban dispersion models - Part II: Evaluation against laboratory and full-scale concentration measurements in street canyons". In: *Environmental Fluid Mechanics* 3.2, pp. 145–172.
- Ketzel, M., R. Berkowicz, and A. Lohmeyer (2000). "Comparison of Numerical Street Dispersion Models With". In: *Environmental Monitoring and Assessment* 65.1-2, pp. 363–370.
- Ketzel, M., P. Wählin, R. Berkowicz, and F. Palmgren (2003). "Particle and trace gas emission factors under urban driving conditions in Copenhagen based on street and roof-level observations". In: *Atmospheric Environment* 37.20, pp. 2735–2749.
- Keuken, M., M. Moerman, M. Voogt, P. Zandveld, H. Verhagen, U. Stelwagen, and D. Jonge de (2016). "Particle number concentration near road traffic in Amsterdam (the Netherlands): Comparison of standard and real-world emission factors". In: *Atmospheric Environment* 132, pp. 345–355.
- Klose, S., W. Birmili, J. Voigtländer, T. Tuch, B. Wehner, A. Wiedensohler, and M. Ketzel (2009). "Particle number emissions of motor traffic derived from street canyon measurements in a Central European city". In: *Atmospheric Chemistry and Physics Discussions* 9.1, pp. 3763–3809.
- Lawson, D. R. (1993). "Passing the Test: Human Behavior and California's Smog Check Program". In: *Air & Waste* December 1993, pp. 1567–1575.
- Li, T., X. Chen, and Z. Yan (2013). "Comparison of fine particles emissions of light-duty gasoline vehicles from chassis dynamometer tests and on-road measurements". In: *Atmospheric Environment* 68, pp. 82–91.
- McCormick, R. L., M. S. Graboski, T. L. Alleman, J. R. Alvarez, and K. G. Duleep (2003). "Quantifying the emission benefits of opacity testing and repair of heavy-duty diesel vehicles". In: *Environmental Science and Technology* 37.3, pp. 630–637.
- Moradpour, M., H. Afshin, and B. Farhanieh (2017). "A numerical investigation of reactive air pollutant dispersion in urban street canyons with tree planting". In: *Atmospheric Pollution Research* 8.2, pp. 253–266.
- Nakashima, Y. and Y. Kajii (2017). "Determination of nitrous acid emission factors from a gasoline vehicle using a chassis dynamometer combined with incoherent broadband cavity-enhanced absorption spectroscopy". In: *Science of The Total Environment* 575, pp. 287–293.
- Ntziachristos, L. (2001). "An empirical method for predicting exhaust emissions of regulated pollutants from future vehicle technologies". In: *Atmospheric Environment* 35.11, pp. 1985–1999.
- Ntziachristos, L., Z. Samaras, C. Kouridis, D. Hassel, I. McCrae, J. Hickman, K.-h. Zierock, M. Andre, M. Winther, N. Gorissen, P. Boulter, R. Joumard, R. Rijkeboer, S. Geivanidis, and S. Hausberger (2012). "EMEP/EEA emission inventory guidebook 2009, updated May 2012 1". In: May.
- Palmgren, F., R. Berkowicz, A. Ziv, and O. Hertel (1999). "Actual car fleet emissions estimated from urban air quality measurements and street pollution models". In: *Science of The Total Environment* 235.1-3, pp. 101–109.
- Pang, Y., M. Fuentes, and P. Rieger (2014). "Trends in the emissions of Volatile Organic Compounds (VOCs) from light-duty gasoline vehicles tested on chassis dynamometers in Southern California". In: *Atmospheric Environment* 83, pp. 127–135.
- Rey deCastro, B., L. Wang, J. N. Mihalic, P. N. Breysse, A. S. Geyh, and T. J. Buckley (2008). "The Longitudinal Dependence of Black Carbon Concentration on Traffic Volume in an Urban Environment". In: *Journal of the Air & Waste Management Association* 58.7, pp. 928–939.
- Riccio, A., E. Chianese, D. Monaco, M. Costagliola, G. Perretta, M. Prati, G. Agrillo, A. Esposito, D. Gasbarra, L. Shindler, G. Brusasca, A. Nanni, C. Pozzi, and V. Magliulo (2016). "Real-world automotive particulate matter and PAH emission factors and profile concentrations: Results from an urban tunnel experiment in Naples, Italy". In: *Atmospheric Environment* 141, pp. 379–387.

- Shunxi, D. and C. Johansson. *Traffic emission factors of particle number measured in a street canyon in Stockholm , Sweden*.
- Smit, R., P. Kingston, D. Wainwright, and R. Tooker (2017). “A tunnel study to validate motor vehicle emission prediction software in Australia”. In: *Atmospheric Environment* 151, pp. 188–199.
- Sokhi, R. S., H. Mao, S. T. Srimath, S. Fan, N. Kitwiroon, L. Luhana, J. Kukkonen, M. Haakana, A. Karppinen, K. Dick van den Hout, P. Boulter, I. S. McCrae, S. Larssen, K. I. Gjerstad, R. San José, J. Bartzis, P. Neofytou, P. van den Breemer, S. Neville, A. Kousa, B. M. Cortes, and I. Myrtveit (2008). “An integrated multi-model approach for air quality assessment: Development and evaluation of the OSCAR Air Quality Assessment System”. In: *Environmental Modelling & Software* 23.3, pp. 268–281.
- Subramanian, R., E. Winijkul, T. C. Bond, N. Thi, K. Oanh, I. Paw-armart, and K. G. Duleep (2009). “Climate-Relevant Properties of Diesel Particulate Emissions : Results from a Piggyback Study in Bangkok , Thailand Climate-Relevant Properties of Diesel Particulate Emissions : Results from a Piggyback Study in Bangkok , Thailand”. In: *Environmental Science & Technology* 43.11, pp. 4213–4218.
- Ubanwa, B., A. Burnette, S. Kishan, and S. G. Fritz (2003). “Exhaust Particulate Matter Emission Factors and Deterioration Rate for In-Use”. In: *Journal of Engineering for Gas Turbines and Power* 125.April, pp. 513–523.
- Vardoulakis, S., B. E. Fisher, K. Pericleous, and N. Gonzalez-Flesca (2003). “Modelling air quality in street canyons: a review”. In: *Atmospheric Environment* 37.2, pp. 155–182.
- Wang, L., Q. Pan, X.-P. Zheng, and S.-S. Yang (2017). “Effects of low boundary walls under dynamic inflow on flow field and pollutant dispersion in an idealized street canyon”. In: *Atmospheric Pollution Research* 8.3, pp. 564–575.
- Yan, F., E. Winijkul, S. Jung, T. C. Bond, and D. G. Streets (2011). “Global emission projections of particulate matter (PM): I. Exhaust emissions from on-road vehicles”. In: *Atmospheric Environment* 45.28, pp. 4830–4844.
- Yan, F., E. Winijkul, T. C. Bond, and D. G. Streets (2014). “Global emission projections of particulate matter (PM): II. Uncertainty analyses of on-road vehicle exhaust emissions”. In: *Atmospheric Environment* 87, pp. 189–199.
- Yanowitz, J., R. L. McCormick, and M. S. Graboski (2000). “In-use emissions from heavy-duty diesel vehicles”. In: *Environmental Science and Technology* 34.5, pp. 729–740.
- Zarate, E., L. C. Belalcazar, A. Clappier, V. Manzi, and H. van den Bergh (2007). “Air quality modelling over Bogota city: combined techniques to estimate and evaluate emission inventories”. In: *Atmospheric Environment* 41.29, pp. 6302–6318.
- Zhang, Y., X. Wang, G. Li, W. Yang, Z. Huang, Z. Zhang, X. Huang, W. Deng, T. Liu, Z. Huang, and Z. Zhang (2015). “Emission factors of fine particles, carbonaceous aerosols and traces gases from road vehicles: Recent tests in an urban tunnel in the Pearl River Delta, China”. In: *Atmospheric Environment* 122, pp. 876–884.
- Zhang, Y., D. H. Stedman, G. A. Bishop, P. L. Guenther, and S. P. Beaton (1995). “Worldwide On-Road Vehicle Exhaust Emissions Study by Remote Sensing”. In: *Environmental Science & Technology* 29.9, pp. 2286–2294.

Chapter 4

Screening differences between a local inventory and the Emissions Database for Global Atmospheric Research (EDGAR)

In the vast majority of Latin American and South American countries, global emission inventories (EIs) are often used for modelling air quality. In particular the Emission Database for Global Atmospheric Research EDGAR is widely deployed but several studies have pointed to some gaps in comparison with national/regional inventories which incur errors in interpreting results. In Cuba, due to scarcity of a spatially distributed national inventory, EDGAR has been used as entry data for air quality modelling without verifying their reliability over the region. Our goal in this article is to compare and contrast EDGAR with a local inventory and to evaluate similarities or discrepancies. We use advanced comparison techniques developed by the Forum for Air Quality Modelling in Europe –FAIRMODE. This approach differs from others in the detailed way in which it points out to the differences and gets insights in possible explanations. Overall, EDGAR provided spatially smoother results and relatively lower values in hotspot areas. Differences in terms of total activities were low for all analyzed sectors. However, EDGAR overestimates emission factors (EFs) of stationary sources for CO by a factor of 3 and SO₂ by a factor of 1.5 while underestimates those of PPM₁₀ by a factor of 25. Most of the road transport EFs are overestimated in EDGAR; PM₁₀, CO and NO_x are 2 times higher, while CH₄ and SO₂ are 5 to 20 times higher. Large differences were found on the spatial distribution of energy and industrial sources. EDGAR can be regionally accepted as a reference but it is not recommended for air quality simulation over Cuba. A more complete reporting must be expected when more official national data are due. A review and evaluation of local emission inventories over Cuba can be useful for identifying potential areas for future improvement.

Note: This chapter is the accepted manuscript (*preprint*) version of an article published in the journal Science of The Total Environment on August 2018.

Scientific paper: Madrazo, J., Clappier, A., Carlos, L., Cuesta, O., Contreras, H., Golay, F., 2018. Screening differences between a local inventory and the Emissions Database for Global Atmospheric Research (EDGAR). Sci. Total Environ. 631–632, 934–941.

Please see the final published version: <https://doi.org/10.1016/j.scitotenv.2018.03.094>. Cited as Madrazo et al. 2018b

4.1 Introduction

Air quality problems currently affect many cities worldwide. To mitigate this pollution issue, governments are developing policies to control air pollution emission sources (cf. Bel et al. 2015; Font et al. 2016; Gil-Alana et al. 2017; Grigoroudis et al. 2016; Zhanga et al. 2017). Policies are usually supported by air quality models able to predict the effect of changes on the sources' emission rate. Studies point out to emissions as the most uncertain factor among different components of air quality models; e.g. meteorology, boundary conditions, model parameters (François et al. 2005; Russell et al. 2000; Viaene et al. 2012). A good understanding of all sources (i.e. anthropogenic and biogenic emission sources) and the quantification of their pollution rate is required. This information is commonly reported in Emission Inventories (EIs). At continental scale, various inventories have been developed (Zhao et al. 2017) including the Emission Database for Global Atmospheric Research (EDGAR, (JRC) et al. 2011), the inventory of the Intergovernmental Panel on Climate Change (IPCC 2006; Penman et al. 2006), the inventory of Reanalysis of TROpospheric chemical composition over the past 40 year (RETRO, Pulles et al. 2003) and the new global emission inventory from the Community Emission Data System (CEDS, Smith et al. 2015). They are all useful for many reference purposes, especially for geographical areas in which data are not available, such as is the case in the vast majority of countries in South America (Alonso et al. 2010) and Latin America. Among them, most air quality simulations have relied on EDGAR (Alonso et al. 2010; Garcia et al. 2015; Kumar et al. 2010; Mena-Carrasco et al. 2009). EDGAR is considered unique in its provision of historical emission data for 20 year prior to 1990, and has been widely used by the global scientific community and by policy makers worldwide ((JRC) 2009). Nevertheless, EDGAR project uses scientific information and data from international statistics in order to model emissions for all countries of the world in a comparable and consistent manner. This fact can be a source of significant uncertainties -especially where there is no officially registered nation based emission data; and therefore it limits their use on decision support analysis. At country-scale, with the exception of a group of countries (i.e. group world 2 -mostly developing countries), national inventories are reported to the United Nations Framework Convention on Climate Change (UNFCCC). In addition, increasing attentions have been paid on regional/local inventories, motivated mainly by the urgent needs for haze pollution mitigation (Fu et al. 2013; Wang et al. 2010; Zhao et al. 2015; Zheng et al. 2009; Zhou et al. 2017).

Given the diversity in terms of methodology and data sources, global and local/regional inventories often do not lead to comparable emission estimates. Inventories' comparison has become an useful approach to quickly scan inventory data for such gaps, mistakes or differences. Specific comparisons over EDGAR have been performed worldwide. For example, Amstel et al. 1999 compared national inventories as reported to the Climate Convention Secretariat with EDGAR CO₂ and CH₄ data. For CO₂, differences were more than 10% in Eastern Europe + former USSR, and the Rest of the World Group 1, mostly developing countries. Large differences were found in some Latin American countries: emissions from fossil fuels were 24% higher in Bolivia national estimates, while EDGAR estimates were 90% and 23% higher than Costa Rica and Venezuela estimates. For CO₂ from biofuels, EDGAR estimates were 175% and 124% of Bolivia and Costa Rica national estimates. Emissions mostly agree within the scope of 5% for Australia, Czechoslovakia, Germany, Italy Iceland, Hungary, Romania and United Kingdom. Substantial differences on CH₄ global emissions from coal, oil and gas were also observed; EDGAR estimates were almost a half of global total of national estimates. In contrast, global total methane emissions from fossil fuel combustion were lower in a factor of 10 in national data with respect to EDGAR. In most of the cases, differences were traced down to the use of different emission factors or the use of national statistic that differed from the internationally available ones. Parrish et al. 2009 indicated that the substantial decrease (something like an order of magnitude) in US non-methane hydrocarbons (NMHC) emissions experienced between 1975 and 2005 is inconsistent with the EDGAR inventory; EDGAR suggests increasing emissions until a maximum reached in 1995. This is probably due to misapprehensions of successful emission control strategies within the period. Regarding spatial patterns, Sheng et al. 2017 results have shown large differences with EDGAR oil/gas emissions in Canada and Mexico; EDGAR largely misses areas of production, and instead allocates total oil/gas emissions mainly according to population. Methane emissions from non oil/gas anthropogenic sources in EDGAR are higher for Canada (14%) as compared to Environment Canada (2015), and for Mexico (12%) as compared to INECC 2015. EDGAR error patterns for other anthropogenic sectors including livestock and waste resulted smaller. Abdallah et al. 2016 highlighted high discrepancies in terms of emission estimates and spatial distribution: EDGAR emissions were higher than regional estimates for NH₃ and SO₂ by a factor about 3, and lower for CO, PPM₁₀ and PM₂₅ by a factor between 2 and 4. These differences were mainly due

to the use of global datasets, occasionally inconsistent with respect to the base year, for the estimations of key factors such as the quantity of fuel, the distributions of fleet compositions and population. This led to high spatial differences in the modeled O₃ and PM_{2.5} concentrations, compared to a regional EI. Jena et al. 2015 indicated that over large NO_x emitting point sources simulated daytime 8-hr, averaged O₃ mixing ratios with EDGAR NO_x emissions during winter shows the lowest O₃ values compared to ensemble mean of other four inventories (i.e. Intercontinental Chemical Transport Experiment-Phase B INTEX-B (Zhang et al. 2009), MACCity Indian National Emission Inventory INDIA NO_x (Zhang et al. 2009), the MAACity emission inventories developed for chemistry-climate studies (Granier et al. 2011) and Regional Emission Inventory in Asia REAS (Ohara et al. 2007)). This study argued that it is likely due to the very high NO_x emissions in EDGAR inventory which leads to titration of O₃ during coolest winter months. G. Janssens-Maenhout et al. 2015 pointed out that EDGAR can be recommended as a global baseline emission inventory, which is regionally accepted as a reference.

In Cuba, there have been national EIs since 1990 (cf. ONE 2016c). They report total emissions by compound and activity sector but not the temporal/spatial disaggregation. Instead EDGAR has been used as reference for national emissions disaggregation (Contreras Peraza et al. 2014) and even as entry for air quality modelling over the country (Turtós Carbonell et al. 2011). Thus, no evidence so far about their reliability over Cuba have been provided. The aim of this article is to evaluate the differences between EDGAR and a local emission inventory developed in Havana Cuba. We use advanced comparison techniques developed by the Forum for Air Quality Modelling in Europe –FAIRMODE. This approach differs from others in the detailed way in which it points out to the differences and gets insights in possible explanations.

4.2 Data and Method

4.2.1 Local inventory

We developed a local air pollutants inventory of emissions from fossil fuel combustion, by end-use sector (transportation, industry and electricity power). The inventory includes emissions of nitrogen oxides (NO_x), carbon monoxide (CO), Non Methane Volatile Organic Compounds (NMVOCs), ammonia (NH₃), Sulphur dioxide (SO₂) and Particulate Matter (PM₁₀). Emissions were calculated based on local data: values of emission factors from measurements and national reports while activities information from local statistic. Emissions were spread across the Selected Nomenclature for reporting Air Pollutant (SNAP) classification (cf. table 4.1).

Table 4.1: SNAP sectors classification. Source: CORINAIR / SNAP 97 version 1.0 dated 20/03/1998.

ID	Description
S1	Combustion in energy and transformation industries
S2	Non-Industrial combustion plants. Residential
S3	Combustion in manufacturing industry
S4	Production processes
S5	Extraction and distribution of fossil fuels and geothermal energy
S6	Solvent and other product use
S7	Road transport
S8	Other mobile sources and machinery
S9	Waste treatment and disposal
S10	Agriculture
S11	Other sources and sinks

Road transport sector

Road transport emissions were estimated by using the EMISENS model especially developed to quickly calculate traffic-generated emissions (Quoc Ho et al. 2014). EMISENS combines the well-known top-down and bottom-up approaches to force them to be coherent on the emission estimation. The basic inputs are road transport activity levels (i.e. vehicle fluxes and street network densities) and vehicular emission factors.

According to the Cuban Vehicle Registration Office, Havana’s road fleet is distributed by categories as shown in table 4.2. Their average covered mileage was collected from Cuban statistic and scientific reports (Álvarez Hymelín 2010; transporte) 2000); and then activity levels calculated as the product of the vehicle number and their mileage. Activity levels can be also calculated as the product of street lengths and average vehicle flows. According to estimations from Open-road plugin maps (QGIS Development Team 2015), the vehicular traffic in Havana is spread over 7’290 km length, including urban, rural and local streets (table 4.3). The average vehicle flow was estimated from manual traffic counting of 50 road network segments, assuming rhythmic and repetitive traffic variations to relate volumes of these segments with volumes of other streets under the same category.

The difference in total activity levels from both approximations is around 5%; so estimations are considered coherent. Regarding fleet composition by road category, activities were subsequently split on a cross-classification (see table 4.4).

EFs were collected by vehicle category and compound (see table 4.5) from different information sources. For CO, we used the results (non-published) of Biart Hernández 2000; this study statistically analyzed the end-pipe measurements of a CE8690 gas analyzer on a 380 samples’ static test to compute EFs of Havana’s gasoline passenger cars. For PM10, we used the results of Madrazo et al. 2018a; their methodology is based on regression analyses of traffic counting, concentration levels and meteorological parameters to compute EFs of Havana’s transport fleet aggregated on four vehicle categories (i.e. motorcycles, modern passenger cars, old passenger cars and heavy vehicles). EFs of other pollutants and vehicle categories were set out from Fernández Martínez et al. 1996 -the cuban national emissions report.

Hourly and weekly traffic profiles (i.e. coefficients defined from daily traffic counting) as well as road network lengths repartition (i.e. vector layers of distances defined in Qgis at 3km spatial resolution) lead to temporal and spatial emission distributions.

Table 4.2: Vehicle categories. The total number of vehicles was set according the vehicle registration system office of Havana. Average mileage in a working day is collected from literature.

Vehicle gories	Cate-	Number of vehicles	Average mileage (km/day)	Activity levels (veh- km/h)
Passenger vehicles and light gasoline vehicles, including small vans (AG)		120’288	160	801’918
Passenger vehicles and light diesel vehicles, including small vans (AD)		27’461	220	251’724
Heavy vehicles and Trucks(HT)		15’494	90	58’101
Buses (B)		14’397	250	149’967
Motorcycles (MT)		52’603	40	87’672

Table 4.3: Street categories: Havana road network categorized according to the Cuban technical standards NC 53-80 y NC 53-81. These norms provide a functional classification of urban and rural streets. Road network lengths were measured by category from the world editable Open Street Map QGIS plugin.

Road categories	Main characteristics	Traffic flow (veh/h)	Activity levels (veh-km/h)
Main Street, Average Speed > 80 km/h, Street length 877.9 km	Motorway – For limited-access restricted divided highways. Motorway link – For linking roads to, from or between motorways beyond the point where non-motorways traffic can joint or leave the link or other roads where motorways rules apply. MainStreet of the city	325	285'318
Semi Urban Street, Average Speed 60-80 km/h, Street length 1652.4 km	Trunk – For inter-regional routes that are not motorways, often limited-access divided highways for general traffic, but sometimes undivided. Trunk link – For linking roads to, from or between trunk roads beyond from the point where traffic is required to joint or leave trunk road.	45	74'358
Urban Street1, Average Speed 40-50km/h, Street length 414.5 km	Primary - often have traffic signal and housing/retain/industry with direct access. Primary link – For link-lanes to, from or between primary roads beyond the point where traffic is required to joint or leave a primary road.	500	207250
Urban Street2, Average Speed 40-50km/h, Street length 450.1 km	Secondary – Typically one lane each direction, wide enough for 2 passager cars with less long distance traffic	60	27'006
Urban Street3, Average Speed 40-50km/h, Street length 737.3 km	Tertiary – For minor roads connecting local neighborhoods.	50	36'865
Locals, Average Speed 30-40 km/h, Street length 1723.3 km	Locals and unclassified– For local roads and roads where the classification cannot be determined.	440	75'8252
Neighborhood Streets, Average Speed < 40 km/h, Street length 3063.3 km	Residential – For roads in primarily residential areas that are not of a specific classification.	15	45'950

Table 4.4: EMISENS input data. Activity levels disaggregated by vehicle and road categories (veh.km/h)

	Main-Street	SemiUrb-Street	Urban-Street1	Urban-Street2	Urban-Street3	Local	Neighb-Street
AG	80192	272652	152364	152364	40096	40096	64153
AD	25172	85586	47828	47828	12586	12586	20138
HT	5810	19754	11039	11039	2905	2905	4648
B	14997	50989	28494	28494	7498	7498	11997
MT	8767	29808	16658	16658	4384	4384	7014

Table 4.5: Emission factors (g/km-veh) by vehicle category (Passenger vehicles and light gasoline vehicles, including small vans (AG), Passenger vehicles and light diesel vehicles, including small vans (AD), Heavy vehicles and Trucks(HT), Buses (B), Motorcycles (MT))and compound including Carbon monoxide (CO), nitrogen oxides (NOx), volatile organic compounds (NMVOC), particulate matter (PM10), methane (CH4) and sulfur dioxide (SO2).

	NOx	CO	SO2	NMVOC	PM10	CH4
AG	0.952	47.08	0.82	6.37	0.108	0.090
AD	0.731	0.80	0.80	0.20	0.108	0.006
HT	6.683	29.92	1.50	1.59	0.413	0.066
B	13.511	114.24	1.50	1.86	0.413	0.077
MT	0.122	33.09	0.06	24.03	0.111	0.227

Industrial, non-industrial and electricity sectors

The stationary sources of Havana are mainly associated with public electricity generation, a group of industries and self-producers (i.e. hospitals, schools, enterprises, etc.). Their emissions were computed on basis of a bottom-up approach using data collected and/or measured by Cuban institutions (i.e. National Institute of Meteorology -INSMET and Information Management and Energy Development Centre-CUBANERGIA).

Data includes emission factors, activity levels and geo-locations of each stationary source. Temporal operation regime were segregated on three day types (i.e. working days, Saturdays and Sundays). In addition, a source classification was made according to applicable sector of the Selected Nomenclature for reporting Air Pollutant (SNAP); it included fuel combustion activities in energy industries SNAP-1, combustion on manufacturing industries SNAP-3, production processes SNAP-4 and non-industrial combustion plants SNAP-2, cf. data in table 4.6.

Each individual activity for any given stationary source can be easily aggregated on a cell grid; either spatially (e.g. the sum of emissions sources located in a cell at any given spatial resolution), temporally (e.g. the sum of hourly emission of any given source) or by sectors (e.g. individual activities are assigned to an applicable activity sector). A simple algorithm was created to compute hourly emissions by day, week and a year at each cell of the study domain.

Table 4.6: Stationary sources, data available.

Example entities: (HOSJT) Hospital “Julio Trigo”, (GEAPO) Electrogen Group “Apolo”, (GEMAN) Electrogen, Group “Managua”, (ANTAC) Iron-steel company “Antillana de acero”, (REFÑL) Crude-oil refinery “Nico Lopez”

Column head description: **(a)** latitude (degree); **(b)** longitud (degree); **(c)** SNAP sector; **(d)** regimen (hrs/day); **(e)** regimen (days/week); **(f)** EF-Nox (g/s) national; **(g)** EF-SO2 (g/s) national; **(h)** EF-PM10 (g/s) national; **(i)** EF-PM2.5 (g/s) national; **(j)** EF-CO (g/s) international reference; **(k)** EF-NMVOC (g/s) international reference

	a	b	c	d	e	f	g	f	i	j	k
HOSJT	23.06	-82.36	SNAP2	8	7	0.108	0.1153	0.0692	0.0514	0.0115	0.0008
GEAPO	23.08	-82.35	SNAP1	2	7	20.1119	10.5919	0.9775	0.1983	0.0992	0.0864
GEMAN	22.97	-82.35	SNAP1	5	7	2.2194	2.0889	0.188	0.0326	0.0163	0.0235
ANTAC	23.04	-82.28	SNAP4	24	7	1.213	NA	51.415	25.707	.776	0.169
REFÑL	23.14	-82.32	SNAP1	24	7	162.04	91.566	13.82	6.91	149.8	3.1

4.2.2 EDGAR inventory

The EDGAR anthropogenic emission dataset (version 4.2) was compiled by the European Commission, Joint Research Center (JRC)- Netherlands Environmental Assessment Agency. This dataset includes emissions of nitrogen oxides (NO_x), carbon monoxide (CO), Non Methane Volatile Organic Compounds (NMVOCs), ammonia (NH₃), Sulphur dioxide (SO₂), Black Carbon (BC), methane and Particulate Organic Matter (POM) from anthropogenic and biomass burning sectors and includes no carbonaceous aerosol emissions. The annual emissions have a resolution of $0.1 \times 0.1^\circ$ and cover the period from 1970 to 2008. Activity data is set from international statistics comparable between countries in definition and units. The International Energy Agency (IAE) 2008 database leads fuel consumption activities, which includes combustion in the energy, manufacturing and transformation industries, combustion in oil refineries and the residential sector (Muntean et al. 2014). The Food and Agricultural Organization of the United Nations (FAO) et al. 2008 database is used for agriculture. Fuel-based emission factors are established from the tier 1 approach of the Intergovernmental Panel on Climate Change (IPCC 2006) guidelines; i.e. “uncontrolled” emission factors common across countries when developers judged comparable. Emission reduction effects of control measures are also applied according to EMEP-EEA guidelines. Grid maps are used for allocating EDGAR sectoral emissions of a country to a grid. Combustion-related emissions from residential and industrial activities are distributed, by default, according to a population proxy data (CIESIN et al. 2010) and urban-rural population in-house EDGAR proxy database (Janssens-Maenhout et al. 2013). The distribution of road transport activities is derived from a specific EDGAR proxy data (i.e. “Population Roads”). For other sectors, point source data for power plants and industrial factories are used. EDGAR disaggregates emissions based on IPCC 2006 categories by sources (see also Barker et al. 2007; Penman et al. 2006 for detailed sectors description). In this study, we convert categories’ IPCC into SNAP sectors by applying Janssens-Maenhout et al. 2015 guidelines.

4.2.3 Benchmarking tools

For comparison of the Havana’s EI with EDGAR, we firstly display total differences in a bar plot on horizontal axes. It shows emission ratios by pollutant on a logarithmic scale. The difference between emission ratios can evidence inconsistencies in emission factors (i.e. dissimilar bar sizes) or in activity data (i.e. similar bar sizes). A second evaluation is made by applying the methodology proposed by Thunis et al. 2016a in the framework of FAIRMODE (2015) -a Forum for Air Quality Modelling created for exchanging experience and results from air quality modelling in the context of the Air Quality Directive (AQD) (Guevara et al. 2017). This approach expresses the emission factor ratio and the activity ratio from the two emission totals; nor the emission factors neither the activities need to be known a priori. To do that, it is assumed that for a given sector, one pollutant species serves as a reference of confidence and that activities by macro-sector are independent of the pollutants. The evaluation is supported by a diagram (i.e. Diamond diagram) aiming at getting additional insights and possible explanations for discrepancies between emissions over the selected areas. Indeed, it unmask information of whether discrepancies are mostly related to differences in the use of emission factors and/or in the choice of activity data (López-Aparicio et al. 2017). For more details about the theory behind the diamond diagram and its interpretations, refer to Thunis et al. 2016a. In addition and to capture inconsistencies in term of the spatial distributions, we extrapolate the methodology of Thunis et al. 2016a to a cell by cell analysis. Emission ratios are computed by cell assuming that each cell activity ratio is independent of the pollutant. Results are displayed as a cloud of points in the “diamond diagram”. The sectors considered for these analyses are SNAP-7 and a macro-sector referred to SNAP-1,3,4 (note that SNAP-2 was excluded because it must account for emissions from the residential sector, which is not available on the local EI). The pollutants considered are CO, NMVOC, PM₁₀, NO_x, SO₂ (all sectors) and CH₄ (only for road transport sector).

4.3 Results and discussion

The final-local EI is a set of hourly layers (grid-maps) covering Havana and adjacent areas on three day types (i.e. working-day, Saturday and Sunday). In correspondence with EDGAR temporal resolution, annualized local emissions were calculated by considering the weighted average of daily emission grids.

Fig.4.1 gives information on the differences of annual emissions (in tons per year) between the local EI and EDGAR based on $0.1 \times 0.1^\circ$ gridded maps for six pollutants (i.e. CO, NMVOC, PM₁₀, NO_x, SO₂ and

CH₄) and two macro-sectors (i.e. Road Transport as SNAP-7 and Stationary sources as SNAP-1,3,4).

For SNAP-1,3,4, EDGAR provided spatially smoother results and has relatively lower values in hotspot areas (e.g. cells in the north area between latitudes 23° 0-12'N and longitudes 82° 12-30'W aggregate a crude-oil refinery, a thermoelectric power plant, several electro-generators and an iron-steel industry) This can be explained by the fact that the local EI is mainly based on bottom-up approaches from sources; large emission entities are not continuously distributed. Therefore, it may provide more discernible results which allow for finer scale emission analysis.

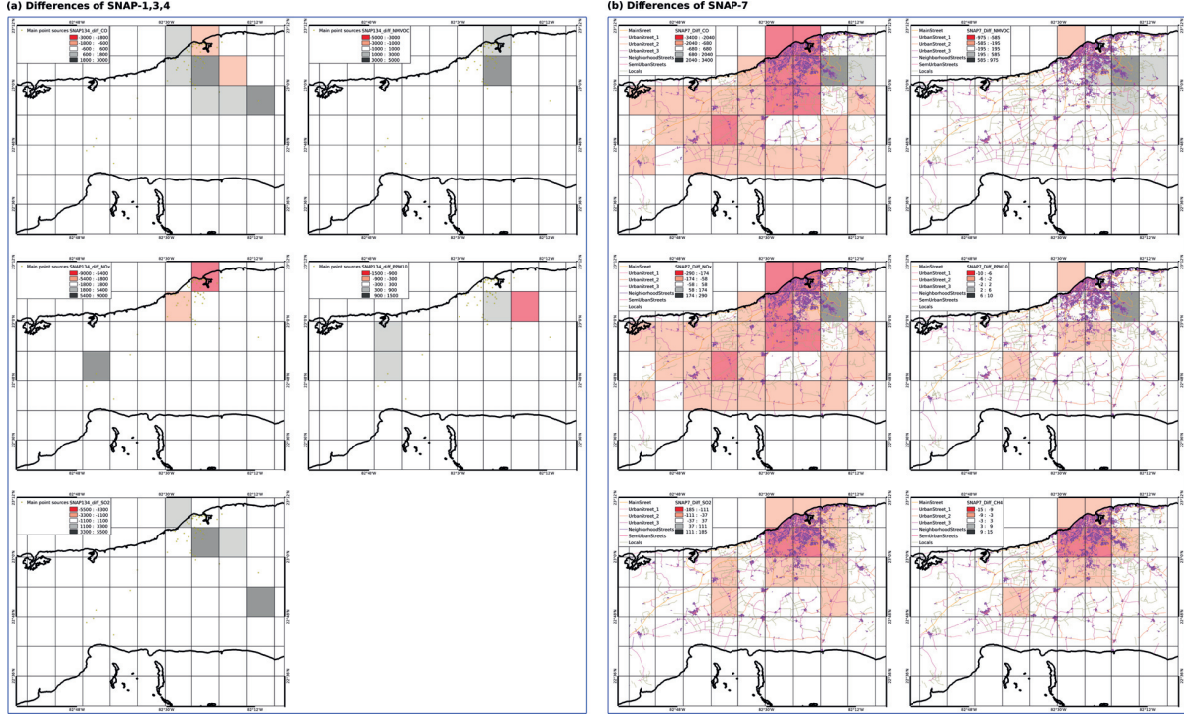


Figure 4.1: Spatial comparison of CO, NMVOC, PM₁₀, NO_x, SO₂ and CH₄ emissions in ton/year; differences as EDGAR - Local EI: (a) SNAP-7 (b) SNAP-1,3,4. Pollutants are mentioned in the legend of each panel.

At this stage, annual emission grids of SNAP-7 and SNAP-1,3,4 can be visually compared. Important differences in terms of emission quantities and their spatial distributions were appreciated but no inferences can be reached about the reason for these discrepancies.

Fig.4.2 shows the bar plot on horizontal axes comparing total emission ratios in a logarithmic scale. In order to facilitate interpretations it is important to mention that the average activity data is considered constant by sector. Therefore, similar E_{Local}/E_{Edgar} ratios (i.e. bar of equal sizes) between pollutants are associated with issues of total activity data but dissimilar ones, as is the case, are mostly due to issues in emission factors. For SNAP-1,3,4, EDGAR overestimates the EF of CO, NO_x and SO₂ while underestimates the PPM₁₀ and NMVOC (with respect to the regional EI). In SNAP-7, with the exception of NMVOC, EFs are underestimated by EDGAR.

Fig. 4.3 offers a more complete overview of the discrepancies since the diamond diagram interprets the emission ratios in two axes (i.e. horizontal and vertical) representing the differences in emission factors and activity data separately. It must be noticed that the emissions corresponding to a macro-sector aggregate quantities from different technologies, and thus activities and emission factors. They should be seen as “coarse” aggregations within macro-sectors. For more details on the mathematical implications of these aggregations, the reader is referred to the original paper Thunis et al. 2016a. In Fig. 4.3, the diamonds symbolize factor thresholds (e.g. red diamond set a threshold of factor 2). The graph suggests that the differences in terms of activities are low for both sectors: Coarse activity levels are slightly overestimated in both, SNAP-7 (circle style points) and SNAP-1,3,4 (triangle style points) sectors, by EDGAR with respect to the local EI. Concerning EFs of SNAP1,3,4, EDGAR emissions were higher than local estimates for

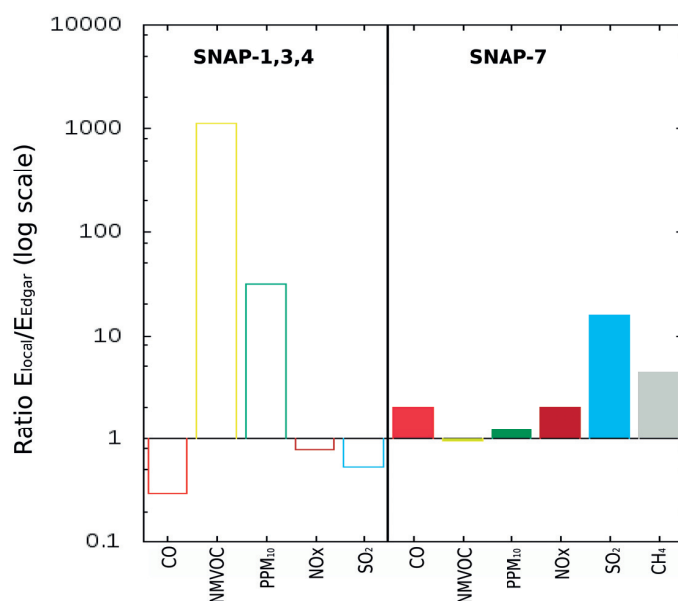


Figure 4.2: Bar plot on horizontal axes: comparison of CO, NMVOC, NOx, PM10, SO2 and CH4 emissions of local inventory with EDGAR data.

CO by a factor of 3 and for SO2 by a factor of 1.5; they were lower for PPM10 by a factor of 25. The reason behind the differences is probably linked to the fact that local EFs- obtained from measurements or national reports- include considerations on technology conditions and the type of fuel used. For NOx and SO2, it considers the actual nitrogen, lead and sulfur content of the fuels burning in Cuban boilers and power plants. For PPM10, it must also refer to the high content of sulfur in fuels combined with poor technical conditions of sources. Many of these sources have been exploited for more than 15 years resulting in obsolete technology for burning fuel and particles control devices. For CO, local EFs are mostly based on experts' recommendations from international references, so they could tend to be underestimated with respect to real values. The high NMVOC differences (out of ranges in Fig.4.3) are not clear, Cuban experts indicate low emissions are logical since a few measurements show insignificant NMVOC emissions. Future work should enhance CO and NMVOC emission factors including local measurements on stationary sources. In SNAP-7, the EF of PM10, CO and NOx are within a factor of 2, while CH4 and SO2 are around 5 and 20 times higher. The poor combustion, technical conditions and operational inefficiency of most of Cuban vehicles –very peculiar with respect the rest of the world- would be the reason for these differences. In addition, it is possible that the sulfur content level of Cuban gasoline-cars has not been taken into account in the EF of SO2 proposed by EDGAR.

The discrepancies in terms of emissions spatial distributions can be observed in Fig.4.4 and 4.5. The points' deviations on the X axis indicate how much the cell's EFs are moving away from the coarse EF ratio; the same applies to deviation on the Y axis with respect to the cell's activity levels.

In SNAP-7 (see Fig.4.4), the points describe a non-perfect but clear vertical alignment indicating that EFs suffer, overall, the same over/underestimations for all cells. It is important to note that these ratios (i.e. points in the diamond diagram) are relating “average” EFs of both inventories cell by cell and these “averages” are ponderations which consider the vehicle fleet distribution at each particular cell. Therefore, the cause of discrepancies can be due to either the vehicle category EFs value by itself or to differences in assumptions of vehicle fleet distribution. The points' dispersion around the X axis suggests, in contrast, high inconsistencies on location/aggregation of SNAP-7 activities; spatial repartition differs in a range of factor 0.2 -5. In SNAP-1,3,4 (see Fig.4.5), points are completely spread; meaning that both, EFs and activity data, disagree spatially between EDGAR and the local EI.

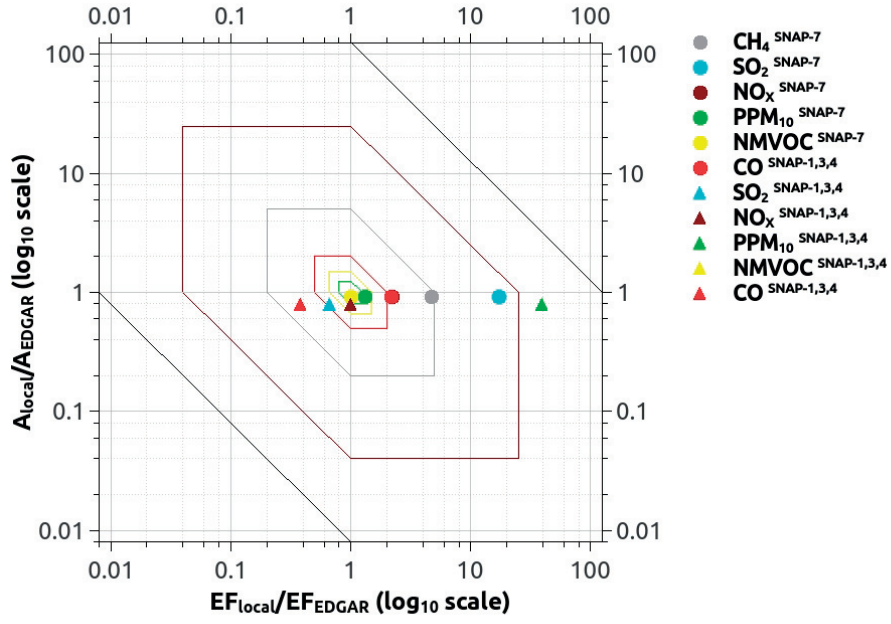


Figure 4.3: Diamond diagram: Activity-emission factor diagram for the macro-sectors SNAP-1,3,4 and SNAP-7, and pollutants CO, NMVOC, NO_x, PPM₁₀, SO₂, CH₄

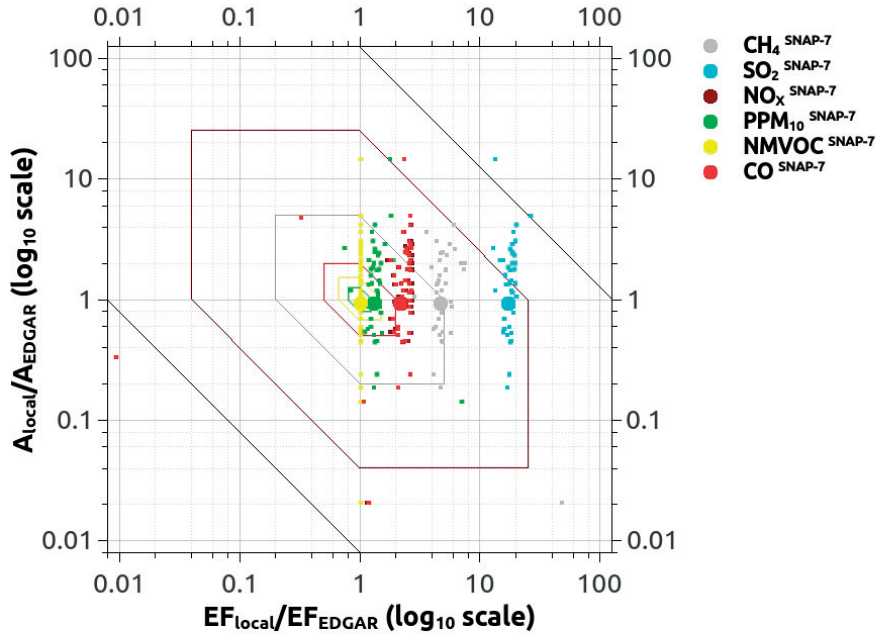


Figure 4.4: Diamond diagram for SNAP-7 with cell by cell ratios. The circles represent coarse comparison by pollutant. The point cloud presents a cell by cell comparison

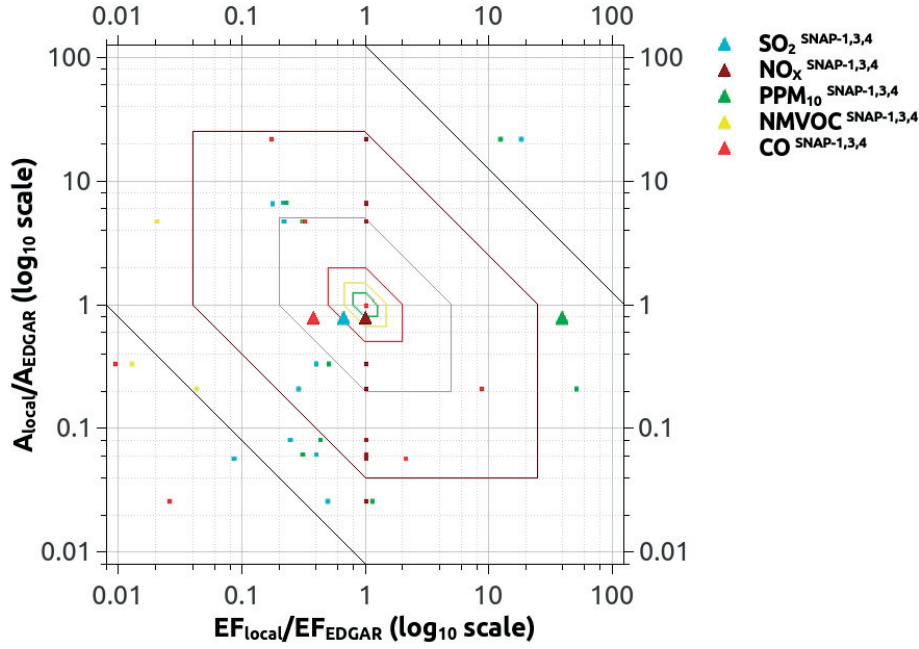


Figure 4.5: Diamond diagram for SNAP-7 with cell by cell ratios. The circles represent coarse comparison by pollutant. The point cloud presents a cell by cell comparison

4.4 Conclusions

A local inventory was compared with EDGAR CO, NMVOC, PM10, NOx, SO2 and CH4 data over Havana by applying benchmarking tools. This kind of comparison allows for an informed evaluation of whether discrepancies are related to differences in the use of emission factors or in the choice of activity data. Differences due to total activity levels are relatively low. EDGAR slightly overestimated total activities of road transport, energy and industrial sectors with respect to the local EI. This can point to the fact that EDGAR uses internationally available activity data and approximations. Differences as a result of different EFs are relatively large. For instance in the case of CO, SO2 and PPM10 from combustion in the energy, manufacturing and transformation industries, EDGAR use higher EFs than local ones by factors 3, 1.5 and 25 respectively. For road transport sector, the EF of PM10, CO and NOx are within a factor of 2, while CH4 and SO2 are around 5 to 20 times higher. Differences due to spatial distribution of emissions were also analyzed. Overall, EDGAR provided spatially smoother results and has relatively lower values in hotspot areas. In particular the spatial patterns from road transport sources are fairly consistent for NMVOC and PM10. However, in the case of NOx, SO2 and CH4, EDGAR estimates are lower for most of grid-cells. These are likely due to the aforementioned differences in EFs. Hotspots areas for stationary sources differ between both inventories; it seems that the choices on both, EFs and activity data, differ spatially. In the gridded local inventory, CO and NOx hotspots were in correspondence with the activity of important sources of combustion in the energy sector, while manufacturing and transformation industries (e.g. cement and iron industries) have high contributions to hotspot areas of PM10. No inventory is 100% accurate, nor is the inventory of Havana. Both, the country and EDGAR could improve emissions report. However local ones should probably be more accurate than global ones. Thus, EDGAR can be regionally accepted as a reference but it is not recommended for air quality simulation over Cuba. A more complete reporting must be expected when more official national data become available. A review and evaluation of local emission inventories over Cuba can be useful for identifying potential areas for future improvement.

References

- Abdallah, C., K. Sartelet, and C. Afif (2016). “Influence of boundary conditions and anthropogenic emission inventories on simulated O₃ and PM_{2.5} concentrations over Lebanon”. In: *Atmospheric Pollution Research* 7.6, pp. 971–979.
- Alonso, M. F., K. M. Longo, S. R. Freitas, R. Mello da Fonseca, V. Marécal, M. Pirre, and L. G. Klenner (2010). “An urban emissions inventory for South America and its application in numerical modeling of atmospheric chemical composition at local and regional scales”. In: *Atmospheric Environment* 44.39, pp. 5072–5083.
- Álvarez Hymelín, R. (2010). “Modelos de emisión para la evaluación de la contaminación ambiental provocada por el tráfico urbano”. PhD thesis. CUJAE.
- Amstel, A. van, J. Olivier, and L. Janssen (1999). “Analysis of differences between national inventories and an Emissions Database for Global Atmospheric Research (EDGAR)”. In: *Environmental Science & Policy* 2.3, pp. 275–293.
- Barker, T., I. Bashmakov, L. Bernstein, J. E. Bogner, P. R. Bosch, R. Dave, O. R. Davidson, B. S. Fisher, S. Gupta, G. J. Heij, S. K. Ribeiro, S. Kobayashi, M. D. Levine, D. L. Martino, O. Masera, B. Metz, L. A. Meyer, A. Najam, N. Nakicenovic, J. Roy, J. Sathaye, R. Schock, P. Shukla, R. E. H. Sims, P. Smith, D. A. Tirpak, D. Zhou, and U. Kingdom (2007). *IPCC Technical Summary. Contribution of Working Group III to the Fourth Assessment Report of the Intergovernmental Panel on Climate Change*. Tech. rep.
- Bel, G. and S. Joseph (2015). “Emission abatement: Untangling the impacts of the EU ETS and the economic crisis”. In: *Energy Economics* 49, pp. 531–539.
- Biart Hernández, R. (2000). “Determinación de factores de emisión para el monóxido de carbono, provocado por el transporte automotor por carretera en Cuba.” PhD thesis. Instituto Superior Politécnico “José Antonio Echeverría. CUJAE.
- CIESIN, C. f. I. E. S. I. N. and S. D. A. C. SEDAC (2010). *Gridded population of the world - for population 1990, 1995, 2000, 2005, 2010*. Tech. rep.
- Contreras Peraza, H., L. M. Turtós Carbonell, and J. A. Rodríguez Zas (2014). “Inventario de emisiones espacialmente distribuido para estudios de la química atmosférica en Cuba”. PhD thesis.
- (FAO), F. and A. O. of the United Nations (2008). “Background Paper 4 FAO datasets on land use , land use change , agriculture and forestry and their applicability for national greenhouse gas reporting A background paper for the IPCC Expert meeting on Guidance on Greenhouse Gas Inventories of Land Uses su”. In: *Agriculture* May, pp. 1–16.
- Fernández Martínez, P. I., R. W. I. Manso Jiménez, A. I. Wallo Vázquez, A. V. I. Guevara Velazco, A. I. León Lee, M. E. O. García Sampedro, E. O. Martínez Mendoza, G. O. Legañoa Martínez, J. J. C. Alea Díaz, I. C. López López, D. C. Pérez Martín, J. M. C. Ameneiros, and S. C. Pire Rivas (1996). *Inventario nacional de emisiones y absorciones de gases de invernadero*. Tech. rep.
- Font, A. and G. W. Fuller (2016). “Did policies to abate atmospheric emissions from traffic have a positive effect in London?” In: *Environmental Pollution* 218, pp. 463–474.
- François, S., E. Grondin, S. Fayet, and J. L. Ponche (2005). “The establishment of the atmospheric emission inventories of the ESCOMPTE program”. In: *Atmospheric Research* 74.1-4, pp. 5–35.
- Fu, X., S. Wang, B. Zhao, J. Xing, Z. Cheng, H. Liu, and J. Hao (2013). “Emission inventory of primary pollutants and chemical speciation in 2010 for the Yangtze River Delta region, China”. In: *Atmospheric Environment. Part A. General Topics* 70, pp. 39–50.
- Garcia, F., G. Curci, and M. Lanfri (2015). “First Implementation of the WRF-CHIMERE-EDGAR Modelling System Over Argentina”. In: 14.8, pp. 1–11.
- Gil-Alana, L. A. and S. A. Solarin (2017). “Have U.S. environmental policies been effective in the reduction of U.S. emissions? A new approach using fractional integration”. In: *Atmospheric Pollution Research*.
- Granier, C., B. Bessagnet, T. Bond, A. D’Angiola, H. D. van der Gon, G. J. Frost, A. Heil, J. W. Kaiser, S. Kinne, Z. Klimont, S. Kloster, J. F. Lamarque, C. Lioussé, T. Masui, F. Meleux, A. Mieville, T. Ohara, J. C. Raut, K. Riahi, M. G. Schultz, S. J. Smith, A. Thompson, J. van Aardenne, G. R. van der Werf, and D. P. van Vuuren (2011). “Evolution of anthropogenic and biomass burning emissions of air pollutants at global and regional scales during the 1980-2010 period”. In: *Climatic Change* 109.1, pp. 163–190.
- Grigoroudis, E., F. D. Kanellos, V. S. Kouikoglou, and Y. A. Phillis (2016). “Optimal abatement policies and related behavioral aspects of climate change”. In: *Environmental Development* 19, pp. 10–22.

- Guevara, M., S. Lopez-Aparicio, C. Cuvelier, L. Tarrason, A. Clappier, and P. Thunis (2017). “A benchmarking tool to screen and compare bottom-up and top-down atmospheric emission inventories”. In: *Air Quality, Atmosphere and Health* 10.5, pp. 627–642.
- (IAE), I. E. A. (2008). *World energy outlook*. Tech. rep. International Energy Agency.
- INECC (2015). *Inventario Nacional de Emisiones de Gases y Compuestos de Efecto Invernadero*. Tech. rep.
- IPCC, I. P. o. C. C. (2006). *EFDB – User Manual for WEB Application. Appendix A : Criteria to be used in the evaluation by the EFDB Editorial Board*. Tech. rep., pp. 37–57.
- Janssens-Maenhout, G., M. Crippa, D. Guizzardi, F. Dentener, M. Muntean, G. Pouliot, T. Keating, Q. Zhang, J. Kurokawa, R. Wankmüller, H. Denier Van Der Gon, J. J. Kuenen, Z. Klimont, G. Frost, S. Darras, B. Koffi, and M. Li (2015). “HTAP-v2.2: A mosaic of regional and global emission grid maps for 2008 and 2010 to study hemispheric transport of air pollution”. In: *Atmospheric Chemistry and Physics* 15.19, pp. 11411–11432.
- Janssens-Maenhout, G., V. Pagliari, D. Guizzardi, and M. Muntean (2013). *Global emission inventories in the Emission Database for Global Atmospheric Research (EDGAR) – Manual (I): Gridding: EDGAR emissions distribution on global gridmaps*. Tech. rep. JRC Report, EUR 25785 EN, ISBN 978–92–79–28283–6.
- Jena, C., S. D. Ghude, G. Beig, D. Chate, R. Kumar, G. Pfister, D. Lal, D. E. Surendran, S. Fadnavis, and R. van der A (2015). “Inter-comparison of different NOX emission inventories and associated variation in simulated surface ozone in Indian region”. In: *Atmospheric Environment* 117, pp. 61–73.
- (JRC), E. C.-J. R. C. (2009). *EDGAR shows worldwide greenhouse gas emissions growing faster*.
- (JRC), E. C.-J. R. C. and N. E. A. A. (PBL) (2011). *Emission Database for Global Atmospheric Research (EDGAR), release version 4.2*. Tech. rep. European Commission, Joint Research Centre (JRC)/Netherlands Environmental Assessment Agency (PBL).
- Kumar, A., A. Rincón, and N. Rojas (2010). “Application of WRF-Chem model to simulate ozone concentration over Bogota Key words : WRF-Chem , Air Quality Modeling , Ozone , Bogota Model Description and Evaluation Episode Selection WRF-Chem Model Configuration”. In: pp. 1–6.
- López-Aparicio, S., M. Guevara, P. Thunis, K. Cuvelier, and L. Tarrasón (2017). “Assessment of discrepancies between bottom-up and regional emission inventories in Norwegian urban areas”. In: *Atmospheric Environment* 154, pp. 285–296.
- Madrazo, J. and A. Clappier (2018a). “Low-cost methodology to estimate vehicle emission factors”. In: *Atmospheric Pollution Research* 9.2, pp. 322–332.
- Madrazo, J., A. Clappier, L. Carlos, O. Cuesta, H. Contreras, and F. Golay (2018b). “Screening differences between a local inventory and the Emissions Database for Global Atmospheric Research (EDGAR)”. In: *Science of the Total Environment* 631-632, pp. 934–941.
- Mena-Carrasco, M., G. R. Carmichael, J. E. Campbell, D. Zimmerman, Y. Tang, B. Adhikary, A. D’Allura, L. T. Molina, M. Zavala, A. García, F. Flocke, T. Campos, A. J. Weinheimer, R. Shetter, E. Apel, D. D. Montzka, D. J. Knapp, and W. Zheng (2009). “Assessing the regional impacts of Mexico City emissions on air quality and chemistry”. In: *Atmospheric Chemistry and Physics* 9.11, pp. 3731–3743.
- Muntean, M., G. Janssens-Maenhout, S. Song, N. E. Selin, J. G. J. Olivier, D. Guizzardi, R. Maas, and F. Dentener (2014). “Trend analysis from 1970 to 2008 and model evaluation of EDGARv4 global gridded anthropogenic mercury emissions.” In: *The Science of the total environment* 494-495, pp. 337–50.
- Ohara, T., H. Akimoto, J. Kurokawa, N. Horii, K. Yamaji, X. Yan, and T. Hayasaka (2007). “An Asian emission inventory of anthropogenic emission sources for the period 1980–2020”. In: *Atmospheric Chemistry and Physics* 7, pp. 4419–4444.
- ONE (2016c). *Anuario Estadístico de Cuba. Section 2: Medio Ambiente*. Tech. rep.
- Parrish, D. D., W. C. Kuster, M. Shao, Y. Yokouchi, Y. Kondo, P. D. Goldan, J. A. de Gouw, M. Koike, and T. Shirai (2009). “Comparison of air pollutant emissions among mega-cities”. In: *Atmospheric Environment* 43.40, pp. 6435–6441.
- Penman, J., M. Gytarsky, T. Hiraishi, W. Irving, and T. Krug (2006). *2006 IPCC GUIDELINES FOR NATIONAL GREENHOUSE GAS INVENTORIES*. Tech. rep.
- Pulles, T. T.-M., R. T.-M. Brand, J. . I. Pereira, B. . I. Mota, L. A. M. f. B. Spessa, P. Schulz, Jena Michael (LSCE, and H. Hoelzemann, Judith (MPI for Meteorology (2003). *REanalysis of the TRpospheric chemical composition over the past 40 years. A long term global modeling study of tropospheric chemistry funded under the 5th EU framework programme*. Tech. rep.
- QGIS Development Team (2015). *QGIS Geographic Information System. Open Source Geospatial Foundation Project*.

- Quoc Ho, B., A. Clappier, and N. Blond (2014). “Fast and Optimized Methodology to Generate Road Traffic Emission Inventories and Their Uncertainties”. In: *CLEAN - Soil, Air, Water* 42.10, pp. 1344–1350.
- Russell, A. and R. Dennis (2000). “NARSTO critical review of photochemical models and modeling”. In: *Atmospheric Environment* 34.12-14, pp. 2283–2324.
- Sheng, J.-X., D. J. Jacob, J. D. Maasakkers, M. P. Sulprizio, D. Zavala-Araiza, and S. P. Hamburg (2017). “A high-resolution (0.1 0.1) inventory of methane emissions from Canadian and Mexican oil and gas systems”. In: *Atmospheric Environment* 158, pp. 211–215.
- Smith, S., Y. Zhou, P. Kyle, H. Wang, and H. Yu (2015). *A Community Emissions Data System (CEDS): Emissions for CMIP6 and beyond*. Tech. rep.
- Thunis, P., B. Degraeuwe, K. Cuvelier, M. Guevara, L. Tarrason, and A. Clappier (2016a). “A novel approach to screen and compare emission inventories”. In: *Air Quality, Atmosphere and Health* 9.4, pp. 325–333.
- transporte), D.-C. del (2000). *Estudio del transporte en la capital*. Tech. rep. La Habana.
- Turtós Carbonell, L. M., G. Mastrapa Capote, E. Ruiz Meneses, D. Alonso García, O. Santos Cuesta, L. Escudero Alvarez, A. Morlot Bezanilla, I. Montejó Borrajero, and M. Fonseca Hernández (2011). *Estimación del impacto del ozono troposférico derivado de fuentes del sector energético. Código del proyecto: PRN/4-1/1 -2008. Salida No3: Resultados de la modelación de la formación de ozono troposférico: Evaluación de la contaminación atmosférica por oz.* Tech. rep. 3.
- Viaene, P., S. Janssen, C. Carnevale, G. Finzi, E. Pisoni, M. Volta, A. Miranda, C. Gama, A. Martili, J. Douros, E. Real, A. Clappier, J.-l. Ponche, A. Graff, P. Thunis, and K. Juda-rezler (2012). *at regional and local scale 1 Summary*. Tech. rep. 303895.
- Wang, S. X., L. Zhang, G. H. Li, Y. Wu, J. M. Hao, N. Pirrone, F. Sprovieri, and M. P. Ancora (2010). “Mercury emission and speciation of coal-fired power plants in China”. In: *Atmospheric Chemistry and Physics* 10, pp. 1183–1192.
- Zhang, Q., D. G. Streets, G. R. Carmichael, K. He, H. Huo, A. Kannari, Z. Klimont, I. Park, S. Reddy, J. S. Fu, D. Chen, L. Duan, Y. Lei, L. Wang, and Z. Yao (2009). “Asian emissions in 2006 for the NASA INTEX-B mission”. In: *Atmospheric Chemistry and Physics Discussions* 9.1, pp. 4081–4139.
- Zhanga, X. and Y. Wanga (2017). “How to reduce household carbon emissions: A review of experience and policy design considerations”. In: *Energy Policy* 102, pp. 116–124.
- Zhao, B., W. Shuxiao, N. M. Donahue, C. Wayne, L. H. Ruiz, N. L. Ng, Y. Wang, and J. Hao (2015). *Evaluation of one-dimensional and two-dimensional volatility basis sets in simulating the aging of secondary organic aerosol with smog-chamber experiments*. Tech. rep. May.
- Zhao, Y., Y. Zhou, L. Qiu, and J. Zhang (2017). “Quantifying the uncertainties of China’s emission inventory for industrial sources: From national to provincial and city scales”. In: *Atmospheric Environment* 165, pp. 207–221.
- Zheng, J., L. Zhang, W. Che, Z. Zheng, and S. Yin (2009). “A highly resolved temporal and spatial air pollutant emission inventory for the Pearl River Delta region, China and its uncertainty assessment.” In: *Atmospheric Environment* 43, pp. 5112–5122.
- Zhou, Y., Y. Zhao, P. Mao, Q. Zhang, J. Zhang, L. Qiu, and Y. Yang (2017). “Development of a high-resolution emission inventory and its evaluation and application through air quality modeling for Jiangsu Province, China”. In: *Atmospheric Chemistry and Physics* 17, pp. 211–233.

Chapter 5

Setting a Source-Receptor Relationship (SRR) for the assessment of emission reduction strategies over Cuba

Quantifying the contribution from emission sources to pollutant concentration is a crucial step on designing effective air quality strategies. These quantifications are commonly performed through simulations from deterministic chemical transport models. The approach is very accurate but high-demanding on data and computational performances. It results in a challenging issue for a region in developing world to afford these tools. Thus, the use of simplified approaches usually referred to as source-receptor relationships SRR, can make substantial helping to cope with computing power limitations. In this regard, this chapter presents an example study which sets up a SRR over Cuba. It was built upon the approach of Pisoni et al., 2017 –a weighted kernel function that spatially links emissions and concentrations over a given domain-, and includes two different techniques for enhancing the Cuban forecaster. The model was derived at 24 km spatial resolution and accounts for the effects of NH₃, SO₂, PPM, NO_x and VOC emission reductions on annual average concentrations of PM₂₅, NO_x and O₃. It opens up a new outlook in designing pollution reduction strategies in Cuba.

5.1 Introduction

In recent years, air pollution has been widely regarded as intensifying climate change effects and human health risks. Its economic burden is immense; it stunts economic growth and exacerbates poverty and inequality (World Bank 2018). Their impacts are overwhelmingly felt in low and middle-income countries where emissions rise in the absence of strict air quality policies (WHO Regional Office for Europe 2016) and live about 94% of adults and children affected by pollution-related illnesses (Landrigan et al. 2016).

In order to curb pollution effects, it is important to know which emissions to reduce and to which extent (Meij et al. 2009). So that, quantifying the contribution from emission sources to pollutant concentration is a crucial step to develop effective strategies. Scenarios analysis through deterministic chemical transport modelling (CTM) is the most commonly used approach to deal with such assessments (Carnevale et al. 2014). It includes the complex nature of physical-chemical processes and treat several precursors simultaneously, each modifying concentration levels of a particular pollutant. The approach is very accurate to forecast improvements and to understand the causes of pollution; but concerns arise from the requirement of detailed information on the regional situation (i.e. meteorological conditions and regional emissions), and its high demanding computational time (Thunis et al. 2016b). As consequence, in most of developing countries, it is challenging for scenarios analysis from CTM implementations. There, the use of simplified approaches usually referred to as source-receptor relationships SRR (cf. Amann et al. 2004; Andrew Kelly 2006; Carnevale et al. 2012a,b; Clappier et al. 2015; Oxley et al. 2013; Pisoni et al. 2009), can make substantial helping on designing pollution reduction strategies. Indeed, SRR includes simplifying assumptions to cope with the lack of computer resources (Pisoni et al. 2017; Thunis et al. 2015); it handles limits on time-scale operations and levels up emission reductions.

This chapter presents an example study which sets up a SRR over Cuba. The first step consisted in performing simulations with a full CTM based on a regional emission inventory (referred to as the base-case); results are analysed statistically for understanding the interrelationships of atmospheric pollutants, and the temporal variation in their concentration profiles. That is providing insights into the behaviour and key relationships among them. Since the focus is on simplifying tools for scenarios analysis we explore model responses of proxy pollutants (EEA 2008), such as ozone, particulate matter and nitrogen oxides; and perform emission reductions of associated precursors (i.e. NO_x, VOC, NH₃, SO_x and primary particulate matter PPM). For arbitrary percentages of emission reductions covering a desired range of applications, a set of CTM simulations allow to understand the relationships among abatement scenarios and then to construct the simplified forecaster (SRR, cf. Clappier et al. 2015; Pisoni et al. 2017) of Cuban concentrations. An evaluation of the SRR capacity to mimic the CTM on different applications is finally performed as a validation step.

5.2 Model set up

The CTM CHIMERE (Mailler et al. 2017; Menut et al. 2013) was used to perform the simulations over Cuba. Their chemical mechanism Melchior describes 120 reactions involving 44 species including processes like chemistry, transport, vertical diffusion, photo-chemistry, dry deposition, in-cloud and below-cloud scavenging and heterogeneous hydrolysis on aerosol surfaces. The model consists of 8 hybrid sigma pressure levels, up to 500hPa (± 5500 m), with the top of the first layer around 40m. At a resolution of 0.2°, simulations were driven by a regional anthropogenic EI and WRF meteorological fields; biogenic emissions were built up on runtime from MEGAN database (Guenther et al. 2012) and monthly mean values of LMDZ-INCA database (Hauglustaine et al. 2004) delivered the chemical boundary conditions.

5.2.1 Emission inventory

The regional EI focused on seven pollutant precursors (i.e. CO, NO_x, SO_x, NH₃, NMVOC, PM₁₀ and CH₄) from anthropogenic sources spread on SNAP sector classification. Emissions from combustion in energy and transformation industries (S1) were calculated for each source location by using local activity levels and emission factors either measured (Abreu Elizundia et al. 2016; Meneses-ruiz et al. 2018), or carefully set out from “AP42, Compilation of Air Pollutant Emission Factors”, EPA 2016. For residential sector (S2), emissions were estimated according to carburant consumptions reported by the energy section of (ONE 2016b) and emission factors from (EPA 1998, 2016; GCE 2006; Haneke 2003). They were distributed as polygon area sources with boundaries defined by population percentages as surrogate spatial dataset.

Emissions from transport sector (S7) were computed by using the EMISENS model (Quoc Ho et al. 2014) according to the average activity levels of Cuban vehicular fleet (ONE 2016a), classified in five vehicle categories (i.e. gasoline and diesel passenger, heavy vehicles, buses and motorcycles) and spared into five road categories (i.e. semi-urban, urban, locals and neighbourhood streets) –for examples on data and methods behind the transport EI of Cuba, the reader is referred to (Madrado et al. 2018a,b). The road network lengths repartition provided by (OpenStreetMap contributors, 2017) was judged as the most closely spatial representation and therefore traffic emissions distributed as such. Emissions from combustion in manufacturing industry (S3), production processes (S4), solvent and other product use (S6), waste treatment and disposal (S9) and agriculture (S10) were compiled from the environmental section of (ONE 2016c). The geographical location (latitude and longitude) of stationary sources were set out from the Cuban State Registration of Companies and Budgeted Units in (ONE 2010); then, GIS tools used to spatially summarize emission-sectors uniformly at location-grids. For agriculture, the spatial distribution was driven by the Global Land Cover Facility GLCF-Cropland database, which supplies an extensive agricultural land classification from remotely sensed satellite data including built-up, water, snow, forest, savannas and shrub, grass and crop lands (Channan et al. 2014; Friedl et al. 2010).

5.2.2 Meteorological fields

Meteorological fields needed to model aerosol and photochemistry in CHIMERE (e.g. humidity, air temperature, pressure, wind fields and planetary boundary layer height, etc.) were produced with WRF model (National Centers for Environmental Prediction NOAA, U.S. Department of Commerce 2000). This model has been previously used for Cuban meteorological studies (cf. Hernández Garces et al. 2017; Moya Álvarez et al. 2014; Rodríguez Roque et al. 2016; Verde Valdés et al. 2015). Bits of advice for setting up parametrizations and in data entries better forecasting Cuban weather were provided by (Baró Pérez et al. 2018; Sierra-Lorenzo et al. 2014; Turtós Carbonell et al. 2013); such as they supported, the present study selects settings already tested in countries of the Caribbean region. It uses NCEP database (National Centers for Environmental Prediction NOAA, U.S. Department of Commerce 2000) -spatial and temporal resolutions of 1 degree and 6 hours respectively, and 28 eta levels in height- for boundary and initial conditions, as well as the lowest resolution options of the static geographic data available. For details on selected physical parametrizations see Sierra-Lorenzo et al. 2014 which provides the more suitable for WRF forecasts in Cuba. The grid model uses one-domain of 12 km resolution (rectangular mesh of 130 and 46 cells) over one-year period from 1/1/2015 to 31/12/2015 inclusive. Simulations cover the Cuban island with a Lambert Conic Conformal (LCC) projection centred at 22.19 N and 79.52 W.

5.3 Statistical analysis

The CTM delivered pollutant concentration fields describing the complex mixture of pollution in ambient air. Some pollutants such as particulate matters (PM₂₅), ozone (O₃) and nitrogen oxides (NO_x) are investigated as proxies of this mixture. The impact attributed to a single one may actually be partly due to the other pollutants (WHO Regional Office for Europe 2016), their precursors and the influence of meteorological fields, e.g. temperature variation. Therefore, a good understanding of the model responses in terms of these pollutant interrelationships and profiles could be the key for concisely representing the entire mix under all circumstances, and to facilitate further scenarios-based analysis. In this attempt, the study of non-linear effects which are explicitly incorporated in CTMs results challenging. According to (Thunis et al. 2015), those that are associated with precursor interactions can be neglected for yearly average pollutant levels. That is for here, we investigate the kind of statistical relationships resulting from yearly averages of computed hourly concentrations.

5.3.1 Relationships between the main species

Firstly, Pearson correlation coefficients relating pairwise data series on hour-by-hour base (i.e. a data series at each hour from 00h00 to 23h00 indexed in cell-by-cell order) of yearly average concentrations were calculated for NO_x, PM₂₅ and O₃. For NO_x, all series of one-hour data were strongly correlated each other in a range of 0.83-0.98. Good correlations (0.60-0.99) were also found between series of PM₂₅. O₃ exhibited a diurnally varying temporal correlation structure which can be explained by mechanisms of diurnal production, accumulation and depletion of ozone; and its dependency on air temperature and

solar radiation: The series within the bunches of 13h00-16h00 and 21h00-08h00 internally correlated very well, i.e. 0.83-0.98 and 0.84-0.99 respectively; but the crossed series from both bunches uncorrelated. The remaining series (i.e. do not belonging to any bunch) of O3 are less-correlated with the series in bunches and interpreted as transition situations in which ozone varies from day to night average levels. Following these bits of pollutant profiles, PM25 and NOx concentrations were summarized in hourly averages of a year as “NO2 mean” and “PM25 mean” while ozone levels were aggregated on “O3 day” and “O3 night” averages. In addition to these sorts of indicators, we consider important to calculate the yearly averages of nitrogen dioxides and primary particulate matters (here referred to as “NO2 mean” and “PPM mean”) as they can complement information on NOx and PM respectively; as well as SOMO35 (i.e. sum of maximum 8-hours ozone levels over 35 ppb for a year) since it summarizes ozone diurnal variations.

Secondly, we analyse whether these indicators are related linearly. In Fig.5.1 -cf. table 5.1, the bipolar plot of a Principal Component Analysis (PCA) shows several interrelationships: (i.) “NO2 mean” and “NOx mean” loading arrows closed in direction and orientation to “PPM mean” in the main principal component evidence their strong correlations; the three pollutant do vary together, locations of hotspots may be similar and likely induced by common emission sources; (ii.) the high loading arrow of “O3 night”, pointing also closed to the most-varying direction of the main principal component but with opposite orientation to “NOx mean” is probably due to simulating night reaction of ozone with the nitrogen dioxides concentrations that remain from nitric oxides titration effects; (iii.) the orthogonality between “O3 day” loading arrow with respect to “O3 night” indicates situations subject to linear unrelationshipness; it may indeed consider particular photochemistry mechanisms of “O3 day” formation which are in reality complex and highly non-linear processes (EEA, 2008b); (iv.) SOMO35 is strongly correlated with the second principal component and “O3 day” correlates very well; it suggests that SOMO35 primarily varies with “O3 day” levels; (v.) “PM25 mean” loading arrow between the primarily measures of “PPM mean” and “O3 day” firstly suggests that PM25 variation is partly due to PPM but may be highly influenced by the reaction of other gases and particles; and secondly that areas with high “O3 day” levels may tend to experience high PM25 levels.

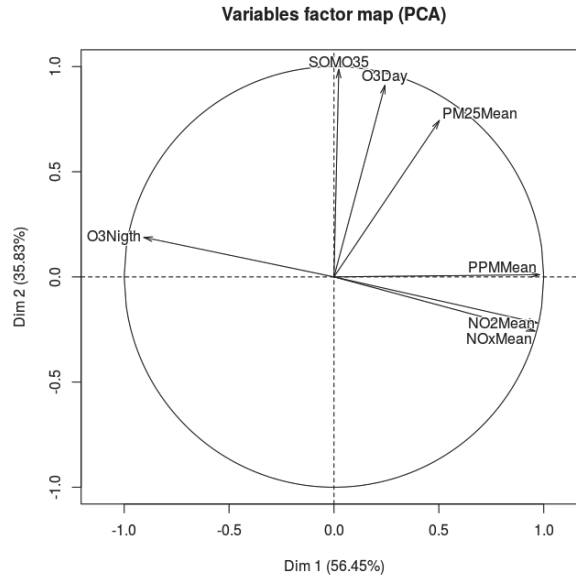


Figure 5.1: Bipolar plot showing relationships between hourly mean of PPM, PM25, NOx, NO2, O3 day and night, as well as the indicator SOMO35.

Fig.5.2 shows the scatter plots of identified interrelationships: As expected, SOMO35 values appear highly influenced by O3 day levels. A positive linear relationship does appear between PPM mean and NOx mean concentrations; it means that a rise in PPM is indeed coupled with a rise in NOx for each individual grid point. The best fit relationship of O3 night vs NOx mean pass through an exponential function: For most of grid points (between 5-20ppb-vol NOx levels), O3 night rates decrease with increasing NOx at almost equal amounts. At grid points of low NOx levels (<5ppb-vol) a higher rate of O3 night production are estimated with decreases in NOx; in contrast at higher NOx levels, O3 night lower production rates

Table 5.1: Overview of PCA results, correlations (Corr) and loadings (Contrib) of variables with respect to the main principal components (PC)

	PC1 (56.4%)			PC2 (35.8%)		
	Correl	Contrib	p.value	Correl	Contrib	p.value
PPM mean	0.98	24.33	3.33e-187	-	0.01	-
PM25 mean	0.50	6.39	2.65e-18	0.74	22.06	9.27e-48
NO2mean	0.97	23.77	1.32e-161	-0.22	1.90	3.48e-04
NOx mean	0.96	23.21	1.05e-143	-0.26	2.62	2.28e-05
O3day	0.24	1.50	6.37e-05	0.91	33.15	2.57e-103
O3night	-0.91	20.78	5.79e-100	0.18	1.41	2.15e-03
SOMO35	-	0.01	-	0.99	38.83	1.08e-209

appear with increasing NOx. The scatter plot NO2 and NOx shows that these pollutants almost perfectly fit by a polynomial function of second order. According to Wesseling et al. 2008, CTMs often calculate the basic dispersion of NOx while adding chemical effect functions on NO2 formation; and so NO2 may depends on the approach added to determine its value. Indeed, this relation does set non-linearly influenced by a photo-chemical conversion function between nitric oxide and ozone.

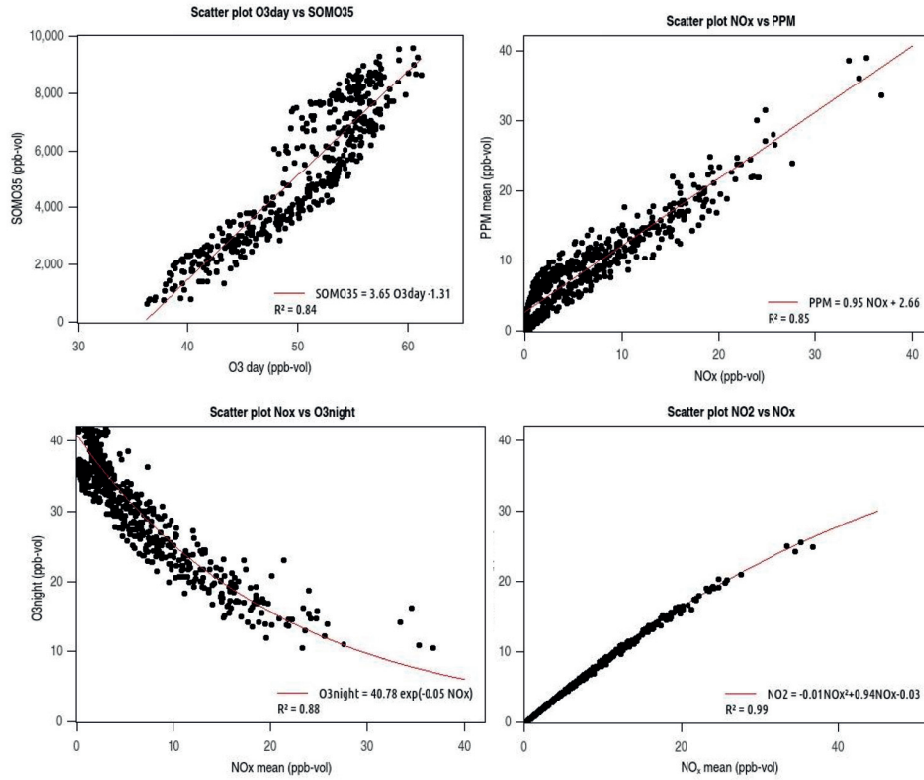
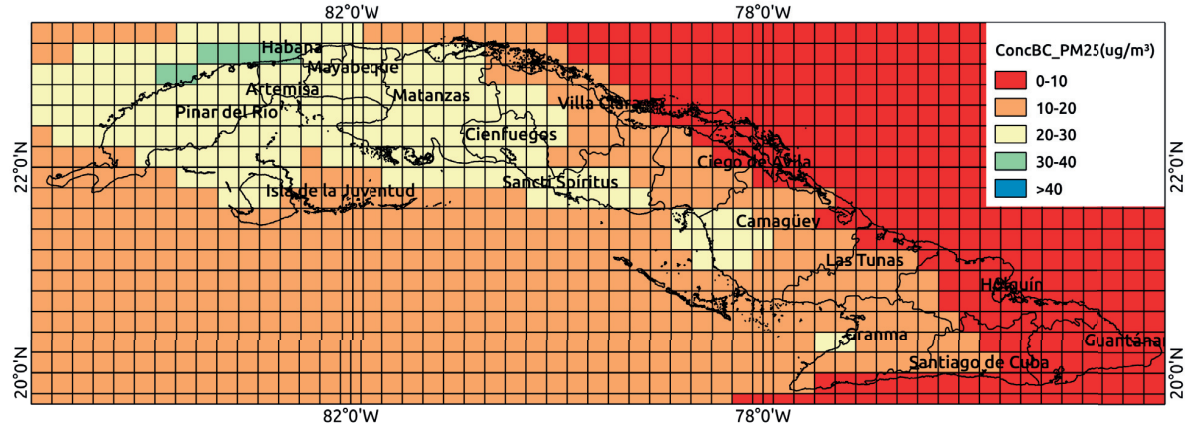


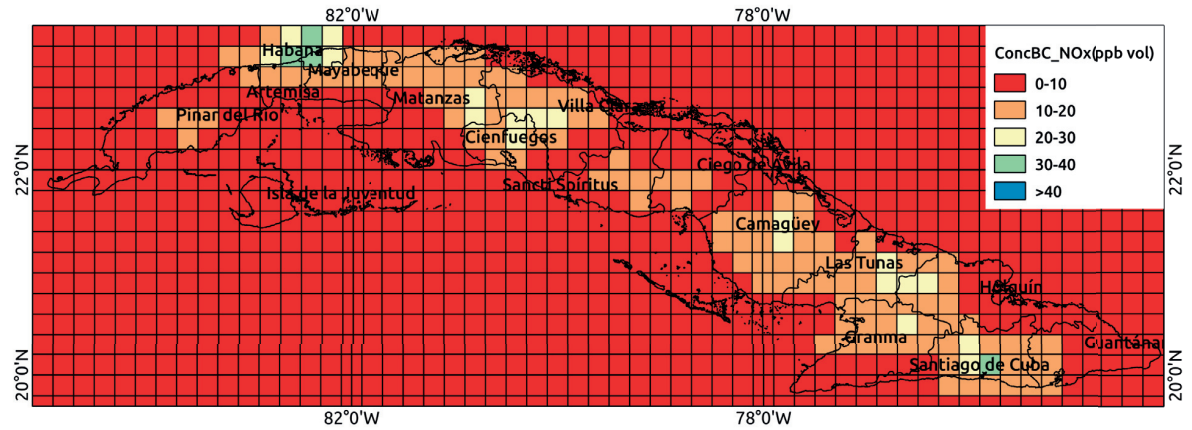
Figure 5.2: Scatter plots of NOx mean vs PPM mean (top-left), NOx mean vs O3 night mean (top-right), O3day vs SOMO35 (bottom-left) and NOx mean vs NO2 mean (bottom-right). Fit line in red colour.

Referring all aforementioned relationships, we consider that NOx mean, PM25 mean and SOMO35 could effectively represent pollution conditions in this study since other pollutant levels of interest could be reasonable derived from them. Its levels do vary spatially depending on prevailing conditions favouring NOx, PM25 and O3 formation. In Fig.5.3, highest NOx levels of 10-40ppb are estimated on urban areas with maximum of 56.8ppb; it points to areas with substantial contributions from road transport emissions.

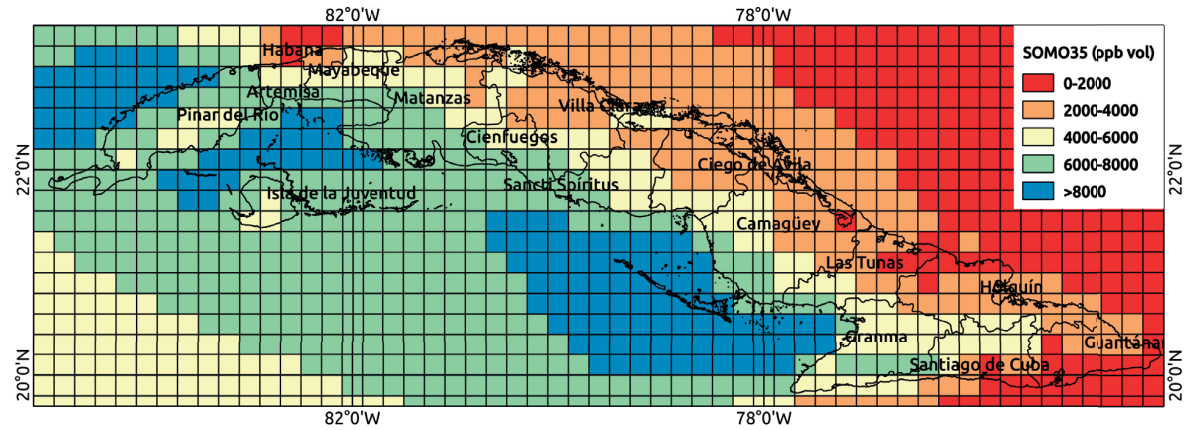
For most of the country land-area, PM₂₅ levels range from 10 to 40 $\mu\text{g}/\text{m}^3$ with a maximum of 75.1 $\mu\text{g}/\text{m}^3$; the highest PM₂₅ levels were computed at western regions which lead to Havana, the capital city. SOMO35 was computed higher in the south-western areas compared to north-eastern ones keeping with lower values in most of urban areas (e.g. for city centres of the provinces Pinar del Río, Havana, Matanzas, Villa Clara, Ciego de Avila). It is probably due to the simulating high NO_x average concentration in urban areas destructing O₃ by rapid reaction with nitric oxides for strong NO titration effects.



(a) Yearly averages of computed PM₂₅ hourly concentrations ($\mu\text{g}/\text{m}^3$)



(b) Yearly averages of computed NO_x hourly concentrations (ppb)



(c) Computed SOMO35 index (ppb)

Figure 5.3: Cuba's pollution maps from CTM simulation

5.3.2 Relationship between abatement scenarios

As the main objective of this study is to simplify the procedure for assessing emission reductions over Cuba, we investigate relationships between possible abatement scenarios. According to Thunis et al. 2015, for yearly average levels, the concentration delta (i.e. the difference between a base-case and an emission reduction scenario) reached from a simulation in which all precursors (denoted by the letter p) are reduced simultaneously by given percentages δ (referred to as $\Delta C_{\{\delta_p\}}^{\{p\}}$ with $\{p\}$ a set of precursors and $\{\delta_p\}$ the set of percentages of emissions which are reduced simultaneously in a given simulation) can be decomposed in individual amounts of pollution (considering δ_p the individual percentages reduced for one precursor at one simulation) triggered by each precursor (the non-linear contributions arising from the interaction among precursors can be neglected):

$$\Delta C_{\{\delta_p\}}^{\{p\}} = \sum_p \Delta C_{\delta_p}^p \quad (5.1)$$

Where $\Delta C_{\delta_p}^p$ is the concentration delta resulting from the emission reduction ($\Delta \bar{E}_{\delta_p}^p$) of one precursor at a time. According to Clappier et al. 2015, this link can be also assumed linear and then mathematically formalized using linear coefficients a^p as:

$$\Delta C_{\delta_p}^p = a^p \Delta \bar{E}_{\delta_p}^p \quad (5.2)$$

When the same set of emission reductions is consistently applied over the whole geographical area, the resulting delta concentration values are directly linked with the average of the base-case emissions (\bar{E}^p) by means of the amount of imposed reduction (δ^p):

$$\Delta \bar{E}_{\delta_p}^p = \delta_p \bar{E}^p \quad (5.3)$$

$$\Delta C_{\delta_p}^p = a^p \delta_p \bar{E}^p \quad (5.4)$$

Thus, the delta concentrations resulting from two different amounts of reductions are expected to relate linearly $\frac{\Delta C_{\delta_1}^{p1}}{\Delta C_{\delta_2}^{p2}} = \frac{\delta_1}{\delta_2}$; and the concentration deltas resulting from a set of simultaneous emission reductions in eq.5.1 can be estimated as follow:

$$\Delta C_{\{\delta_p\}}^{\{p\}} = \sum_p \frac{\{\delta_p\}}{\delta_p} \Delta C_{\delta_p}^p \quad (5.5)$$

In order to corroborate these assumptions for the three selected indicators (i.e. PM25 mean, NOx mean and SOMO35), a set of eight CTM simulations have been performed with different reduction levels. It includes five scenarios setting individual reductions of precursors NOx, VOC, PPM, NH3 and SOx to 50%, and other three resulting from simultaneous reductions at low, middle and high levels, i.e. Scn-low: NOx(10%) SOx(10%) VOC(40%) PPM(40%) NH3(10%); Scn-middle: NOx(50%) SOx(50%) VOC(50%) PPM(50%) NH3(50%); Scn-high: NOx(60%) SOx(60%) VOC(90%) PPM(90%) NH3(60%).

By applying eq.5.5, delta PM25 mean, NOx mean and SOMO35 values of scenarios accounting for simultaneous reductions were estimated from the individual precursor simulations. Fig.5.4 shows that estimates are comparable and scenarios relate linearly regardless of the level of simultaneous reductions. For PM25 and NOx, the bias of estimates are limited to less than $\pm 10\%$; however it seems that strong reductions ($> 50\%$) introduce non-linear effects on ozone concentrations which results in less performant SOMO35 estimations (bias $\pm 30\%$).

This allows us to state that a series of five CTM simulations resulting from individual emission reductions could be effectively used to assess the impacts of simultaneous reductions on yearly average concentrations. It was even effective for applications considering high level simultaneous precursor reductions, with the exception of SOMO35. Only notice that it is valid when emission reductions are applied over the same entire domain because pollutant concentration changes at a given geographical point are affected by the same amount of abatement at every point within the domain. The implicit linear assumptions limit the applicability of this approach to work properly at regional abatements –scenarios in which emissions are reduced over a smaller area than the domain.

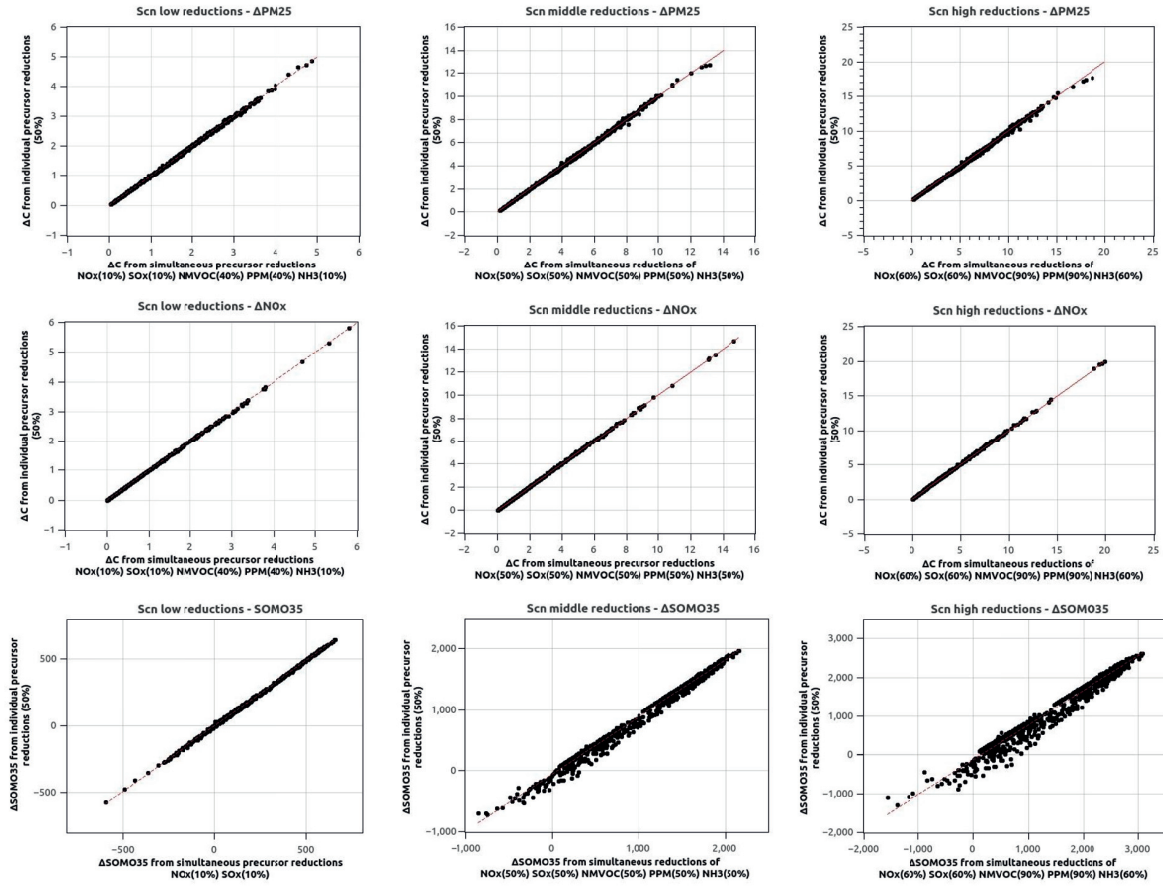


Figure 5.4: Comparison between simulations resulting from simultaneous precursor reductions and the estimates made from individual precursor reductions.

5.4 Source-Receptor relationship

5.4.1 Methodology

To extend the range of the study to regional abatements, we explore the approach of Pisoni et al. 2017 which considers possible spatial differences of the linear relationships (the so-called “spatial flexibility”) between emissions and concentrations deltas in the following way:

$$\Delta C_i = \sum_p^P \sum_j^N a_{ij}^p \Delta E_j^p$$

$$a_{ij}^p = \alpha_i^p (1 + d_{ij})^{-w^p}$$

Where N is the number of grid cells within the domain and P the number of precursors. ΔE_j^p and ΔC_i^p are the emission and concentration deltas; notice they continue linked linearly, so the approach remains valid and could be applied as long as the relationships between emissions and concentrations can be assumed linear. Coefficients a_{ij}^p (unknown parameters) relate each precursor (p) in each emission “source” cell (j) with a concentration “receptor” cell (i) by mean of a “bell-shape” function depending on distance d_{ij} with α_i^p and w^p the amplitude and width respectively. α_i^p is interpreted as the relative importance of each precursor in producing pollutant concentration while w^p indicates how the contribution of a precursor decreases with the distance.

The computational procedure can be performed by a least square estimation; it needs at least $(2 \times P + 1)$ equations available by receptor cell. The solver uses the concentration and emission deltas provided by different scenarios runs as inputs. Thus, each receptor cell provides a different set of inputs (d_{ij} , ΔC_i

and ΔE_j^p) which are used to estimate a unique set of outputs α_j^p and w^p . A “good practice” approach to the robustness and accuracy implies a two steps implementation: the first step treats each precursor individually by using independent simulations that reduce each precursor at a time and performs a least square optimisation using all cells in the domain to estimate α_i^p and w^p . In a second step emission weighted average deltas (i.e. $\sum_j \Delta E_j^p (1 + d_{ij})^{-w^p}$) are computed at each receptor cell by using the coefficient w^p identified in step 1; then a multiple linear regression fit is implemented to calculate more precise values for α_i^p . For more details on the mathematical principles and procedures behind the approach, the reader is referred to the original paper Pisoni et al. 2017, section 3.

5.4.2 Application for NOx, PM25 and SOMO35

In order to implement the SRR bell-shape approach (i.e. from Pisoni et al. 2017) in the Cuba case, we used a set of CTM simulations (see an overview in Table 4) including the 8 scenarios of section 5.3.2 and other 4 that complete the series enough to identify the coefficients. All scenarios applied reductions over the entire modelling domain between 10-90%. Another series of scenarios is dedicated to assess whether SRR is able to reproduce the CTM results for low and high levels of regional emission reductions (see selected regions in Fig.5.5 and their set of emission reductions in table 5.2, scenarios 14-15).

Table 5.2: Set of emission reduction scenarios needed to implement the SRR over Cuba. Scenario 1 represents the base-case set-up in Sec.5.3.2, while the other scenarios are computed applying the % emission reductions as shown in table.

Scen No.		Geog. Area	NOx	VOC	NH3	PPM	SO2
1	BC	Cuba	-	-	-	-	-
2		Cuba	50%	-	-	-	-
3			-	50%	-	-	-
4			-	-	50%	-	-
5			-	-	-	50%	-
6			-	-	-	-	50%
7	Sec.5.3.2	Scn-low	10%	40%	10%	40%	10%
8	Sec.5.3.2	Scn-mid	50%	50%	50%	50%	50%
9	Sec.5.3.2	Scn-high	60%	90%	60%	90%	60%
10			10%	10%	10%	40%	10%
11			10%	40%	40%	40%	10%
12			60%	60%	60%	90%	60%
13			60%	90%	90%	90%	60%
14		Regions in Fig.6	20%	20%	20%	20%	20%
15			80%	80%	80%	80%	80%

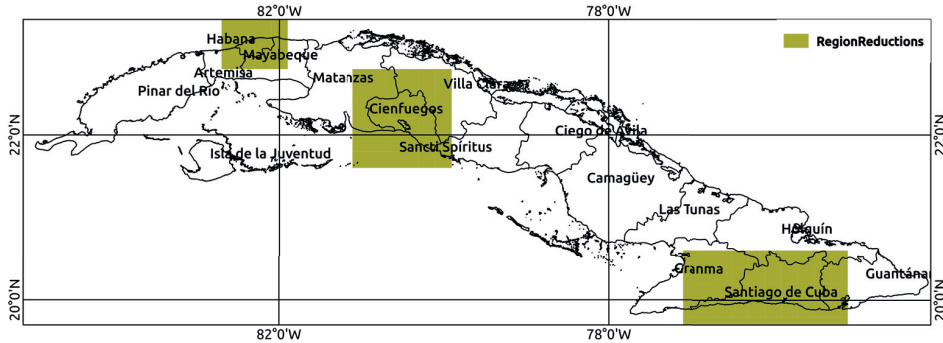


Figure 5.5: Regions selected for validating the SRR.

Results of the SRR are compared with those of CTM in Fig.5.6. In summary, each pollutant indicator exhibited similar dispersion patterns either at low or high reduction levels (i.e. $R(\text{PM}_{25}) \sim 0.73$, $R(\text{NO}_x) \sim 0.93$ and $R(\text{SOMO35}) \sim 0.52$). Among them, NO_x estimates experienced the best fit in comparison to PM_{25} and SOMO35 . For PM_{25} , the larger percentage errors are localized in the outline of the regions where emission reductions were imposed, while for SOMO35 it mostly occurs inside these regions. Next section explores strategies to improve estimates of PM_{25} and SOMO35 .

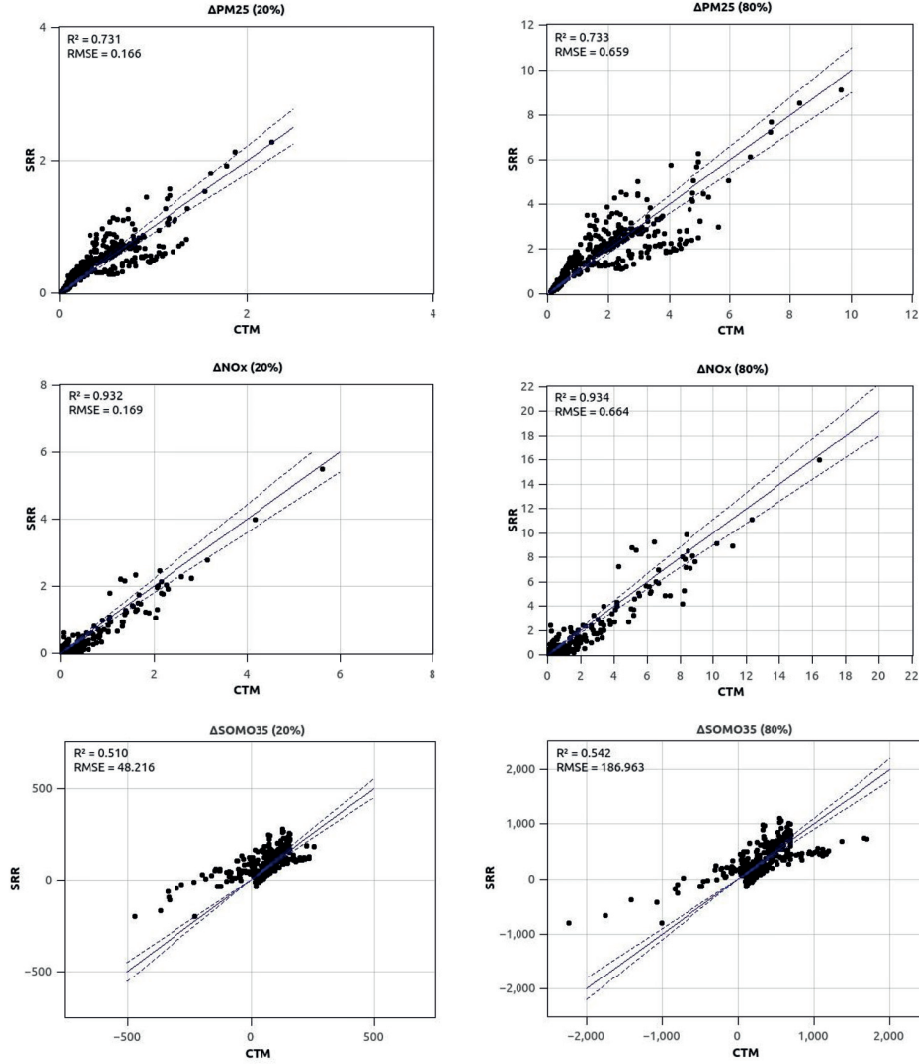


Figure 5.6: Comparison between CTM and SRR bell-shape approach for yearly PM_{25} , NO_x , SOMO35 , with emission reductions applied over Havana, Cienfuegos and Santiago de Cuba at 20 and 80%. Blue dotted lines represent the ± 10 error range

5.4.3 Improvements for PM_{25} and SOMO35

Two different approaches were explored in order to improve the Cuban SRR:

- The first one consists in spatializing the coefficient that indicates how far the contribution of each precursor gets (w^p). It is built on the assumption that each precursor contribution could decrease differently with the distance. So, in the first computational step, each receptor cell accounts for a surrounding window inside which this coefficient is assumed to be constant. The minimum number of

cells (i) inside the windows is forced to be enough to perform a least square calculation of the following formulation:

$$\Delta C_i = \sum_p^P \sum_j^N \alpha_i^p (1 + d_{ij})^{-w_i^p} \Delta E_j^p$$

- (b) The second strategy adds terms of interactions between precursors to the second computational step in order to capture possible non-linear effects. In summary the delta concentrations are computed as:

$$\Delta C_i = \sum_p^P \alpha_i^p \Delta \bar{E}_i^p + \sum_{p'}^P \beta_i^{pp'} |\tilde{E}_i^p| \Delta \bar{E}_i^p$$

with

$$\Delta \bar{E}_i^p = \sum_j \Delta E_j^p (1 + d_{ij})^{-w^p}$$

and

$$|\tilde{E}_i^p| = \sum_j |E_j|^p (1 + d_{ij})^{-w^p}$$

Where $|E_j|^p$ are values resulting from averaging base-case and abatement emissions in a cell j and $\beta_i^{pp'}$ measures the relative weight of each pairwise (p and p') precursors' interactions in producing pollutant concentration.

Applying the proposed approaches, subtle enhancements were found on statistical parameters R and RMSE; it produces lower errors than the traditional Bell-shape approach. Fig5.7-left shows the validation of PM25 for 20% simultaneous-regional emission reductions (scenario 14 in Table 5.7, to be compared with Fig.5.6 top-left). Estimates are basically improved by spatializing the parameter at each cell i with surrounding windows of 2-3 cells (50-70km radius). It points to the fact that PM25 dispersion may have indeed a regional behaviour turning precursors around proximity concentration changes. In Fig.5.7-right (scenario 14 in Table 5.2, to be compared with Fig.5.6 bottom-left), SOMO35 estimates are improved by considering NOx and VOC as precursors, plus the interactions of PPM with NOx, VOC, SOx and NH3. It agrees with the ozone dependency on NOx and VOC chemical reactions; which may actually depends on both precursor variations as a function of their rapid interactions with other precursors sharing reactive processes.

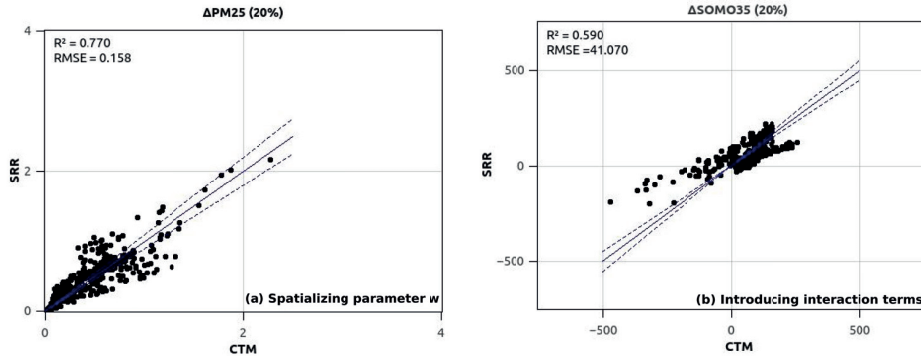


Figure 5.7: Comparison between CTM and SRR improvement strategies for yearly PM25 and O3day, with emission reductions applied over Havana, Cienfuegos and Santiago de Cuba at 20%.

5.4.4 Absolute values, PM25, SOMO35 and NO2 estimates

PM25, SOMO35 and NOx absolute values can be simply retrieved from SRR estimates (i.e. concentration deltas). For NO2, the relationship found in Sec.5.3.1 must be used. Fig.5.8 shows comparisons between CTM and SRR implementations for 80% simultaneous emission reduction (table 5.2, scenario 15). It clearly shows that SRR can mimic CTM responses for yearly average concentrations with good level of accuracy even in case of high emission reduction levels.

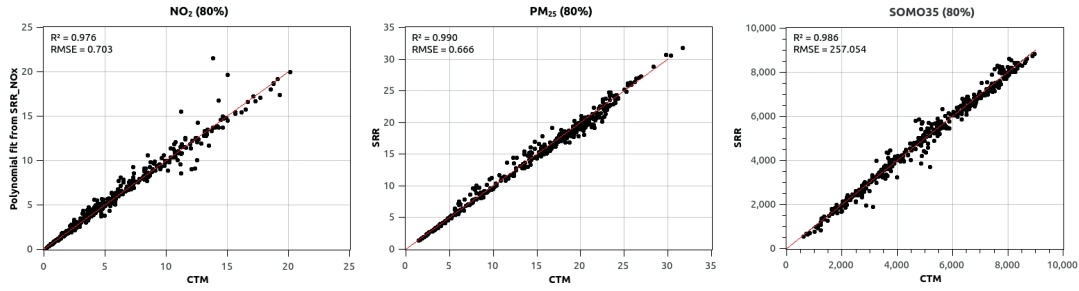


Figure 5.8: Comparison between CTM and SRR for absolute NO₂, PM₂₅ and SOMO₃₅, with emission reductions applied over Havana, Cienfuegos and Santiago de Cuba at 80%.

5.5 Conclusions

In accordance with the attempt of facilitating the assessment of emission reduction strategies over Cuba, this chapter presented an example study of setting up a SRR able to satisfactory mimic CTM behaviours. The SRR were derived at 24 km spatial resolution and accounts for the effects of NH₃, SO₂, PPM, NO_x and VOC emission reductions. It was built upon the approach of Pisoni et al., 2017 which considers a “bell-shape” function of distances to spatially link emissions and concentrations over a given domain. Two strategies of improvement were further added to the already satisfactory approach; they consisted in spatializing the coefficient that indicates how far the contribution of each precursor gets and in adding terms of interactions between precursors.

Concentrations from SRR were compared to those resulting from CTMs simulations. This validation focused on emission reductions on three different regions of the country. The applications showed a good level of accuracy even for high abatements; the level of performance of the Cuban SRR is satisfactory for annual average concentrations of PM₂₅, NO_x, as well as for SOMO₃₅ index. The added improvements provided subtle enhancements to statistical parameters R and RMSE producing lower errors than the traditional bell-shape approach. Additional relationships were provided for analyse NO₂, O₃ and PPM annual average concentrations. The approach can assess the pollution impacts of emissions scenarios applied over a given region from few CTM simulations. The low requirement on computational time (i.e. few minutes simulating a scenario) opens up a new outlook to design pollution reduction strategies in Cuba.

References

- Abreu Elizundia, H., O. Rico Ramírez, M. González Cortés, M. Espinosa Pedraja, and M. Z. Rubén (2016). “Evaluation of energy cogeneration from sugar cane bagasse”. In: *Centro Azucar* 43.1, p. v.
- Amann, M., C. Heyes, R. Mechler, J. Cofala, and Z. Klimont (2004). “RAINS REVIEW 2004 The RAINS model . Documentation of the model approach prepared for the RAINS peer review 2004 The Regional Air Pollution Information and Simulation (RAINS) model February 2004”. In: pp. 1–156.
- Andrew Kelly, J (2006). *An Overview of the RAINS Model Environmental*. Tech. rep.
- Baró Pérez, A., C. Lynch, A. L. Ferrer Hernández, I. Montejo Borrajero, and A. Rodríguez Roque (2018). “Kalman Filter bank post-processor methodology for the Weather Research and Forecasting Model wind speed grid model output correction”. In: *International Journal of Sustainable Energy* 0.0, pp. 1–15.
- Carnevale, C., G. Finzi, E. Pisoni, M. Volta, G. Guariso, R. Gianfreda, G. Maffei, P. Thunis, L. White, and G. Triacchini (2012a). “An integrated assessment tool to define effective air quality policies at regional scale”. In: *Environmental Modelling & Software* 38, pp. 306–315.
- Carnevale, C., G. Finzi, G. Guariso, E. Pisoni, and M. Volta (2012b). “Surrogate models to compute optimal air quality planning policies at a regional scale”. In: *Environmental Modelling & Software* 34, pp. 44–50.
- Carnevale, C., G. Finzi, A. Pederzoli, E. Turrini, M. Volta, G. Guariso, R. Gianfreda, G. Maffei, E. Pisoni, P. Thunis, L. Markl-Hummel, N. Blond, A. Clappier, V. Dujardin, C. Weber, and G. Perron (2014). “Exploring trade-offs between air pollutants through an Integrated Assessment Model.” In: *The Science of the total environment* 481, pp. 7–16.
- Channan, S., K. Collins, and W. R. Emanuel (2014). *Global mosaics of the standard MODIS land cover type data*. Tech. rep. Maryland, USA: University of Maryland and the Pacific Northwest National Laboratory, College Park.
- Clappier, A., E. Pisoni, and P. Thunis (2015). “A new approach to design source–receptor relationships for air quality modelling”. In: *Environmental Modelling & Software* 74, pp. 66–74.
- EEA (2008). *Air pollution harms human health and the environment*. Tech. rep. European Environmental Agency.
- EPA (1998). *Residential Wood Combustion Technology Review Volume 1 . Technical Report*. Tech. rep. December. United States Environmental Protection Agency.
- (2016). *AP 42. Chapter 1: External combustion sources. Fifth edition Vol 1*. Tech. rep. United States Environmental Protection Agency/Office of Transportation and Air Quality, pp. 8–11.
- Friedl, M., D. Sulla-Menashe, B. Tan, A. Schneider, N. Ramankutty, A. Sibley, and X. Huang (2010). *MODIS Collection 5 global land cover: Algorithm refinements and characterization of new datasets, 2001-2012, Collection 5.1 IGBP Land Cover*. Tech. rep. Boston, MA, USA.: Boston University.
- GCE, U. G. c. d. e. d. l. N. U. (2006). *Manual del sector de energía. Quema de combustibles*. Tech. rep.
- Guenther, A. B., X Jiang, C. L. Heald, T. Sakulyanontvittaya, T. Duhl, L. K. Emmons, and X Wang (2012). “The Model of Emissions of Gases and Aerosols from Nature version 2.1 (MEGAN2.1): an extended and updated framework for modeling biogenic emissions”. In: *Geoscientific Model Development* 5.6, pp. 1471–1492.
- Haneke, B. H. (2003). “A National Methodology and Emission Inventory for Residential Fuel Combustion”. In: *12th International Emission Inventory Conference - "Emission Inventories - Applying New Technologies"*.
- Hauglustaine, D. A., F. Hourdin, L. Jourdain, M. Filiberti, S. Walters, J. Lamarque, and E. A. Holland (2004). “Interactive chemistry in the Laboratoire de Météorologie Dynamique general circulation model: Description and background tropospheric chemistry evaluation”. In: *Journal of Geophysical Research: Atmospheres* 109.D4.
- Hernández Garces, A., M. Reinoso Valladares, and F. Hernández Bilbao (2017). “Contaminantes atmosféricos emitidos por centrales azucareros cienfuegueros”. In: *Universidad y Sociedad*, pp. 70–74.
- Landrigan, P. J. and R. Fuller (2016). “Pollution , health and development : the need for a new paradigm”. In: *Rev Environ Health* 31.1, pp. 121–124.
- Madrado, J. and A. Clappier (2018a). “Low-cost methodology to estimate vehicle emission factors”. In: *Atmospheric Pollution Research* 9.2, pp. 322–332.
- Madrado, J., A. Clappier, L. Carlos, O. Cuesta, H. Contreras, and F. Golay (2018b). “Screening differences between a local inventory and the Emissions Database for Global Atmospheric Research (EDGAR)”. In: *Science of the Total Environment* 631-632, pp. 934–941.

- Mailler, S., L. Menut, D. Khvorostyanov, M. Valari, F. Couvidat, G. Siour, L. Interuniversitaire, A. Lisa, U. M. R. Cnrs, U. Paris, and E. Créteil (2017). “CHIMERE-2017 : from urban to hemispheric chemistry-transport modeling”. In: *Geoscientific Model Development* 10, pp. 2397–2423.
- Meij, A. D., P. Thunis, B. Bessagnet, and C. Cuvelier (2009). “The sensitivity of the CHIMERE model to emissions reduction scenarios on air quality in Northern Italy”. In: *Atmospheric Environment* 43.11, pp. 1897–1907.
- Meneses-ruiz, E., A. Roig-rassi, E. Paz, D. Alonso, and J. Alvarado (2018). “Factores de emision de CO , CO 2 , NOx y SO 2 para instalaciones generadoras de electricidad en Cuba Factors of emission of CO , CO 2 , NOx AND SO 2 for electricity generating plants in Cuba”. In: 24.1, pp. 1–9.
- Menut, L., B. Bessagnet, D. Khvorostyanov, M. Beekmann, N. Blond, A. Colette, I. Coll, G. Curci, G. Foret, A. Hodzic, S. Mailler, F. Meleux, J.-L. Monge, I. Pison, G. Siour, S. Turquety, M. Valari, R. Vautard, and M. G. Vivanco (2013). “CHIMERE 2013: a model for regional atmospheric composition modelling”. In: *Geoscientific Model Development* 6.4, pp. 981–1028.
- Moya Álvarez, A. S. and J. M. Ortega León (2014). “Aplicación del modelo meteorológico de precipitaciones en período lluvioso de Cuba, 2014”. In: *Apunt.cienc.soc.* 5, pp. 135–145.
- National Centers for Environmental Prediction NOAA, U.S. Department of Commerce, N. W. S. (2000). *NCEP FNL Operational Model Global Tropospheric Analyses, continuing from July 1999*. English. Boulder, CO.
- ONE (2010). *Cuban State Registration of Companies and Budgeted Units*.
- (2016a). *Anuario Estadístico de Cuba. Section 10: Minería y Energía*. Tech. rep.
- (2016b). *Anuario Estadístico de Cuba. Section 13: Transporte*. Tech. rep.
- (2016c). *Anuario Estadístico de Cuba. Section 2: Medio Ambiente*. Tech. rep.
- Oxley, T., A. J. Dore, H. ApSimon, J. Hall, and M. Kryza (2013). “Modelling future impacts of air pollution using the multi-scale UK Integrated Assessment Model (UKIAM).” In: *Environment international* 61, pp. 17–35.
- Pisoni, E, C Carnevale, G Finzi, and M Volta (2009). “The RIAT project : a multi objective nonlinear optimization approach to design effective air quality control policies Acknowledgments”. In: 2008, p. 4842.
- Pisoni, E, A. Clappier, B Degraeuwe, and P. Thunis (2017). “Adding spatial flexibility to source-receptor relationships for air quality modeling”. In: *Environmental Modelling and Software* 90, pp. 68–77.
- Quoc Ho, B., A. Clappier, and N. Blond (2014). “Fast and Optimized Methodology to Generate Road Traffic Emission Inventories and Their Uncertainties”. In: *CLEAN - Soil, Air, Water* 42.10, pp. 1344–1350.
- Rodríguez Roque, A., A. Hernández Ferrer, I. Montejo Borrajero, M. Sierra Lorenzo, and A. Verde Valdés (2016). “Pronóstico de viento a corto plazo utilizando el modelo WRF en tres regiones de interés para el Programa Eólico Cubano Short-term wind forecast using the WRF model in three regions of interest for the Cuban Wind Program Introducción”. In: *Revista Cubana de Meteorología* 22.2, pp. 164–187.
- Sierra-Lorenzo, M., A. L. Ferrer Hernández, R. Hernández Valdés, Y. González Mayor, R. C. Cruz-Rodríguez, I. Borrajero Montejo, and C. F. Rodríguez Genó (2014). *Sistema automático de predicción a mesoescala de cuatro ciclos diarios Proyecto Sistema de Predicción Resolución de Datos Informe de Resultado on a mesoescala de cuatro ciclos diarios Autores : Maibys Sierra Lorenzo Adri an Luis Ferrer Hern Roilan*. Tech. rep. Centro de Física de la Atmósfera. Instituto de meteorología de Cuba.
- Thunis, P., A. Clappier, E. Pisoni, and B. Degraeuwe (2015). “Quantification of non-linearities as a function of time averaging in regional air quality modeling applications”. In: *Atmospheric Environment* 103, pp. 263–275.
- Thunis, P., B Degraeuwe, E Pisoni, F Ferrari, and A. Clappier (2016b). “On the design and assessment of regional air quality plans : The SHERPA approach”. In: *Journal of Environmental Management* 183, pp. 952–958.
- Turtós Carbonell, L. M., G. Capote Mastrapa, Y. Fonseca Rodriguez, L. Alvarez Escudero, M. Sanchez Gacita, A. Bezanilla Morlot, I. Borrajero Mojena, E. Meneses Ruiz, and S. Pire Rivas (2013). “Assessment of the Weather Research and Forecasting model implementation in Cuba addressed to diagnostic air quality modeling”. In: *Atmospheric Pollution Research* 4.1, pp. 64–74.
- Verde Valdés, A., R. C. Cruz Rodríguez, and A. Roque Rodríguez (2015). “Evaluación del pronóstico de viento del modelo Weather Research Forecast (WRF) en torres de prospección eólica”. In: *Revista Cubana de Meteorología* 21.
- Wesseling, J and F Sauter (2008). *Non-linearity in the NOx/NO2 conversion*. Tech. rep. 680705009. rivm-National Institution for Public Health and the Environment.

WHO Regional Office for Europe (2016). *Health risk assessment of air pollution - general principles*. Tech. rep.

World Bank (2018). *Reducing air pollution*.

Chapter 6

Cuban's energy strategy into 2030: General design features toward a sustainable transition

This work aims to explore scenarios for a reliable energy transition in Cuba. The energy fluxes between final energy demand and resources were computed for the year 2015. Then, the energy demand was projected to 2030 and a set of scenarios based on different mix of energy resources and technologies were designed to fulfil this demand. These scenarios were compared according to three criteria that seemed the most relevant for Cuba given its geopolitical and economic situation: energy security, energy sustainability and air quality impacts. The results show that when wind and solar energy fulfil 20% of the electricity demand, the fossil fuel requirements are significantly reduced. Once this penetration reaches 50%, Cuba can achieve complete independence from energy imports. The scenario fulfilling 100% of electricity demand from wind and solar resources shows the maximum sustainability. The use of renewable resources also has positive effects on air quality.

6.1 Introduction

Cuba is a socialist developing country located in the Caribbean region. Its economic development has been characterized by a relatively low average per capita income and per capita energy use. Like most Latin American countries, Cuba's economy showed steady growth between 1940 and 1960. With the revolutionary Government coming in 1960, the country experienced strong economic and social development. This growth was highly supported by favorable trade relationships with the countries of the Council for Mutual Economic Assistance (CMEA) which provided a stable supply of oil and oil by-products, making the country's energy mix depends significantly on the imports (Suarez et al. 2012).

During 1990s, after the collapse of the Soviet Union, this dependency led to a major setback of the Cuban economy. The state was forced to slash its energy imports which affected its capability to satisfy its energy requirements. The government responded by implementing important reforms which led to a change of society with respect to energy use, resulting in a less-demanding energy system. The policies included: increasing production of domestic crude oil and associated gas, considerably reducing energy demands, reducing electricity losses, and improving energy infrastructures. Between 1992 and 2003, the domestic oil production grew annually by 7% (Suarez et al. 2012) but this fuel showed to be far from optimal in terms of generating power (its high levels of sulphur damaged the power plants due to extensive corrosion); and many power plants had to shut down for periods of time, leading to severe power shortages. This triggered a new crisis in 2005; which the government replied with to the so-called "Energy Revolution". It again instituted measures to reduce electricity demands and increase energy efficiency with investments on distributed electricity generation systems. A couple of thousand diesel-fueled mini-generators were scattered across the island and distributed to 70% of the municipalities (Belt 2010). The Energy Revolution increased the reliability of the electricity supply and was successful in changing the energy use patterns of the Cuban households by replacing appliances with more efficient and safe equipment. However, the energy system in general continued to be highly dependent on imports, which was at that time supported by preferential trading agreements with Venezuela. Because of this, the political crisis that developed in Venezuela in 2013 caused the Cuban energy sector to once again enter a period of uncertainty. During July 2016, following difficulties with imports, the state announced new goals to reduce electricity consumption by 6% and fuel consumption by 28% in the second half of the year (Panfil et al. 2017; Reuters 2016). Currently, the country does not cease in exploring ways of fostering energy efficiency. The necessity caused by economic crises enforced moving toward a less-demanding energy system, but it has been and still is heavily reliant on fossil fuels, with a considerable amount in the share of imports (cf. citeONE2016). The country is in need of a new energy lifeline.

In this regard, the main goal of this work is to explore scenarios for a reliable Cuban energy transition. We firstly draw up an overview of the current energy system, including the resources, technologies, and services with base-case in 2015, as well as the country projection to 2030. This reveals the main challenges and opportunities to provide general design features for the transition. A set of indicators to address energy security, sustainability and air quality impacts are presented in order to facilitate the analysis of different energy scenarios.

6.2 Overview of the Cuban energy system

6.2.1 The situation in 2015

Energy demand

Energy consumption is an inevitable consequence of human activities which are connected with all the aspects of daily life through the vast use of energy, from household to industries. In Cuba (see table 6.1), industrial processes encompass major consumers (41%), followed by residential sector (37%) and then the transports (11%). The various other sectors (i.e. water supply, construction and agriculture) use 12% of the total energy consumed. The demand is fulfilled with two different branches of energy resources: Oil sub-product (63%) and electricity (37%).

Table 6.1: Energy demands (GWh) by key sectors in 2015. Adapted from (ONE, 2016)

Services	Electricity	Oil Sub-prod.	Total
Residential	12440	4376	16816
Industries	4713	13939	18651
Transport	0	5048	5048
Other	0	5459	5459
Total	17153	28821	45974

Electricity production

The largest part of electricity (59%) is produced by seven thermoelectric power plants that consume large amounts of crude oil as well as, in smaller quantities, fuel oil and diesel. A further 22% of electricity is produced by a set of distributed generators (so-called “Generator set”) reliant on fuel oil and diesel, 15% comes from natural gas by combined-cycle generating plants, 3.5% from bioelectric plants from bagasse (i.e. the dry pulp residue left over after sugar extraction from sugar cane), and around 0.5% from other renewables resources such as water, sunlight and wind. See table 6.2 for the breakdown of the Cuban electricity generation technologies and resources.

Table 6.2: Electricity production (GWh) 2015: Technologies and resources

Technologies	Electricity production	Energy consumption	Resources
PV panels	15		Sun radiation
Wind turbines	35		Wind
Hydroelectric	48		Water
Sugar factory	898	5900	Bagasse
Gas turbine	2950	12100	Gas
Thermoelectric	11943	37768	Oil and Oil sub-product
Generator set	4399	11321	Oil sub-product
Total	20288	79149	

Thermoelectric power plants produce a total of 2’588 MW. Presently, the obsolescence of these technologies joined with the use of low-quality crude oil lead to high rates of failure and inefficiencies on electricity generation. This hampers the full use of the existing capacities. Indeed, most of the major power plants run at only 60-65% of their potential (Berg et al. 2013), which is a rather modest figure by international standards.

Generator set technologies account for 2’520 MW providing services at or near points of consumption. These technologies are a singular aspect of Cuban electric grid that offers benefits against centralized power (Panfil et al. 2017): they help when facing natural disasters, such as hurricanes, as each affected plant contributes a smaller individual capacity to the grid. They also reduce electricity loss as they do not rely to the same extent on extended transmission networks, and they can be brought back online more quickly than centralized generation (Momoh et al. 2012). They have increased efficiency rates (i.e. lower specific consumption rates). The only concern arises from their contingency upon burning high-properties’ oil sub-products, which leads to a costly option to match daily load profiles (Benjamin-Alvarado 2010). According to Berg et al. 2013, they are not a viable solution in the long run and may only serve as a supplementary power source to the major thermoelectric power plants.

Combined cycle generating plants sum-up to 580 MW. The technology was commissioned and is currently operated by the foreign company Energas (i.e. a joint venture between Canada’s Sherritt and Cuba’s Cupet and Unión Eléctrica). The largest facilities are located near the country’s capital city.

Bioelectric power plants account for 470 MW spread among 40 sugar factories. The sugar industry has longstanding experience in the use of biomass to cogenerate heat and electricity, but currently only small amounts of electricity are exported to the grid as the industry self-consumes over 85% of produced energy (Jimenez Borges et al. 2017; MINAS et al. 2016; Rodríguez-Machín et al. 2012; Sagastume et al. 2018). In

addition, its capacities are in use for merely 3600 h (150 days) per year.

The renewable power generation also share 62.8 MW of hydroelectric plants, 11.7 MW of onshore wind turbines, 24.4 MW of utility scale PV and 0.66 MW of bio-power from gasification of forest biomass. The renewable resources are not significantly exploited. They are mainly used in remote locations, inaccessible to the supply with conventional resources (Sagastume et al., 2017). Nowadays, the electricity losses represent 15.5% of the total electricity generated.

Fuel production

In 2015, the country used 108'993 GWh of primary resources: ~ 42% imported and ~ 58% produced domestically. The domestics (47'771 GWh) include 3 million tons of crude oil, 1'200 million cubic meters of natural gas and 1.2 million tons of sub-products from oil and gas. The Cuban crude oil is a product extracted from shallow waters just off the coasts with extra-heavy and high-sulphur properties (Käkönen et al., 2014), while the natural gas is a production of all associated natural gas found within the crude oil reservoirs (Benjamin-Alvarado 2010).

The imports (45'871 GWh) account for 0.7 million tons of crude oils and 3.3 million tons of oil sub-products. Around 1.2 million tons of oil sub-products are produced from refining processes of either domestic or imported fuels at Cuban facilities. A part of them are known to be exported, so in our analysis we only take into account the part locally used. The country spends more money in energy (mainly imports) as a percent of GDP than most nations; the total value of the energy consumed is estimated at 14% of Cuba's GDP, whereas the world average is roughly 10% (Panfil et al., 2017).

Fig.6.1 summarizes the Cuban energy system for the year 2015 in a flow Sankey diagram. Absolute numbers are given for the different resources at the left in the diagram. Final consumption (at the right) was represented as the sum of two main components: electricity and all other services using oil sub-products. The diagram also shows the amount of energy "left after production". So mainly it is the non-efficiency of the production expressed as a relative part figures that is shown. It can be seen that electricity sector plays the main role as it consumes around 73% of all resources managed by the country, and accounts for around 40% of those imported.

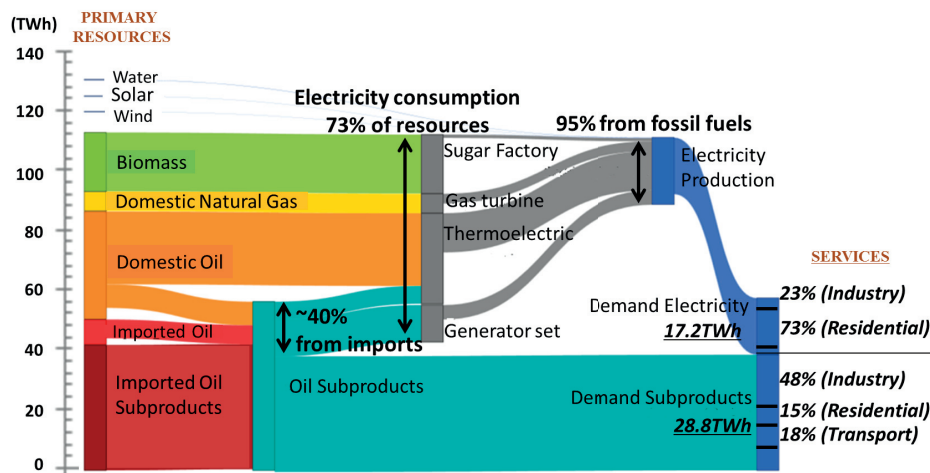


Figure 6.1: Energy flow Sankey diagram of Cuba for the year 2015

6.2.2 The projection into 2030

Energy demand

Over the last twenty years, electricity generation steadily increased (ONE 2016c; Sagastume et al. 2018). In Fig.6.2, the electricity consumption trend from 2002 to 2015 shows an average increase of 3.6% per year, with 4.8% from 2014 to 2015 alone. This trend can be mainly explained by an increased demand from residential sector (around 4.7% per year during the last five years). According to Reuters 2016, the opening of the private segment of the economy during the 2000s (where Cubans were allowed to set up businesses in their homes and front porches) highly influenced this drift. For all other sectors the increase is lower (less than 3% per year). Following the trend, the Cuban electricity consumption is expected to raise in the future (Käkönen et al. 2014), where official estimations foresee an increase of 3.28% per year (MINAS et al. 2016), reaching 27'834 GWh in 2030. The direct consumption of oil sub-products, by services other than electricity, experienced a decreasing trend. Official projections regarding future consumption were not found. So that, at the risk of being too pessimistic about the planning horizon, such demand is assumed to remain constant at 28'821 GWh. Consequently the total energy demand will increase from 45'974 GWh in 2015 to 56'655 GWh in 2030 with a share of 51% of oil sub-product and 49% of electricity.

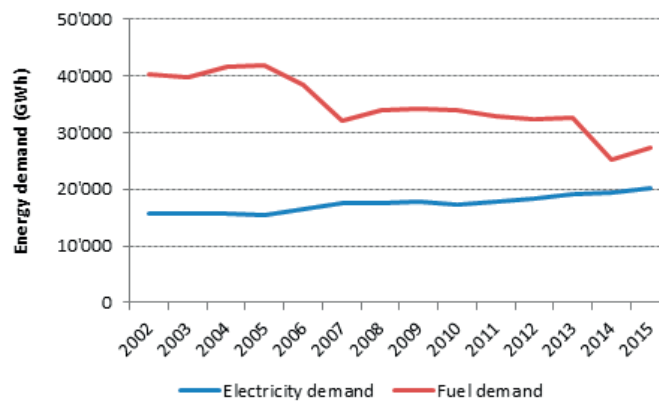


Figure 6.2: Trend of energy demand from 2002 to 2015

Electricity production

The government is aiming to match the future energy needs with a more self-reliant supply. Its strategy consists in cutting the cost of importing the shortfall by producing more domestic resources. Broadly, the 2030 strategy includes: (i.) increasing technological capacity to use domestic fuels (i.e. crude oil and natural gas), (ii.) increasing efficiency of electricity production, distribution and consumption with energy saving measures, (iii.) and expanding the renewables share to 24% (EFE 2014, documented by "Cartera de oportunidades Cuba").

Around 800 MW (an additional 13% of generating capacity) will raise existing thermoelectric capacities. Combined-cycle natural gas plants will also increase their share in electric generation, in relation with an increasing domestic gas production (cf. Belt 2010). Generator set is maintained at the same level of 2015.

The renewable share will add 74 small hydroelectric plants (375MW), 13 onshore wind farms (583MW) and 19 utility-scale PV plants (263MW). Most of hydropower energy will remain from isolated system areas. Onshore wind farms will be located at specific zones on the northeast coast of the country where historical wind estimations at 50 and 100m favor wind power output at a capacity factor over 30%. The solar system will continue to focus toward urban applications but will also expand beyond on-grid usage. A high betting for bio-power from bagasse combustion is expected, with around 720 MW of increased efficiency technologies (i.e. showing an efficiency increase from 5% to 10%) in 19 of the existing sugar factories. The potential scenarios consider updating bio-power technologies and including the combustion of marabu (i.e. *Dichrostachys-cinerea*: a woody bush considered a plague in Cuba) after the sugar-cane milling season to extend the use of the electric generation infrastructures to a minimum of 50 days above 3600 h per year. See table 6.3 for a summary of the main energy technologies and resources expected to be used in 2030.

Table 6.3: Electricity production 2030: Technologies and resources

Technologies	Electricity production	Energy consumption	Resources
PV panels	518		Sun radiation
Wind turbines	1535		Wind
Hydroelectric	985		Water
Sugar factory	5152	515200	Bagasse and Marabu
Gas turbine	4481	8962	Gas
Thermoelectric	16296	52682	Oil and Oil sub-product
Generator set	3951	11297	Oil sub-product
Total	32914	127493	

Fuel production

To fulfil the projected demand, the country may manage around 158'000 GWh of primary resources including crude oil and sub-products. Domestic crude oil production is expected to amount 58'110 GWh (~ 5000 Mteo) with around 8'962 GWh of associated natural gas. The bagasse may set up to 51'520 GWh. The needs of oil sub-products will be covered by Cuban facilities with refining capacities for 55'786 GWh ($\sim 16'000$ tons) per year.

Fig.6.3 summarizes the Cuban energy system for the year 2030 in a flow Sankey diagram. The increased final electricity demand (around 10.6 TWh with respect to 2015) can be observed. The diagram also shows the raise in the share of electricity produced from renewable resources ($\sim 24\%$) such biomass, water, solar and wind. Despite these prospects, technological capacity of using domestic fuels (i.e. centralized thermoelectric and gas plants) and renewables will still remain insufficient to be totally self-sufficient on fossil fuels. Electricity supply, as well as residential, industrial and transportation activities will leave a deficit of around 39'400 GWh on imports.

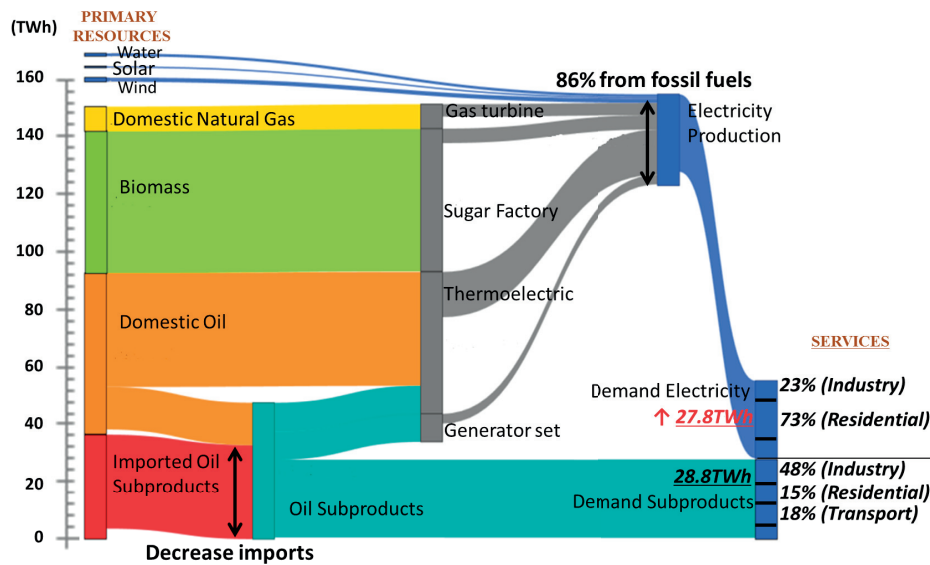


Figure 6.3: Energy flow Sankey diagram of Cuba for the year 2030

6.2.3 Environmental concerns

An important factor when discussing the energy development in Cuba is the local influence of pollutant emissions (Wright et al. 2010). A majority of the Cuban electricity generation is achieved by combusting different kinds of fuels. This joined with the facts of using high-sulphur content oil (i.e. domestic crude oil) and low-efficient technologies, make the energy system prone to high emission levels. In addition, most of the power installations are close to urban zones which may aggravate the impacts on population health.

The emission inventory developed in the previous chapter for Cuba -base year 2015, was used here to assess the projection into 2030. Since this projection only acts on electric generation (i.e. other services hold steady from 2015), just the emission parameters (i.e. emission factors, activity levels and allocations) of power units need to be modified. Overall, in 2030, the emission rates from electricity generation increase with respect to 2015: for NO_x (19%), SO_x (36%), VOC (17%), PPM (330%) and NH₃ (94%). Increased NO_x, SO_x and VOC emissions are mainly linked with an increase of activities of centralized power plants, while for PPM and NH₃ they mostly lie with the operation of new bioelectric plants on sugar factories. These emissions are all particulate-forming pollutants; their rise will affect the human health risks of exposures to PM_{2.5}. To investigate this issue, the average PM_{2.5} concentration levels were computed by modelling the Cuban emission inventory with the Chemical Transport Model CHIMERE for 2015 and 2030 scenario; then, a population-weighted mean level (Ex-PM_{2.5}) of PM_{2.5} calculated as:

$$Ex_{PM_{2.5}} = \frac{\sum_i C_i^{PM_{2.5}} Pop_i}{\sum_i Pop_i} \quad (6.1)$$

where: $C_i^{PM_{2.5}}$ is the annual average of PM_{2.5} concentration and Pop_i the population at a region “i”. The population-weighted mean of PM_{2.5} concentrations resulted 17.8 $\mu\text{g}/\text{m}^3$ in 2015 and 19.0 $\mu\text{g}/\text{m}^3$ in 2030; this indicates that people will live in the highest polluted areas by 2030.

6.2.4 Comparison between 2015 and 2030

In order to preliminarily evaluate the interests of the country, a set of indicators were designed. The historic dependency on imported fuels has made Cuba vulnerable to political changes abroad and to oil market variations, so that, energy security is center piece in the economic development of the country. In addition, the availability of fossil fuels is likely finite. As a result limited reserves, it is not a long-term sustainable solution for the country’s energy mix. An environmental aspect is also important to take into account for the country, especially the impact on air quality (Sagastume et al. 2018), as the combustion technologies that are currently in use are causing air quality degradation with negative effects on human health.

With the aforementioned in mind, indicators were calculated to allow for a comparison of the Cuban situation between 2015 and 2030, where the criteria on which the indicators are based are: energy security, energy sustainability and air quality impacts (see table 6.6 in Sec.6.4). The three indicators can range from 0 to 1. In short, when an indicator is equal to 1, the criteria does not change with respect to the base-case. When the indicators are less than 1 the criteria improves over time, and likewise, when the indicators are larger than 1 the criteria worsens over time. The ideal situation arises with nulls.

These indicators offer intuitive formulations which compare the needs of primary resources and the consequences on air quality of its use, using 2015 values as a base:

- The energy security criterion is evaluated as the ratio between the needs on imported fuels in 2030 and 2015. It implicitly measures the vulnerability of the country for net-import dependence. For the 2030 base-line the value is 0.83, which means reducing the share of imports from the energy mix. This result mainly lies in the increased use of domestic and renewable primary resources (i.e. biomass, solar and wind).
- The energy sustainability criterion is evaluated as the ratio between the needs of fossil fuels in 2030 and 2015. It directly concerns the fossil resources managed by the country, ranking its ability to provide stable, affordable and environmentally-friendly energy. For the proposed projection the value is 1.16, which implies an increasing dependence on fossil resources.
- The air quality impact criterion is evaluated as the ratio between population exposure to PM_{2.5} concentrations between 2015 and 2030. The indicator is 1.07 and shows a rise in population exposure due to the air quality deterioration in 2030. It is mainly due to an increased combustion of fuels including crude oil and bagasse.

6.3 Alternative scenarios for the Cuban energy mix

In view of improving the energy security, sustainability and air quality indicators, alternative scenarios are explored in this section. To this end two complementary strategies will be analyzed: (i) Switching primary resources and (ii) improving the efficiency of technologies to reduce energy demand.

6.3.1 Insights in energy demand

Until now, the electricity sector plays the main role in energy consumption, which prompted the Cuban government to implement several policies to improve the energy sector's operating rates. The most significant of the policies was implemented in 2005 during the Energy Revolution, which caused a substantial decrease in electricity demand through energy efficiency and saving measures. A fundamental part of the process was the replacement of household and state entities appliances with more efficient equipment. The policy also introduced a new electricity tariff with a reduction of government subsidies to encourage electricity saving (Guevara-stone et al. 2009; Suarez et al. 2012). The industrial sector, although technologically outdated (Sagastume et al. 2018), has also implemented policies to improve energy efficiency. The sector has specific bodies that provide services for saving energy (i.e. technological changes and materials) at affordable costs (Gonzalez Del Toro 2016). Such bodies police industries in such a way that all productive processes meet standard energy consumption requirements.

With these policies Cuba has been able to manage its energy demands. However, an increase in energy demand is stressed: forecasts of climate change have shown predicted increases of the annual average temperature (Angeles et al. 2007) and a regional warming trend in the Caribbean. The region may increase air conditioning demands to achieve human comfort in buildings. The projections of Angeles et al. 2010 show a positive energy demand per capita change of around 9.6/15 kWh per month by the middle of the twenty-first century (Angeles et al. 2018). In Cuba, this phenomenon may also lead to higher energy per capita requirements for air conditioning, mainly in the tourism industry, which is one of the main sources of revenue for the island. The rate of increase estimated by Cuban authorities is a little bit optimistic at 3.28% per year; it is more likely that the increase in electricity demand will be greater than 4% per year.

Moreover, the implemented policies have, so far, not had much impact on transport. This sector in general uses outdated technologies, and the motor vehicle penetration rate is amongst the lowest in Latin America. The demand is currently at around 336'400 tons of fuel, including diesel and gasoline. The vehicle fleet comprises some 362'000 vehicles (Enoch et al. 2004), with only 38 cars per 1'000 inhabitants. Even so, the sector uses 10% of total energy demand which probably lies with the overconsumption of the obsolete fleet.

6.3.2 Insights in potential resources

Official information about estimated reserves and potential of energy resources in Cuba was not found. This work compiles data from different sources and provides some estimation.

Fossil fuels

The size of oil deposits in onshore and offshore territories remains difficult to quantify. The known quantity that would be extracted with available Cuban technologies was estimated by the Cuba oil union, CUPE, to be 97.8 million toe. Nevertheless, the discovery of important crude oil and natural gas reserves in the so-called "Cuban Economic Exclusion Zone (EEZ)" of the Gulf of Mexico is expected (cf. "Cuba. Cartera de oportunidades de la inversion extranjera 2016-2017" 2017). The Cuban government has estimated that at least 2.7 billion tons can be found deep in the sea, while the United States Geological Survey's estimate a more modest 630 million tons, which is still a significant number (Schenk2004). On the basis of historical extraction rates for crude oil and gas (5 million tons), and considering hypothetically that all the reserves can be extracted, estimated onshore reserves will last approximately 22 years and offshore reserves approximately 155 years (IAEA 2008).

Biomass

Bagasse from sugar-cane and marabu are expected to be the most important biomass sources in Cuba. The country has around 6'279 100 ha of agricultural surface. During the last 10 years, more than 400'000 ha of sugar-cane have been cultivated (see Fig.6.4) for an average annual production of 14'610 million tons , with harvest yield at 36 tons/ha. In 2015, sugar-cane was harvested across 436'600 ha (7% of agricultural surface), with the total production increasing up to 19.3 million tons (ONE, 2016). One ton of sugar-cane processed in a sugar factory yields on average around 240 kg of bagasse. Their cogeneration potential is documented in ranges of 20-25 kWh/ton-of-cane (Alonso-pippo et al. 2008), 580 kWh/ton-of-bagasse (Sagastume et al. 2018) or 35-40 kWh/ton-milled-sugarcane (Alonso-pippo et al. 2008; Jimenez Borges et al. 2017; Sagastume et al. 2018), based on different sugar factory generation pressures (18-23 bar) and efficiencies. Opportunities exist to increase the rates of production from bagasse, which includes enhancements on harvest yields (90 tons /ha) and electricity production efficiency (140 kWh/ton-milled-sugarcane). Considering an average harvest of 47.5 million tons of sugarcane (i.e. following the trend 2010-2015 which increase production at 2 million tons per year), the 2030 production of bagasse is estimated at 8.4 million tons. The potential cogeneration ranges between 1'700 and 6'500 GWh depending on current and optimal efficiencies.

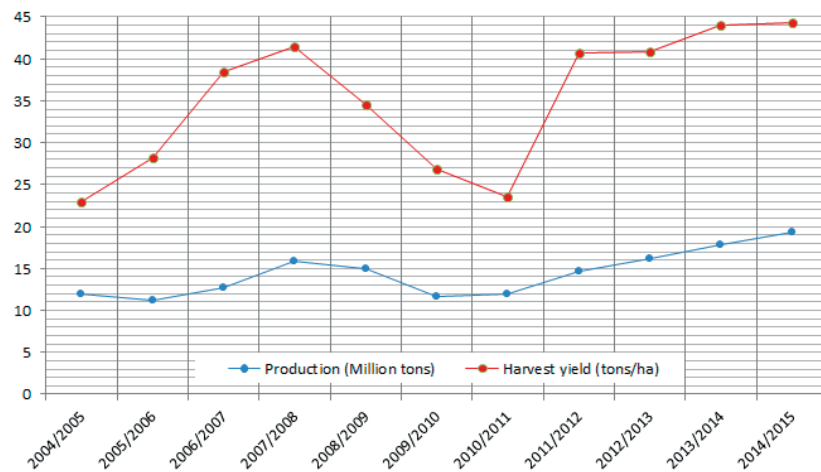


Figure 6.4: Trend of sugarcane production from 2005 to 2015

The marabu covers over 1.7 million ha (15% of the Cuban territory) (Käkönen et al. 2014; Rodríguez-Machín et al. 2012; Sagastume et al. 2018). The shrub expands quickly at an average occupancy of 37 tons/ha and a natural renewability period of 3 years. Currently, about 63 million tons of marabu are available all over the country. This resource could either be progressively eradicated to release agricultural surface for other applications or be re-used. The combustion properties of this biomass is documented to be between 120 kWh/t (MINAS and JICA, 2016) and 1268 kWh/t (Sagastume et al. 2018). Considering a capability of harvesting 21 million tons (1/3 of availability) every year (which is an optimistic estimation considering the difficulties that are currently faced in eradicating the shrub, cf. Rodríguez-Machín et al. 2012), the potential electric generation ranges between 2'520 and 26'628 GWh.

Water, wind, solar

Average annual precipitation in Cuba is 1400 mm. There are about 900 runoff water streams, though they are not very extensive owing to the long and narrow shape of the country (with an average width of 97 km). The estimated hydropower potential of annual generation is around 1300 GWh (IAEA 2008); however, it cannot be completely exploited because of environmental protection constraints. In this work, we consider the hydropower potential as estimated in Cuban 2030 projection where only 985GWh (75%) can be used.

The Cuban wind potential was found to be a very controversial topic. Estimations for the Caribbean derived a considerably large potential with good to exceptional power densities: 200–300 W/m² (Chadee et al. 2014) and 500-1000 W/m² (Maegaard et al. 2013). However, investigations carried out with assistance from Cuban meteorological stations identified a limited number of suitable sites (20) with potential for

around 2'000 MW (Käkönen et al. 2014) and utilization factor of 23% (4'030GWh). Other Cuban estimations from climate modelling identified 448 km² of land with good wind conditions and merely 63 km² having excellent wind conditions for electric generation; these led an estimated potential of 2'550 MW (Panfil et al. 2017). The lowest figures on the overall annual potential go down to 1200 MW (2418 GWh) (IAEA 2008) while the highest go up to 5'000 and 14'000 MW (Avila 2009).

Due to its geographical location in the tropical latitude, the country is extremely well endowed in solar energy. Studies on climate conditions provide confirmatory evidence of around 2800 sunshine hours (32% of utilization factor) annually. The daily average solar energy that reaches Cuban land throughout the year is 5 kWh/m² (Panfil et al. 2017). This value is relatively uniform across the country and shows little variations (± 0.5 kWh/m²) from winter to summer seasons (MINAS et al. 2016). Jacobson et al. 2017 estimated a PV panel install capacity of 8'726'129 MW, only taking into account suitable rural land areas (i.e. rural land areas receiving a minimum acceptable solar insolation and being appropriated for PV panel installation) . This huge potential represents an energy of around 24'433'161GWh per year.

Table 6.4: Potential of energy resources in Cuba

Resources	Annual potential (million tons)	Annual potential (GWh)	Reserve last (years)
Crude oil and associated gas	5.0	15110- 20870	155
Bagasse biomass	8.4	1700 - 6500	-
Marabu biomass	21.0	2500 - 26628	-
Water	-	985	-
Solar	-	24433161	-
Wind	-	2418-28207	-

The reduction of energy dependence in Cuba entails a more intensive exploitation of local renewable energy resources: biomass (bagasse and marabu), wind or sun. However, the exploitation of these resources depends on the area that is dedicated to them, such that solar panels, wind turbines and biomass crops must compete to occupy land surface across the country. Fig.6.5 provides a comparison of the physical land surface

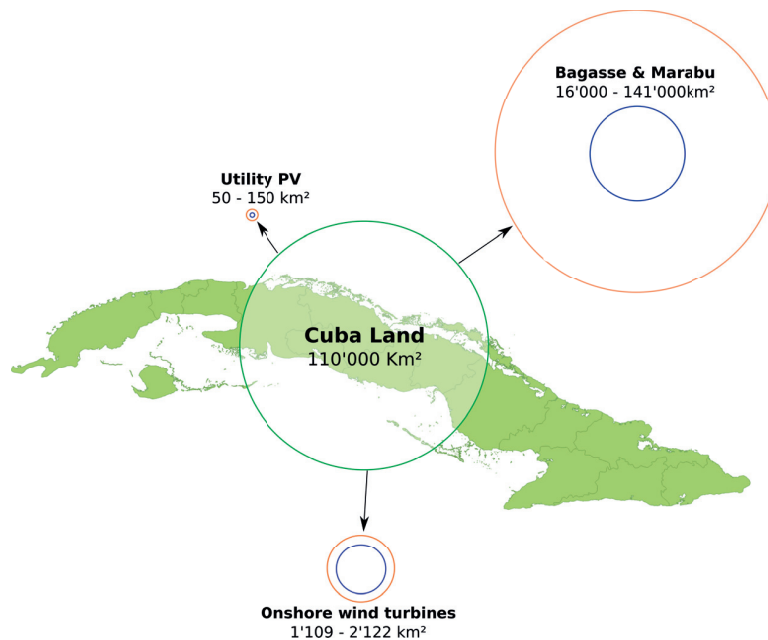


Figure 6.5: Land surface (km²) required to meet Cuban electricity demand from solar, wind and biomass resources

needed for the use of each renewable resource assuming that it will provide 100% of the Cuban electricity demand by 2030. The physical land surface includes the spacing between devices avoiding, for example, the partial shadowing on the energy yield of PV systems or the interference due to the wake of a wind turbine with others downwind. For Utility scale PV has an installed spacing density of 100-300 MW/km², which is assumed on the basis of estimations performed by Al-Khazzar 2017 for different types of PV modules with efficiencies from 0.12 to 0.20 and areas between 1.3 and 1.7 m². For Wind Turbines the assumed range is 7.1 - 13.6 MW/km², taken from Jacobson et al. 2017. In the case of biomass, the estimated occupied surface area is based on the harvesting area needed to generate electricity during 150 days from bagasse and 225 days from marabu. This estimation also combines minimal and maximum expected generation rates in terms of harvesting yields, technological efficiencies and biomass properties. The comparison between the physical land-surfaces needed by the different kind of renewable energies shows that a widespread use of solar or wind energy should account for less than 0.1% and 2% of Cuba land, respectively. The estimation for the biomass is between 15% to 128%. This estimate shows a wide range of uncertainty as biomass crop yields and the efficiency of technologies used for energy production from biomass can vary widely.

6.3.3 Matching electric power supply with demand

Wind and solar resources do not contribute significantly to the Cuban energy production (only 0.5% of the electricity production in 2015). Because they constitute the highest potential of the country's renewable energies, the increase of their part in the Cuban energy mix is an option that deserves to be considered. The main disadvantage of these resources is that they supply energy intermittently and stochastically on a temporal basis. As intermittent penetration increases, electric grid integration issues become more significant and energy storage becomes an important option that needs to be considered.

Basic calculation features

The planning of energy scenarios aiming to increase the part of wind and solar energy requires an assessment of the constraints arising from the temporal match between electricity demand and supply, the use of storage and conventional technologies in the power system. In this study, such assessment is supported on a time series simulation model created for, and readily adapted to, the situation in Cuba. It accounts for estimations of the temporal electricity demand on one side and the solar and wind energy production on the other side.

The simulation model is composed of four components: the intermittent sources, the demand, the storage and the conventional backup. It assumes that the available intermittent power is first used to supply as much as demand as possible. Whatever load remains (if any), the model attempts to supply it from the storage. If there is still load remaining, the model attempts to supply it with the backup (conventional generators). The system operates in an hourly basis: during the hourly time step, the intermittent sources provide an energy flux equal to I_t while the expected demand in an energy flux is equal to D_t . At the beginning of each time step $t - 1/2$, the amount of stored energy is equal to $S_{t-1/2}$, and it is equal to $S_{t+1/2}$ at the end of the time step. The losses are taken into account between each network connection: η^{ID} between the intermittent sources and the demand, η^{IS} between the intermittent sources and the storage, η^{SD} between the storage and the demand, and η^{BD} between the backup and the demand. The energy storage is considered ideal and is allowed to vary from none to infinity. There is also no limit on charging or discharging power levels.

The energy flows can be distributed between the different components of the system in three different ways:

1. The intermittent sources provide enough energy to fulfil the demand: $I_t > \frac{D_t}{(1-\eta^{ID})}$.
The surplus energy which is equal to $-I_t + \frac{D_t}{1-\eta^{ID}}$ goes directed towards the storage (Fig.6.6a).
2. The intermittent sources does not provide enough energy to fulfill the entirely the demand: $I_t(1-\eta^{ID}) \leq D_t$. Then, the energy storage supplies $D_t - I_t(1-\eta^{ID})$ which is sufficient to complement the demand (Fig.6.6b).
3. The intermittent sources and the storage provide respectively $I_t(1-\eta^{ID})$ and $S_{t-1/2}(1-\eta^{SD})$ to the demand but this is not sufficient to fulfill demand entirely. The missing energy demand which should be powered by a backup energy source is B_t (Fig.6.6c).

The description of the three situations a), b) and c) is used to calculate the energy fluxes that drive the storage balance:

$$F_t^{IS} = \max \left[0; \left(I_t - \frac{D_t}{1 - \eta^{ID}} \right) (1 - \eta^{IS}) \right] \quad (6.2)$$

$$F_t^{SD} = \max \left\{ -S_{t-1/2}; \min \left[0; \frac{I_t(1 - \eta^{ID}) - D_t}{1 - \eta^{SD}} \right] \right\} \quad (6.3)$$

F_t^{IS} is the flux provided by the intermittent sources, it leads to an increase of storage. F_t^{SD} is the flux supplied by the storage to powered the demand, it leads to a decrease of storage. These two fluxes are used to compute the storage balance at each time step as follow:

$$S_{t+1/2} = S_{t-1/2} + F_t^{SD} + F_t^{IS} \quad (6.4)$$

The backup source can be estimated starting from the demand balance. In situation a) and b) it is not needed to supply the demand ($B_t = 0$). In situation c), the intermittent sources and the storage are not sufficient and the backup is needed to close the demand balance:

$$D_t = I_t(1 - \eta^{ID}) + S_{t-1/2}(1 - \eta^{SD}) + B_t(1 - \eta^{BD}) \quad (6.5)$$

To fit with the three situations a), b) and c), the backup source can be computed as follow:

$$B_t = \max \left(0; \frac{D_t - I_t(1 - \eta^{ID}) - S_{t-1/2}(1 - \eta^{SD})}{1 - \eta^{BD}} \right) \quad (6.6)$$

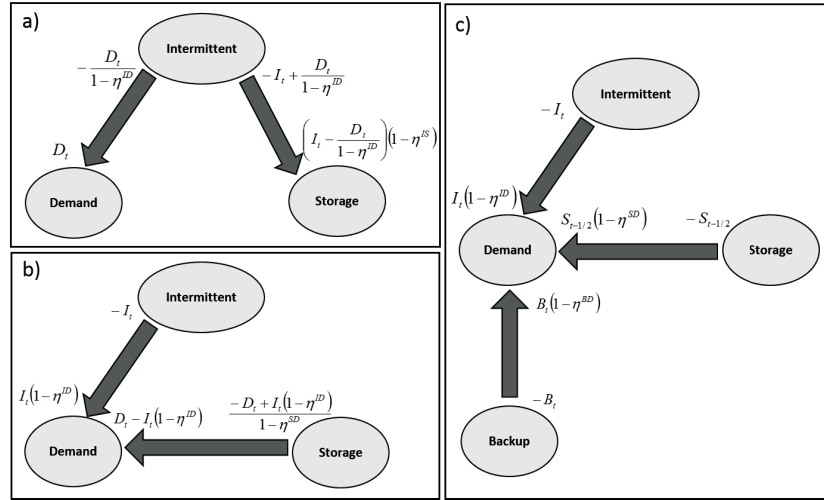


Figure 6.6: Energy fluxes between the intermittent sources, the storage, the demand and the backup: a) the intermittent sources provide enough energy to entirely fulfil the demand, b) the storage completes the intermittent sources to supply the demand, c) intermittent sources and storage are not sufficient to entirely power the demand, so it is necessary to use a backup energy source.

Data and application

Hourly loads of electricity demand at each time step were estimated from modelling historical national electricity data with the tool MAED from (IAE) 2006. These calculations were performed by researchers of CUBAENERGIA for the year 2015 assuming that the time profile of the energy demand remains steady in the future, despite the electricity growth.

Solar hourly capacity factors were simulated using data from the Solaris 2017 dataset NREL 2008 (i.e. five years of hourly global radiation data). It considers that power output of PV systems largely depends

on the amount of global radiation. The nominal power is obtained when the intensity of sunshine reach the ideal condition of 900W/m^2 . PV panels are supposed to be inclined at an angle equal to the average latitude of the country and correctly spaced to avoid shadowing. The losses compared to performance in optimal conditions due to non-ideal alignment of modules in tilt and/or azimuth or higher temperatures are neglected.

Hourly onshore wind turbine output power was estimated using simulation results from the Weather Research Forecasting model. The estimation of the hourly capacity factors is based on the variations of wind speeds assuming a typical power curve which nominal power arise when wind speeds reach $14\text{--}25\text{ m/s}$, cut-in speed at less than 3m/s , and cut-out speed at 25m/s .

A constant wind and solar energy install-capacity is chosen to compute the intermittent energy power available every hour using the hourly solar and wind capacity factors. The difference between the intermittent energy power and the demand load is calculated for every hour. This difference is used to calculate the energy which can be stored and the energy backup (produced by other types of energy sources), which should be introduced when the intermittent sources are not sufficient.

The loss between the energy supply and the demand accounted for 15% in 2015. We assume that this value will be the same in 2030 between the backup and the demand. We also assume that wind and solar energy will be produced locally in each of the country's regions, which should lead to a reduced energy loss (10%) between the intermittent sources and the demand. An increased loss of energy (30%) is specified when the energy supply is ensured through the storage (from the intermittent sources to the storage and then to the demand). The calculation is performed for different installed capacities and each result is expressed according to the percentage of the demand supplied by the intermittent sources.

The calculated results show that the backup energy, and consequently the average fossil fuel consumption, decreases linearly with the percentage of demand, which is fulfilled by the intermittent energy (Fig.6.7a); this will result in an increasing storage capacity. It also showed that three different kind of scenarios can be distinguished (Fig.6.7):

- (i) when less than 20% of the demand is fulfilled by the intermittent sources, no energy storage is required, but the backup capacity (i.e. maximum hourly backup required) remains the same as if there were no intermittent sources.
- (ii) when the percentage of the demand fulfilled by the intermittent sources is between 20% and 80%, the energy stored increases progressively, but the backup capacity decreases minimally.
- (iii) when greater than 80% of the demand comes from intermittent sources the storage increases strongly, while the backup capacity decreases to reach zero when 100% percent of the demand is covered by the intermittent sources.

The model application offer some interesting insights. First it indicates that intermittent resources could supply 20% of the load and save a corresponding amount of fuel without the need for storage. As penetration levels increase, storage would become progressively more useful. For greater penetration levels, significant fuel saving would be possible but a big storage would be required. It is apparent that an intermediate transition (i.e. intermittent resources fulfilling between 20-80% of electricity demand) could not be a desirable option, and beneficial effect can become more pronounced after 80% of penetration level. This is encouraging for providing a large fraction of Cuba's electricity with renewables. However, the overarching conclusion is that energy storage will become progressively more important when supplying very large fractions of electrical networks' load with wind and solar.

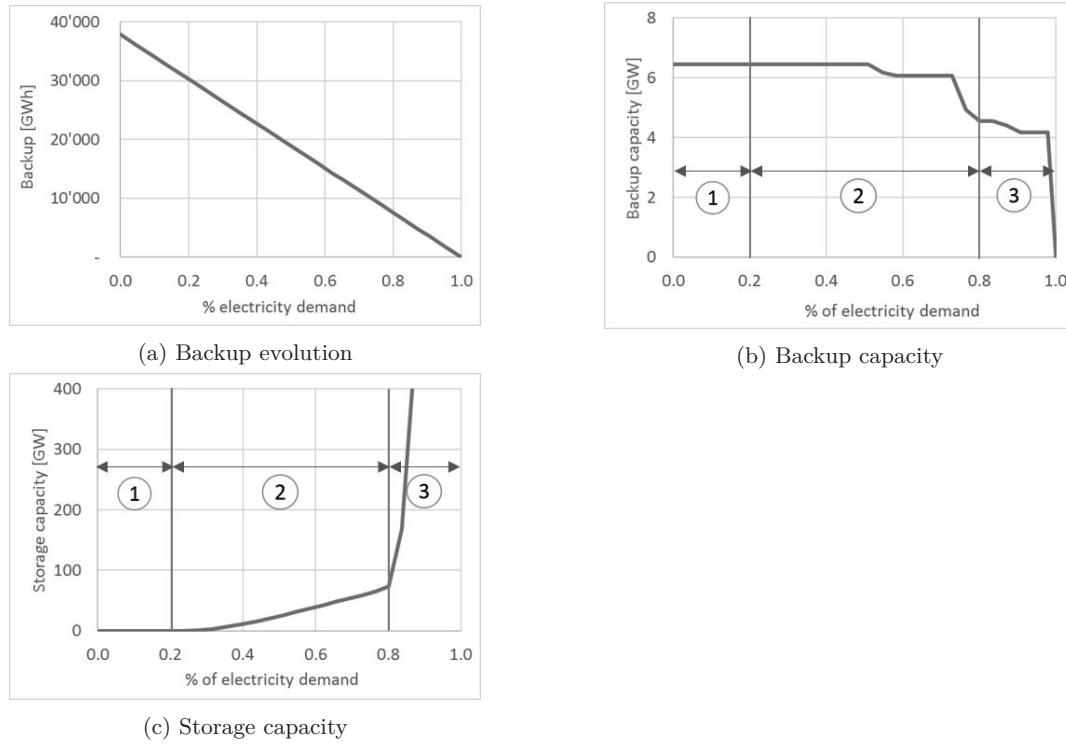


Figure 6.7: Backup energy, storage capacity and backup capacity calculated for different solar installed capacity expressed according to the different percentages of the electricity demand supplied by the solar energy.

6.3.4 Scenarios development

On the basis of the calculated results, a set of scenarios are defined for the year 2030. They show the pathways in which 20, 50 and 100% of final electricity demand is provided from intermittent resources and includes the option of switching existing vehicles by an electric fleet. Table 6.5 lists the scenarios considered. The electricity demand of the transport sector considers that the number of vehicles remains steady from 2015. However, the use of conventional fuels decreases to zero and the rate of energy consumption decreases from 0.63-3.75 kWh/km to 0.02-0.20 kWh/km on the basis of current consumption of different categories of commercial electric vehicles (Osses 2018).

Table 6.5: List of alternative scenarios for 2030

No.	Scenario ID
1a	2030-Int20%
1b	2030-Int20% EV
2a	2030-Int50%
2b	2030-Int50% EV
3a	2030-Int100%
3b	2030-Int100% EV

In scenarios 1a and 1b, 20% of the Cuban electricity demand in 2030 is produced from solar and wind resources. Hydroelectric plants are able to meet 3% (2.8% considering EV) of demand and bioelectric plants meet 15.6% (14.4% considering EV). The 61.4% (62.9% considering EV) will be supplied by oil-based technologies. These scenarios account for the share of oil-based technologies (i.e. backup) less-demanding on imports.

Scenarios 2a and 2b evaluate the option of solar and wind integration at 50% of electricity demands. In agreement with Sec.6.3.3, an energy storage system of around (26GW) could accompany these options. Hydroelectric and bioelectric plants meet the same percentages of scenarios 1 and 2, but the generation of oil-based technologies is reduced down to 31.4% (32.8% considering EV). Scenarios 3a and 3b meet 100% electricity demands from intermittent resources. In addition, hydroelectric and bioelectric plants are supposed to provide electricity up to their full potentials. In the case of bioelectric plants, only the 150 days (i.e. from November to May) of electric generation during the sugarcane milling season are considered. The system is set to over-generation at $\sim 115\%$ of electricity demand and might account for storage at around 2700GW.

6.4 Results

Fig.6.8 shows the primary resources required for each scenario. The first and second bars represent the reference base-case in 2015 and the base-line projection into 2030, such as described in Sec.6.2.1 and 6.2.2. As was mentioned earlier, the base-case energy mix accounts for 84% and 42% of fossil and imported fuels respectively. By 2030, a rise in energy demand is expected and consequently, an increase in reliance on energy resources. The base-line proposed by Cuban authorities achieves a drop in the share of imports (i.e. higher levels of energy security) by intensifying the use of domestic resources (mainly crude oil and biomass from bagasse) but proves to be more reliant on fossil fuels (i.e. decrease sustainability). Accordingly, air quality degradation and an increasing population health risk of pollution exposure are anticipated.

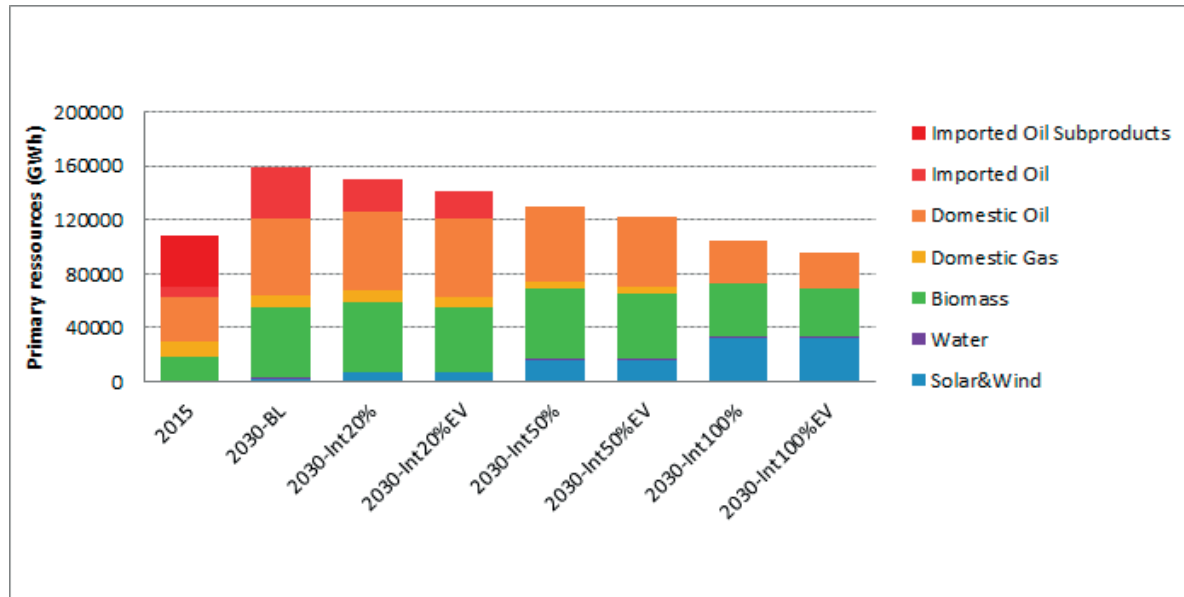


Figure 6.8: Comparison between scenarios for 2030

Table 6.6: Indicators 2030

Criteria	2030BL	2030 Int20%	2030 Int20% EV	2030 Int50%	2030 50% EV	2030 Int100%	2030 Int100% EV
Energy security	0.83	0.52	0.44	0.00	0.00	0.00	0.00
Energy sustainability	1.16	1.00	0.96	0.68	0.63	0.35	0.29
Air quality	1.07	1.01	0.99	0.93	0.90	0.84	0.80

The second to the eighth bars in Fig.6.8 show the consequences of Cuba's penetration of renewable resources to meet the increase of electricity demand, such as described in Sec.6.3.4. In agreement with indicators in Sec.6.2.4, the energy security, sustainability and air quality impact changes can also be perceived (see also table6.6). Overall, the results indicate that energy security and sustainability increase with wind and solar penetration at different rates: a penetration rate of 20% of the electricity demand significantly decreases fuel imports requirements (even more than the base-line scenario) but the share on fossil fuel, as well as the level of population exposure to pollution, remains the same as in 2015. Once the wind and solar penetration rise to 50%, Cuba can achieve complete energy independence and significantly reduce (40%) the use of fossil fuel resources. Finally, when adding solar and wind electric generation at 100% of demand, the dependency on fossil fuels significantly decreases, however the reliance on services such as industrial and production processes still avoids a complete phase out of fossil fuels. Not surprisingly, a high use of renewable energy has positive effects on air quality. Rates over 50% can diminish the level of population exposure to pollution by between 7 and 20%.

The effect of switching the existing vehicles to an entirely electric fleet can be also considered. Despite the increase in electricity demand, the net effect for the energy system is a reduction in total requirements on resources. The switching may help the country to reduce its dependency on oil imports (15%, comparing scenarios Int20% and Int20%EV), and save between 4 and 18% of oil by-products such as diesel and gasoline.

6.5 Summary and conclusions

This work aimed to explore scenarios for a reliable Cuban energy transition. To this end, an overview of the country's energy system (i.e. resources, technologies, and services) and its short-term projection was drawn up. Final energy consumption was characterized as the sum of two main components: electricity demand and oil sub-product demand. Among them, the electricity sector plays the main role as it currently consumes 73% of all resources managed by the country, of which 45% are imported.

It is a fact that the component of electricity demand will increase over time. Although this has already been acknowledged by the country's authorities, the rate of increase that they envisage is likely underestimated. At the same time, there is a wide range of uncertainty over the supply outlook for 2030. The estimated margins of resource availability and recoverability (mainly fossil fuels and biomass) are often optimistic. Following these insights, it is not certain that electricity demand for 2030 could be met. In addition, the dependency on imports makes the country vulnerable to political changes abroad; while the dependence on fossil fuel, combined with the use of outdated technologies, deteriorate the environment.

Our assessment is that there is potential for these risks to be managed by a wider use of renewable resources. The potential of the main renewable energy resources available for Cuba have been evaluated. The required land-surface for its widespread adoption have been computed. It was found that the use of solar and wind resources require less than 0.1% (for the solar) and 2% (for the wind) of Cuban land to be able to entirely fulfil the electricity demand expected in 2030, while the biomass might require a great deal of space land expenses. This issue caused the study to focus more on the analysis of wind and solar systems. These resources are characterized by a large degree of intermittency driven by natural variability of climate factors. Thus, time series simulations that included an intermittent electric supply coupled with storage and backup utilities were performed.

The simulations allowed for rapid estimations of the intermittent deployment: as its penetration rates increase, the average use of conventional technologies (i.e. centralized thermoelectric, combined-cycle generating plants and distributed generator sets) and resources decrease regularly. However, the storage and backup utilities operate differently. Three different regimes were revealed: for intermittent penetration below 20% of electricity demand, the loads can be supplied without the need for storage, but high backup capacities (the same as a conventional supply) must be available to meet peak demands. Above this rate, the regime still needs high traditional backup capacities and storage requirements start subtly increasing until intermittent penetration meets approximately 80% of the electricity demand. As intermittent penetration increases over 80%, storage significantly increases and backup capacities can progressively be stopped until their services are not more required. It is apparent that beneficial effect can become more pronounced after 80% of penetration level. This is encouraging for providing a large fraction of Cuba's electricity with renewables. However, the overarching conclusion is that energy storage will become progressively more important when supplying very large fractions of electrical networks' load with wind and solar.

In order to evaluate the consequences of these regimes to the country development, a set of scenarios were defined for the year 2030. They show the pathways in which 20, 50 and 100% of final electricity demand

is provided from intermittent resources. In addition, a set of indicators allow for quantifying the effects in terms of energy security, sustainability and air quality impacts. Overall, the results indicated that energy security and sustainability increase with wind and solar penetration at different rates. A penetration rate of 20% of the demand significantly decreases fossil fuel imports. Once raised to 50%, Cuba can achieve complete energy independence. Not surprisingly, the penetration of renewable energy sources had positive effects on air quality.

This study is significant in assessing the benefits of renewable resources deployment over Cuba, as well as in evaluating the consequences of the transition. The status of these assessments is very encouraging and it lead one to consider what additional features could be added to guide policy-makers about the main ingredients of a low-carbon and self-sufficient energy transition. Some possibilities include assessments of the effects of different storage types, holding capacity and charging/discharging power varying, as well as estimations about the kind of backup supply (e.g. centralized, bio-electric, hydroelectric power plants) which is needed / available considering the start-up times/frequencies at which conventional energy must supply the shortages of intermittent-storage system. The economical effects of the resulting alternatives - including market prices, investments and operating costs- are important factors that should be also included for upcoming research.

References

- Al-Khazzar, A. (2017). “The Required Land Area for Installing a Photovoltaic Power Plant The Required Land Area for Installing a Photovoltaic Power Plant”. In: *Iranica Journal of Energy & Environment* April.
- Alonso-pippo, W., C. A. Luengo, J. Koehlinger, P. Garzone, and G. Cornacchia (2008). “Sugarcane energy use : The Cuban case”. In: 36, pp. 2163–2181.
- Angeles, M. E., J. E. Gonzalez, J. E. Iii, and J. L. Hernandez (2010). “The Impacts of Climate Changes on the Renewable Energy Resources in the Caribbean”. In: 132.August, pp. 1–13.
- Angeles, M. E., J. E. Gonzalez, J. E. Iii, L. Hern, R. National, and O. Ridge (2007). “Predictions of future climate change in the caribbean region using global general circulation models”. In: 569.October 2006, pp. 555–569.
- Angeles, M. E., J. E. Gonzalez, and N. Ramirez (2018). “Impacts of climate change on building energy demands in the intra-Americas region”. In: pp. 59–72.
- Avila, M. A. A. (2009). “Cuba: Energy and Development.” In:
- Belt, J. A. B. (2010). *The Electric Power Sector in Cuba : Potential Ways to Increase Efficiency and Sustainability*. Tech. rep.
- Benjamin-Alvarado, J. (2010). *Cuba’s Energy Future: Strategic Approaches to Cooperation*. Brookings Institution Press.
- Berg, H. and E. Bäck (2013). “Study of Oil-Fired Electricity Production on Cuba ; Means of Reducing Emissions of SO₂ by Increasing Plant Efficiency”. PhD thesis. KTH School of Industrial Engineering and Management. STOCKHOLM.
- Chadee, X. T. and R. M. Clarke (2014). “Large-scale wind energy potential of the Caribbean region using near-surface reanalysis data”. In: *Renewable and Sustainable Energy Reviews* 30, pp. 45–58.
- EFE (2014). “Cuba aims for 24 pct renewable energy by 2030”. In: *Fox News*.
- Enoch, M., J. P. Warren, and H. Valde (2004). *The effect of economic restrictions on transport practices in Cuba*. Tech. rep., pp. 67–76.
- Gonzalez Del Toro, D. (2016). *Quality and technologies to benefit the country*.
- Guevara-stone, L., M. Alberto, and A. Avila (2009). “La Revolucion Energetica : Cuba’s Energy Revolution”. In: *Renewable Energy World*, pp. 1–13.
- (IAE), I. E. A. (2006). *Model for analysis of Energy demand (MAED-2)*. *Computer Manual Series No.18*. Tech. rep.
- IAEA (2008). *Cuba: A country profile on sustainable energy development*. Tech. rep.
- Jacobson, M. Z., M. A. Delucchi, Z. A. Bauer, S. C. Goodman, W. E. Chapman, M. A. Cameron, C. Bozonnat, L. Chobadi, H. A. Clonts, P. Enevoldsen, J. R. Erwin, S. N. Fobi, O. K. Goldstrom, E. M. Hennessy, J. Liu, J. Lo, C. B. Meyer, S. B. Morris, K. R. Moy, P. L. O’Neill, I. Petkov, S. Redfern, R. Schucker, M. A. Sontag, J. Wang, E. Weiner, and A. S. Yachanin (2017). “100% Clean and Renewable Wind, Water, and Sunlight All-Sector Energy Roadmaps for 139 Countries of the World”. In: *Joule*.
- Jimenez Borges, R., J. Lorenzo Llanes, J. P. Monteagudo Yanes, H. Pérez de Alejo Victoria, R. Alvarez Delgado, and D. D. Carreño Sarmiento (2017). “Potentialities of electricenergy delivery in two sugar mills of Cienguegos province.” In: *Centro Azucar* 44.2, pp. 1–7.
- Käkönen, M., H. Kaisti, and J. Luukkanen (2014). *Energy Revolution in Cuba : Pioneering for the Future* ? January.
- Maegaard, P., A. Krenz, and W. Palz (2013). *Wind Power for the World: International Reviews and Developments*. Vol3. Florida, United States: CRS Press.
- MINAS, M. d. e. y. minas de la republica de cuba) and A. d. c. i. d. J. JICA (2016). *Estudio para la recoleccion de datos sobre el sector de electricidad en la republica de Cuba. Informe Final Informe Final*. Tech. rep.
- Momoh, J. A., S. Meliopoulos, and R. Saint (2012). “Centralized and Distributed Generated Power Systems - A Comparison Approach.” In: *PSERC*.
- NREL (2008). *National Solar Radiation Database (NSRDB)*.
- ONE (2016c). *Anuario Estadístico de Cuba. Section 2: Medio Ambiente*. Tech. rep.
- Osses, M. (2018). “Electric vehicles in urban environment: Energy demand, climate change and technological challenges”. In:
- Panfil, M., D. Whittle, and K. Sinverman-Roati (2017). *The Cuban Electric Grid. Lesson and recommendations for Cuba’s electric sector*. Tech. rep. Environmental Defense Fund (EDF).

- Reuters (2016). “Cuba’s power consumption jumped 4.8 percent in 2015”. In: *Reuters*.
- Rodríguez-Machín, L., D. H. Bretón-Glean, R. Perez-bermudez, and L. E. Arteaga-Pérez (2012). *Métodos de estimación de biomasa potencial*. Tech. rep. July.
- Sagastume, A., J. J. Cabello Eras, D. Huisingsh, C. Vandecasteele, and L. Hens (2018). “The current potential of low-carbon economy and biomass-based electricity in Cuba . The case of sugarcane , energy cane and marabu (*Dichrostachys cinerea*) as biomass sources”. In: 172, pp. 2108–2122.
- Solaris (2017). *Solaris*.
- Suarez, J., P. Anibal, R. Faxas, and O. Pérez (2012). “Energy , environment and development in Cuba”. In: *Renewable and Sustainable Energy Reviews* 16.5, pp. 2724–2731.
- Wright, E. L., J. A. B. Belt, A. Chambers, P. Delaquil, and G. Goldstein (2010). “A scenario analysis of investment options for the Cuban power sector using the MARKAL model”. In: *Energy Policy* 38.7, pp. 3342–3355.

Chapter 7

Summary of main contributions and outlook

This thesis presented alternative methods to facilitate the assessment of air quality and energy strategies in the framework of developing countries. It was implemented in Cuba. The main contributions of this work are summarised in the following two sections: alternatives methods for the assessments of air quality strategies, the case of Cuba (Sec.7.1) and general design features toward a sustainable energy transition, the case of Cuba (Sec.7.2). In the following some recommendations for further develop the methods hereby (Sec.7.3 and 7.4).

7.1 Alternatives techniques for reliable assessments of emission abatement strategies, the case of Cuba

This section summarizes the work performed on air pollution emphasizing the main contributions. The workflow diagram integrates the relationships among research steps, see Fig.7.1.

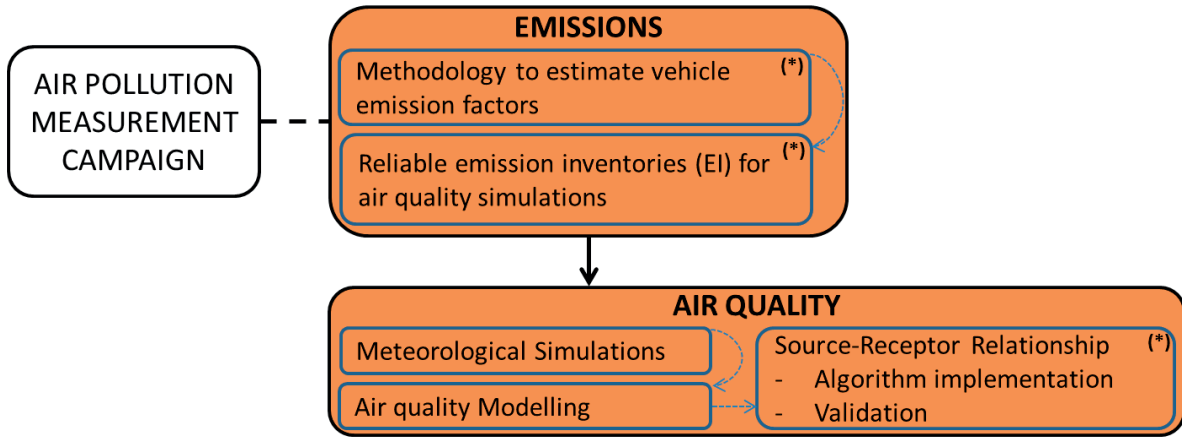


Figure 7.1: Interdependencies of the research in air quality domain and main contributions (*)

A first contribution of this research is to provide relevant data on air quality. A pollution measurement campaign was carried out in Havana, Cuba. Some traffic-related pollutants (i.e. PM₁₀, SO₂ and NO₂) were rated. Observations showed that concentration levels exceeded World Health Organization thresholds for PM₁₀ and SO₂. Subsequence statistical analysis (Sec.2.3) indicated that southeast/northeast wind episodes drag significant amount of PM₁₀/SO₂ to the urban environment from specific sources around the city. However traffic was found responsible for around 50% of PM₁₀ concentrations at the level street (Sec.3.5).

A second important contribution was to use the measurements results to develop and implement a low-cost methodology able to estimate vehicle emission factors. This methodology uses street canyon measurements of traffic fluxes, wind, and pollutant concentration. It improves the approach developed by Belalcazar et al. 2009 reducing its cost and improving its robustness. So far, emission factors have been found only for PM. As expected, results has identified pre-1980 vehicles as the most polluting technologies (see Sec.3.3), and pointed that upgrading this category would be an effective scenario for reducing PM₁₀ air pollution in Havana by between 10 and 17%. These emission factors are also key parameters on the development of road transport emission inventories of Cuba.

A third contribution stems from our reframing of the issue of how to assess the usability of an emission inventory for air quality simulations. The Emission Database for Global Atmospheric Research (EDGAR) was used to generate a preliminary emission inventory (EI) of Havana. A second EI was created from local information provided by the Cuban partner. The implementation of comparison methods developed in the framework of the Forum for Air Quality Modelling in Europe-FAIRMODE showed that the global EI cannot be used as reference for air quality analysis as it is too far from what we locally know: EDGAR overestimates emission factors of stationary sources for CO by a factor of 3 and SO₂ by a factor of 1.5 while underestimates those of PPM by a factor of 25. Most of the road transport emission factors are also overestimated in EDGAR; PPM, CO and NO_x are 2 times higher, while CH₄ and SO₂ are 5 to 20 times higher.

This finding led to the development of a new-regional emission inventory for Cuba (see Sec. 5.2.1). It was used as input for modelling the air quality over the country. Simulations were performed with the deterministic chemical transport model CTM- CHIMERE (Mailler et al. 2017; Menut et al. 2013) and driven by meteorological outcomes from the Weather Research Forecasting model (WRF of National Centers for Environmental Prediction NOAA, U.S. Department of Commerce 2000). Since we focused on simplifying tools for scenarios analysis, we statistically explored the model responses of proxy pollutants (EEA, 2008), such as particulate matter, nitrogen oxides and ozone; and their interrelationships. This provided insights

into the behaviour and key relationships among them (see Sec.5.3) and showed that yearly averages of hourly NOx and PM25, as well as the SOMO35 index (i.e. sum of maximum 8-hours ozone levels over 35 ppb for a year) might concisely represent pollution conditions under all circumstances in Cuban simulations since other pollutant of interest (e.g. PPM, NO2 and O3 night/day levels) can reasonable be derived from them.

A fourth important contribution derives from the development of simplified algebraic relationships able to predict the impacts on concentrations that result from regional emission abatements. Following the statements of linearity (i.e. linear relationships between emission and concentrations) described by Clappier et al. 2015 and Thunis et al. 2015, and implementing the approach of Pisoni et al. 2017, a simplified forecaster of NOx and PM25, SOMO35 pollution was developed for Cuba (i.e. the so-called “Source-Receptor Relationship -SRR”). It worked properly for all tested applications even for those considering high level of simultaneous reductions of pollutant precursors (i.e. PPM, NO2, SOx, NH3, and VOC). To further improve the statistical estimates over Cuba, two different algorithms were explored (Sec. 5.4.3); they subtly enhance PM25 and SOMO35 applications. The SRR is able to assess the impact of projected emission reduction strategies on air quality in a faster way (i.e. it requires low CPU time and computer resources).

7.2 General design features toward a sustainable energy transition. The case of Cuba

This section summarizes the work performed on the issue of energy systems emphasizing the contributions made by the author through the Cuban case study.

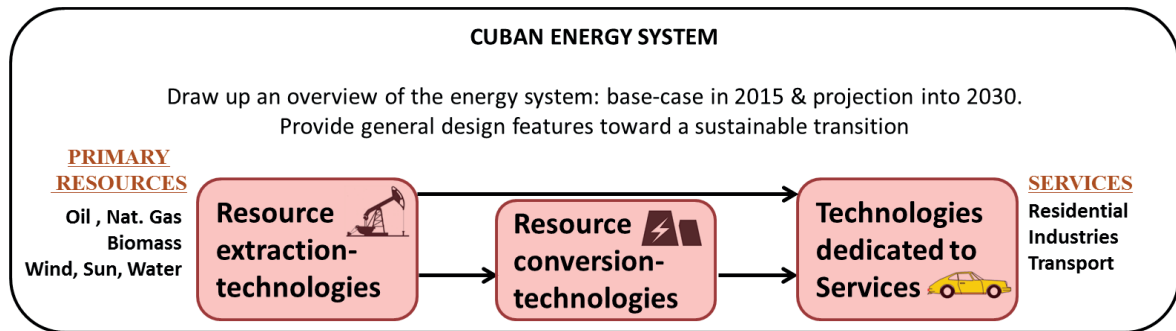


Figure 7.2: Main contribution in energy system domain

The study aimed to explore scenarios for the energy transition of Cuba. To this end, an overview of the country’s energy system (i.e. resources, technologies, and services) and its short-term projection was drawn up. Final consumption was represented as the sum of two main components: electricity and all other services using oil sub-products. Among them, electricity sector plays the main role since it currently consumes 73% of all resources managed by the country and 45% of those imported.

In order to decrease the energy dependency of fossil fuel and imports, an assessment of the potential and consequences of Cuba’s use of local renewable resources (i.e. biomass, wind and solar) was carried out. A widespread adoption of solar and wind systems would require around 0.1% and 2% of Cuba land. However, the biomass might suppose a great deal of space land expenses accounting for at least 15% of Cuba land.

Time series simulations, including solar and wind electric supply coupled with storage and backup utilities showed that an increasing penetration rates of these resources decreases the use of conventional technologies and resources regularly. Solar and wind could supply around 20% of the electricity demand and save a corresponding amount of fossil fuel without the need for storage but as penetration levels increase, storage become progressively more useful. For greater penetration levels, significant fossil fuel saving would be possible but a big storage would be required. It is apparent that beneficial effect of solar and wind use can become more pronounced after 80% of penetration level which is encouraging for providing a large fraction of Cuba’s electricity with renewables. However, the overarching conclusion is that energy storage will become significant when supplying very large fractions of electrical networks’ load with wind and solar.

A set of transition scenarios -designed on the basis of different mix of energy resources- indicated that the energy security and sustainability of the country can also increase with the use of renewable resources:

A penetration rate at 20% of the demand significantly decreases fossil fuel imports. Once raised to 50%, Cuba can achieve complete energy independence. The scenario which fulfils 100% of the electricity demands from solar and wind resources shows the maximum of sustainability. Not surprisingly, the penetration of renewables had also positive effects on air quality.

7.3 Recommendations

In this section we formulate some recommendations for further developing the methods presented in this thesis. But first, a word for the Cuban researchers who will continue developing this work:

- (i) It is important to stress the still remaining need for air pollution measurements over Cuba. Forthcoming measurement campaigns must be organized in other places and over longer time period –if possible covering the two most important seasons of the country, the so-called Cuban dry and wet seasons. This may allow firstly for performing a more complete analysis of the Cuban air pollution processes; and secondly to have reference measurement points for comparing and validating air quality modelling results.
- (ii) It is still necessary to validate the methodology of emission factors estimations for other pollutants; e.g. gases like NO₂ and SO₂. To do that, it is recommended to select a street canyon with significant and diverse traffic conditions, in a way that correctly represents the technological conditions of the fleet to be evaluated. In addition, we strongly recommend measuring pollutant concentration levels at low time intervals -then explore the averaging time period that best fit traffic, concentrations and meteorological data.
- (iii) The example study of setting up the SRR over Cuba is, such as it was stated, just an example; before any definitive version may be released, it is necessary to validate the Chemical Transport Model -CTM results.
- (iv) Although Cuban institutions provide control services for saving energy in industrial sector, a deeper review and evaluation of the technologies used in industrial and production process is recommended. It must be useful for establishing reliable energy policies at a country level in such sectors.

Further improvements can be achieved on the methods presented along this dissertation:

- With respect to the methodology for low-cost estimation of vehicle emission factor

Among several mathematical assumptions, the background concentration level at the street level is assumed constant. It has effects on the accuracy of estimations since it deteriorates the quality of the statistical relations established between traffic flows and pollutant concentration levels. Three intuitive directions could be followed to reduce this source of imprecision: (a) including measurements of background concentrations as inputs in the algorithm –it will reduce the number of unknown variables and could potentially increase the accuracy of calculations, (b) clustering the set of measurements over periods during which background contributions has proven to be constant (e.g. from complementary measurements of surrounding stationary stations), and (c) removing the background concentration from estimations by considering relationships in form of derivatives. This technique was already tested by the author with acceptable preliminary results: they were less accurate than those obtained by the proposed methodology for PM₁₀ but they could be valid for applications to other pollutants. In addition, this methodology was implemented for the specific street configuration. A generalization including different street geometries (i.e. ratio height/width of street canyons) could broaden its range of applications.

- With respect to the Source-Receptor Relationship

The method worked properly for all tested applications but it was less accurate than expected –in comparison with the original applications in Pisoni et al. 2017. The level of accuracy associated with the estimation method might be further increased by establishing other kind of locally weighted kernel functions (e.g. local polynomials) between emissions and concentrations during the training (fit) step. Indeed, the implementation of alternative kernel functions would fit a more adapted smooth surface of concentrations from surrounding emission values. As inconvenient, the number of coefficient (unknown

parameters) relating emissions and concentrations could increase, and consequently, an increased number of simulation runs (scenarios) might be required to perform the calculations. A trade-off between bias (i.e. error from assumptions in the algorithm) and variance (i.e. variability of estimates) must be found.

A current limitation of the approach lies in the spatial resolution; once the algebraic relationships are fit, smaller configurations cannot be analysed. This leads to problem for energy system scenarios analysis as they must consider emission changes at a very local scale. One approach that could overcome this issue is to add downscaling implementations. This is a technique commonly used to extract high-resolution information from regional scale variables produced by coarse resolution models, e.g. CTMs. More specifically, statistical downscaling (e.g. regression-based downscaling) is based on developing a statistical relationship between small-scale variables and large-scale variables (Alkuwari et al. 2013). The main advantage of their use is that it is computationally inexpensive and appropriate when computational resources are limited (Wilby et al. 2004), as in developing regions. Statistical downscaling can provide point-specific forecasts from a set of air quality simulations at high resolution in areas of interest. Regression fits (e.g. linear, principal component or nearest neighbour smoother regression) can be implemented between the grid average values at coarse resolution and local model outputs. In the case of Cuba, computer performance limited the CTM forecasts to a coarse spatial resolution of 24km; however, high-resolution simulations (3km) were performed for Havana. It could be very interesting to link a downscaling method to the SRR of Cuba, in order to forecast emission reductions in Havana. This approach can also be used to improve the forecasts provided by SRR from measurements produced by monitoring stations, which is widely applied in downscaling CTMs from observations of historical data.

- With respect to the time series simulations of intermittent (i.e. wind and solar) energy

In its current form, the time series simulation of intermittent energy production illustrates basic features mismatching the available wind and solar power with electrical load, and the possible benefits of storage and backup systems. It would be also interesting to look at the possible benefit of using the storage to shift energy produced at times of low value to peak hours. In this way storage can be used as part of an overall dispatching strategy to reduce fossil fuel use. It could be also of interest to look at the effect of storage holding fixed capacity and charging/discharging power varying. It could provide interesting insights about the optimum size of storage capable of saving the greater fossil fuel amounts.

The model does not include estimations about the start-up times and frequencies at which conventional energy must supply the shortages of intermittent-storage system. This could be significant in selecting the kind of backup supply (e.g. centralized, bio-electric, hydroelectric power plants) which is needed / available. For planning purposes, it is recommended to provide these sort of outputs.

The assessment framework still does not consider costs. The effect of market prices, investments and operating costs are important factors in real-world operational decisions. So that, these evaluations should be included for upcoming research.

7.4 Outlook

The techniques presented in this thesis can potentially assist the planning of future strategies in air quality and energy fields. However, this work is just a step towards the goal of providing an adapted modelling support in designing sustainable energy strategies for low-income economies. Additional work is still necessary to model other components of this complex system. Forthcoming steps should foster flexibility, simplicity (in terms of data and computational demands) and accuracy required for applications in developing countries.

In this regard, the experience gained along this research let formulate some recommendations.

- (i) Compiling data: The characteristics of the energy systems of developing countries are complex and make their study challenging. To prevent misfit, it is strongly recommended to avoid the use of global data, or at least, carefully evaluate the reliability of data sources in the specific context. The use of local/regional data with adequately adapted models (e.g. approaches of type bottom-up) should be preferred.
- (ii) Modelling support: Computationally intensive modelling, either on air quality or energy fields, is often difficult to perform in developing countries. Outcomes such as interactive graphics or scenarios-based analyses accounting for ad-hoc criteria (of interest for the country) could prove to be helpful for facilitating the assessment of air quality and energy strategies.

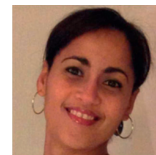
- (iii) Uncertainty: Even considering these cautions, one could ask whether and to what extent a set of solutions is reliable. The level of uncertainty associated with the estimation methods might be further investigated. Uncertainties and/or sensitive analysis are research issues that must be considered when modelling systems in developing countries.

References

- Alkuwari, F. A., S. Guillas, and Y. Wang (2013). “Statistical downscaling of an air quality model using Fitted Empirical Orthogonal Functions”. In: *Atmospheric Environment* 81, pp. 1–10.
- Belalcazar, L. C., O. Fuhrer, M. D. Ho, E. Zarate, and A. Clappier (2009). “Estimation of road traffic emission factors from a long term tracer study”. In: *Atmospheric Environment* 43.36, pp. 5830–5837.
- Clappier, A., E. Pisoni, and P. Thunis (2015). “A new approach to design source–receptor relationships for air quality modelling”. In: *Environmental Modelling & Software* 74, pp. 66–74.
- Mailler, S., L. Menut, D. Khvorostyanov, M. Valari, F. Couvidat, G. Siour, L. Interuniversitaire, A. Lisa, U. M. R. Cnrs, U. Paris, and E. Créteil (2017). “CHIMERE-2017 : from urban to hemispheric chemistry-transport modeling”. In: *Geoscientific Model Development* 10, pp. 2397–2423.
- Menut, L., B. Bessagnet, D. Khvorostyanov, M. Beekmann, N. Blond, A. Colette, I. Coll, G. Curci, G. Foret, A. Hodzic, S. Mailler, F. Meleux, J.-L. Monge, I. Pison, G. Siour, S. Turquety, M. Valari, R. Vautard, and M. G. Vivanco (2013). “CHIMERE 2013: a model for regional atmospheric composition modelling”. In: *Geoscientific Model Development* 6.4, pp. 981–1028.
- National Centers for Environmental Prediction NOAA, U.S. Department of Commerce, N. W. S. (2000). *NCEP FNL Operational Model Global Tropospheric Analyses, continuing from July 1999*. English. Boulder, CO.
- Pisoni, E., A. Clappier, B. Degraeuwe, and P. Thunis (2017). “Adding spatial flexibility to source-receptor relationships for air quality modeling”. In: *Environmental Modelling and Software* 90, pp. 68–77.
- Thunis, P., A. Clappier, E. Pisoni, and B. Degraeuwe (2015). “Quantification of non-linearities as a function of time averaging in regional air quality modeling applications”. In: *Atmospheric Environment* 103, pp. 263–275.
- Wilby, R. L., S. P. Charles, E. Zorita, B. Timbal, P. Whetton, and L. O. Mearns (2004). “Guidelines for Use of Climate Scenarios Developed from Statistical Downscaling Methods”. In: August, pp. 1–27.

Jessie Madrazo Bacallao

Av. Florissant 36
1020 Renens
+41 78 926 8022
jessie.madrazo@epfl.ch



Date of birth : 22/06/1982
Nationality: Cuba
Cohabiting in couple

Strengths: Analytical thinking, strategic planning, international oriented

Profiles on:

www.linkedin.com/in/jessiemadrazo
<http://orcid.org/0000-0001-8750-2967>

Education/Qualifications

- 2014-2018** PhD candidate at Swiss Federal Institute of Technology in Lausanne, EPFL (exp. Oct)
2017-2018 PhD Student –exchange, Stanford University – Atmosphere and Energy Program
2010 Post-graduate degree & Intern-ship for project management and international collaboration, Polytechnic Superior Institute CUJAE.
2006-2009 Master in Civil Engineering M.A., Polytechnic Superior Institute CUJAE.
2000-2005 Bachelor in Civil Engineering, Polytechnic Superior Institute CUJAE.
1997-2000 Vocational Pre-university Institute of Exact Sciences – IPVC Lenin

Professional Experience/Internships

- 2014-2017** **Association UrbamoCuba.ch**
Support to projects related to mobility, energy and the environment in Cuba. As Cuban specialist, I contributed to the definition of technological choices on energy and air pollution strategies.
- 2012-2014** **EPFL Excellence Fellowship**
Research on emission inventories for Cuba.
- 2010-2012** **CUJAE Deputy head of Road Engineering's Department**
Led and coordinated the Road Engineering disciplines: liaising with the general manager in ensuring that teaching resources are in place and on time; taking responsibility to accredit and reaccredit courses with government and professional accreditation bodies; providing timetabling advice for all units; advising the teaching & learning committee; successful interactions with the industry related to Road Engineering disciplines.
- 2009-2010** **SCD Cooperation project Cuba- Switzerland: Renaissance of Havana's Arterias**
Technical team leader of civil engineers and architects. Decided on preliminary solutions to increase bus networks and corridor productivities; improvement of pedestrians' accessibility and enhancement of security at bus stops in harmony with urban development and environmental requirements.
- 2009-2010** **CUJAE – Research and teaching associated**
Participation in teaching and applied research at Civil Engineering Laboratory

Technical skills

Scientific programing, simulation and optimization techniques.
Computer literate: Linux, Windows applications.
Programming languages: C/C++, Matlab
Geographic Information Systems: QGIS, ArcGIS, Spatial statistic
Design: AutoCAD
Emissions - Air pollution – Weather modelling: CHIMERE, WRF, OSPM, Envi-Met
Languages: Spanish: native speaker; French: fluent; English: fluent

List of publications

- Madrazo, J., Clappier, A., 2018. Low-cost methodology to estimate vehicle emission factors. *Atmos. Pollut. Res.* 9, 322–332. <https://doi.org/10.1016/j.apr.2017.10.006>
- Madrazo, J., Clappier, A., Carlos, L., Cuesta, O., Contreras, H., Golay, F., 2018. Screening differences between a local inventory and the Emissions Database for Global Atmospheric Research (EDGAR). *Sci. Total Environ.* 631–632, 934–941. <https://doi.org/10.1016/j.scitotenv.2018.03.094>
- Madrazo, J., Clappier, A., Cuesta, O., Belalcazar, C., Gonzalez, Y., Menendez, L., Sosa, C., Carrillo, E., Manso, R., Golay, F., 2017. Evidence of traffic-generated air pollution in Havana. *Atmosfera*, Manuscript 1–20. *submitted to Atmosphere*
- Oswaldo, C., Bolufé, J., Gonzalez, Y., Sosa, C., Carrillo, E., Manso, R., Madrazo, J., Clappier, A., Barcarcel, C., Fankhauser, R., 2017. Contaminación atmosférica por fuentes móviles en la calle Reina , La Habana Atmospheric pollution for mobil sources in Reina street , La Havana. *Rev. Cuba. Meteorol.*
- Madrazo, J., Sacasas León, C., Pire Rivas, S., Alonso León, L., 2014. Estimation of CO and NOx concentration levels associated to the exploitation of national roads in Havana. *Carreteras* 4, 77–91.
- Madrazo, J., Álvarez Goris, H., 2010. Indicators for evaluating the impacts generated by actions affecting transport systems. *Carreteras* 4.
- Madrazo, J., Miralles, L., Menendez, C., 2012. Modelos para la evaluación de la contaminación atmosférica provocada por el tráfico urbano. Estrategia para la evaluación en La Habana, 1ra ed. Medio ambiente CUJAE-UPV 2009-2011, Madrid.
- Díaz, S., Isaac, C.L., Alba, L., Madrazo, J., Claro, A., Miralles, L., Menendez, C., 2012. Metodología para la ejecución de los diagnósticos ambientales en las vías, 1ra ed. Medio ambiente CUJAE-UPV 2009-2011, Madrid.
- Madrazo, J., Clappier, A., 2018. Implementation of an air quality modelling system to study the impact of futur energy stratagies in Cuba: International Conference on the Management of Energy, Climate and Air for a Sustainable Society. MECAS. La Havana, Cuba.
- Madrazo, J., Clappier, A., 2017. Design a low cost methodology to estimate vehicle emission factor: application in Havana, Cuba, in: International Conference on Atmospheric Sciences and Application to Air Quality. ASAAQ. Strasbourg, France.